

UNIVERSITÀ  
DEGLI STUDI  
DI PADOVA

Università degli Studi di Padova

Dipartimento di Scienze Chirurgiche, Oncologiche e Gastroenterologiche

SCUOLA DI DOTTORATO DI RICERCA IN ONCOLOGIA E ONCOLOGIA  
CHIRURGICA

CICLO XXVI

**The crosstalk between activated T cells and  
Myeloid Derived Suppressor Cells: characterization of molecular  
mechanisms involved in immune suppression**

**Direttore della Scuola :** Ch.ma Prof.ssa Paola Zanovello

**Supervisore :** Dott.ssa Susanna Mandruzzato

**Dottoranda:** Laura Pinton



# INDEX

ABBREVIATIONS .....	3
ABSTRACT .....	7
RIASSUNTO .....	9
INTRODUCTION .....	11
1.1 From immuno-surveillance to the theory of cancer immunoediting.....	11
1.2 Tumor immune tolerance .....	12
1.3 Myeloid derived suppressor cells (MDSCs) .....	15
1.3.1 Factors involved in MDSC expansion .....	15
1.3.2 Murine MDSCs .....	16
1.3.3 Human MDSCs .....	17
1.3.4 Mechanisms of action of MDSCs .....	19
1.3.5 MDSCs as a therapeutic target.....	21
1.3.6 <i>In vitro</i> induction of MDSCs from BM cells .....	24
1.4 Signal Transducer and Activator of Transcription 3 (STAT3): a key factor in promoting tumor growth .....	26
1.5 The B7- family of proteins: surface molecules involved in the modulation of immune response .....	29
1.6 Functional role of PD-1/PD-L1 interaction in tumors .....	33
1.7 T cell anergy, exhaustion and senescence in tumor microenvironment.....	34
2. AIM OF THE PROJECT .....	37
3. MATERIALS AND METHODS .....	39
3.1 BM samples.....	39
3.2 BM-MDSC generation and separation of BM-MDSC subsets.....	39
3.3 Proliferation assay .....	40
3.4 Flow cytometric analysis of BM-MDSCs and activated T cells.....	41
3.5 Analysis of IL-10 production .....	42
3.6 Protein extraction and Western Blot analysis .....	43
3.7 Intracellular staining for P-STAT3 .....	44
3.8 FACS sorting to separate B7-H1 <sup>+</sup> and B7-H1 <sup>-</sup> subsets.....	45
3.9 Analysis of STAT3 target genes by TRANSFAC database.....	45
3.10 Colon cancer patients cohort.....	45

3.11 Enzymatic digestion of biopsies and flow cytometric analysis.....	46
3.12 Statistical analysis .....	46
4. RESULTS.....	47
4.1 Role of IL-10 in the immune suppression induced by MDSCs expanded <i>in vitro</i> .....	47
4.2 Role of STAT3 phosphorylation in MDSC-mediated immune suppression .....	49
4.3 Analysis of the expression of B7-family members on iBM-MDSCs under different experimental conditions.....	54
4.4 Evaluation of the relationship between STAT3 activation and B7-H1 expression .....	57
4.5 Inhibition of STAT-3 phosphorylation in iBM-MDSCs restores the immune response .....	60
4.6 Analysis of STAT3 target genes.....	63
4.7 Analysis of T cell-suppression induced by iBM-MDSCs .....	66
4.8 MDSCs induce markers of cell exhaustion on T cells.....	67
4.9 Analysis of myeloid cells present in liver metastases from colorectal cancer patients.....	72
4.10 Analysis of PD-1 and LAG-3 expression in T cells infiltrating liver metastases from colorectal cancer patients.....	73
5. DISCUSSION.....	75
6. REFERENCES .....	83
RINGRAZIAMENTI .....	95
APPENDIX I.....	97

## ABBREVIATIONS

APC: *antigen presenting cell*  
ARG: *arginase*  
ATRA: *all trans retinoic acid*  
BAT-3: *HLA-B-associated transcript 3*  
B7-H: *B7-homolog*  
BM: *bone marrow*  
BM-MDSC: *BM-derived MDSC*  
BSA: *bovine serum albumin*  
BTLA: *band T-cell lymphocyte attenuator*  
CCL2: *chemokine (C-C motif) ligand 2*  
CDDO-Me: *Methyl 2-cyano-3,12-dioxooleana-1,9(11)dien-28-oate, Bardoxolone methyl*  
CD40L: *CD40 ligand*  
C/EBP- $\beta$ : *CCAAT-enhancer binding protein- $\beta$*   
CIP: *cancer immunotherapy immunoguiding program*  
COX-2: *cyclooxygenase-2*  
CTL: *cytotoxic T lymphocyte*  
CTLA-4: *cytotoxic T-lymphocyte antigen 4*  
CXCL12: *chemokine (C-X-C motif) ligand 12*  
CXCR4: *chemokine (C-X-C motif) receptor 4*  
DC: *dendritic cell*  
ECM: *extracellular matrix*  
EDTA: *ethylenediaminetetraacetic acid*  
EGF: *epidermal growth factor*  
EGFR: *epidermal growth factor receptor*  
Egr2: *early growth response gene 2*  
ELISA: *Enzyme-Linked Immunosorbent Assay*  
ERK: *extracellular signal-regulated kinase*  
FBS: *fetal bovine serum*  
FcR: *Fc receptor*  
FLT3L: *FMS-like tyrosine kinase 3 ligand*

FMO: *fluorescence minus one*  
5-FU: *5-fluorouracil*  
G-CSF: *granulocyte-colony stimulating factor*  
GM-CSF: *granulocyte macrophage-colony stimulating factor*  
G-MDSC: *granulocytic MDSC*  
GvHD: *graft versus host disease*  
HDAC: *histone deacetylase*  
HHLA2: *HERV-H LTR-associating protein 2*  
HLA: *human leukocyte antigen*  
HNSCC: *head and neck squamous cell carcinoma*  
HRP: *Horseradish peroxidase*  
HS: *human serum*  
iBM-MDSC: *immature BM-MDSC*  
ICOS-L: *inducible costimulator ligand*  
iDC: *immature dendritic cell*  
IDO: *indoleamine 2 3-dioxygenase*  
Ig: *immunoglobulin*  
IL: *interleukin*  
IL4I1: *IL4 induced 1*  
IL4R $\alpha$ :  *$\alpha$  chain of IL-4 receptor*  
IL6st: *IL-6 signal transducer*  
IMDM: *Iscove's Modified Dulbecco's medium*  
INF- $\gamma$ : *interferon- $\gamma$*   
iNOS: *inducible nitric oxide synthase*  
ITSM: *immunoreceptor tyrosine-based swith motif*  
JAK: *Janus-activated kinase*  
KLRG-1: *killer cell lectin-like receptor subfamily G, member 1*  
LAG-3: *lymphocyte-activation gene*  
LAP\*: *liver-enriched activator protein*  
L-arg: *L-arginine*  
LCMV: *Lymphocytic choriomeningitis virus*  
L-cys: *L-cysteine*  
Lin: *lineage*  
LPS: *lipopolysaccharide*

mAb: *monoclonal antibody*  
MAPK: *mitogen-activated protein kinase*  
mBM-MDSC: *mature BM-MDSC*  
M-CSF: *macrophage-colony stimulating factor*  
MDSC: *myeloid-derived suppressor cell*  
MFI: *mean fluorescence intensity*  
MHC-I: *major histocompatibility complex*  
MMP9: *matrix metalloproteinase 9*  
MHC-II: *major histocompatibility complex-II*  
Mo-MDSC: *monocytic-MDSC*  
NK: *natural killer*  
NO: *nitric oxide*  
NOS: *nitric oxide synthase*  
NSCLC: *non-small cell lung cancer*  
OS: *overall survival*  
PBMC: *peripheral blood mononuclear cell*  
PBS: *phosphate buffered saline*  
PDGFR: *platelet-derived growth factor receptor*  
PDE-5: *phosphodiesterase type 5*  
PD-1: *programmed death-1*  
PD-L1: *programmed cell death-1 ligand*  
PD-L2: *programmed cell death-2 ligand*  
PGE2: *prostaglandin E2*  
PIAS: *protein inhibitor of activated STAT*  
PI3K: *phosphoinositide 3-kinase*  
PKC: *protein kinase C*  
PMSF: *Phenylmethylsulfonyl Fluoride*  
P-STAT3: *phosphorylated STAT3*  
PTEN: *Phosphatase and tensin homolog*  
PVDF: *polyvinylidene fluoride*  
RAGE: *receptor for advanced glycation end products*  
RANKL: *receptor activator of NF- $\kappa$ B ligand*  
RCC: *renal cell carcinoma*  
rh: *recombinant human*

ROS: *reactive oxygen species*  
RNS: *reactive nitrogen species*  
RPMI: *Roswell Park Memorial Institute medium*  
RT: *room temperature*  
SCF: *stem cell factor*  
SDS: *sodium dodecyl sulphate*  
SE: *standard error*  
SHIP-1: *SH2 domain-containing inositol phosphatase 1*  
SOCS: *suppressor of cytokine signalling*  
SSC: *side-scatter*  
STAT3: *signal transducer and activator of transcription 3*  
TAM: *tumor associated macrophage*  
TCR: *T cell receptor*  
TDF: *tumor-derived factor*  
TGF- $\beta$ : *tumor growth factor- $\beta$*   
Th: *T helper*  
TiDC: *tumor associated-iDC*  
TIL: *tumor-infiltrating lymphocytes*  
TIM-3: *T cell immunoglobulin and mucin-domain-containing molecule-3*  
TLR: *toll-like receptor*  
TNF: *tumor necrosis factor*  
Treg: *regulatory T cell*  
VEGF: *vascular endothelial growth factor*  
VEGFR: *vascular endothelial growth factor receptor*  
VISTA: *V-domain Ig suppressor of T-cell activation*

## ABSTRACT

One of the mechanisms used by cancer to evade the immune response is the expansion of myeloid-derived suppressor cells (MDSCs), a population of immature myeloid cells able to inhibit immune responses in cancer patients and experimental animals with neoplasia. The role of MDSCs in promoting tumor growth and metastasis has gained importance over the years, highlighting the need to find specific target of intervention that could be used in the treatment of cancer patients.

The aim of the present work was to analyze the signaling pathways active in MDSCs, using an *in vitro* model of MDSC generation developed by our group. Our previous studies revealed that the phenotype and suppressive ability of MDSCs were influenced by the presence of activated T cells, thus suggesting the existence of an interplay between the two populations. We therefore focused our attention on soluble molecules and surface markers mediating the interaction.

We demonstrated that IL-10 release is increased in the culture between MDSCs and activated T cells and that this cytokine leads to the activation of STAT3 both in myeloid and lymphoid cells. One of the targets of STAT3 is B7-H1, a molecule that can deliver an inhibitory signal to T cell, interacting with its receptor PD-1. We therefore analyzed the expression of B7-H1 on MDSCs and we found that it is up-regulated in the presence of activated T cells through a STAT3-dependent signaling. By analyzing the fate of suppressed T cells, we observed that they express at higher level two markers of T cell exhaustion, PD-1 and LAG-3. LAG-3 is a negative co-stimulatory receptor on T lymphocytes and the natural ligand of HLA class II, whose expression we found up-regulated in MDSCs after culture with activated T cells. These results thus suggest that the interplay between MDSCs and activated T cells could be mediated by the couples of receptor/ligand PD-1/B7-H1 and LAG-3/HLA class II, leading to T cell exhaustion.



## RIASSUNTO

Uno dei meccanismi utilizzati dalle cellule tumorali per evadere la risposta del sistema immunitario è costituito dall'espansione delle cellule soppressorie di derivazione mieloide (MDSC), una popolazione di cellule mieloidi immature capaci di inibire le risposte immunitarie nei pazienti con tumore e in modelli murini con neoplasie. Il ruolo delle MDSC nel promuovere la crescita tumorale e la metastatizzazione ha acquisito sempre maggiore importanza negli ultimi anni, evidenziando la necessità di trovare specifiche vie di segnalazione attive in queste cellule che possano diventare bersaglio di interventi terapeutici mirati nel trattamento dei pazienti con tumore.

Lo scopo di questo lavoro è stato quello di analizzare le vie di segnalazione attive nelle MDSC, utilizzando un modello sviluppato dal nostro gruppo per la generazione *in vitro* delle MDSC umane. I nostri studi precedenti hanno rivelato che il fenotipo e la capacità soppressoria delle MDSC sono fortemente influenzati dalla presenza dei linfociti T attivati, suggerendo l'esistenza di un'interazione tra le due popolazioni. Abbiamo quindi focalizzato la nostra attenzione su molecole solubili e marcatori di superficie che potrebbero essere coinvolti nell'interazione tra MDSC e cellule T attivate.

Abbiamo dimostrato che il rilascio di IL-10 è aumentato nelle colture tra MDSC e cellule T attivate e che questa citochina porta all'attivazione di STAT3 sia nelle cellule mieloidi che in quelle linfoidi. Uno dei bersagli di STAT3 è B7-H1, una molecola che può fornire un segnale inibitorio alla cellula T, interagendo con il suo recettore PD-1. Abbiamo pertanto analizzato l'espressione di B7-H1 sulle MDSC e abbiamo notato che essa è aumentata in presenza delle cellule T attivate, mediante una via di segnalazione dipendente dall'attivazione di STAT3. Analizzando il destino dei linfociti T soppressi, abbiamo osservato che essi esprimono ad alto livello due marcatori di "exhaustion" delle cellule T, che sono PD-1 e LAG-3. E' noto che LAG-3 è un recettore co-stimolatorio negativo sui linfociti T ed è il ligando naturale di molecole HLA di classe II, che sono

significativamente aumentate nelle MDSC dopo coltura con le cellule T attivate. Questi risultati pertanto suggeriscono che l'interazione tra le MDSC e le cellule T attivate potrebbe essere mediata dalle coppie di recettore/ligando PD-1/B7-H1 e LAG-3/HLA di classe II, portando ad "exhaustion" delle cellule T.

# INTRODUCTION

## 1.1 From immuno-surveillance to the theory of cancer immunoediting

The immunosurveillance theory, that was formally enunciated in 1957 by Burnet and Thomas, states that immune system can eliminate malignant cells before they develop into detectable tumors by recognizing and inactivating them through the existence of tumor antigens, molecules present on neoplastic cells able to elicit a protective immune response<sup>1-3</sup>. However, these data were criticized by part of the scientific community, as studies carried out subsequently on immunodeficient mice (nude mice) showed no higher incidence of tumor development, as compared to immunocompetent mice<sup>4,5</sup>. However, now it has to be acknowledged that there were several limitations in the experimental model, that could not be appreciated at that time. In fact, the nude mouse still possesses  $\alpha/\beta$  T cells and NK cells that could provide a reduced but significant cancer immunosurveillance ability. Only in the last 20 years, with the development of knock-out mice and transgenic technology and the possibility to produce highly specific monoclonal antibodies, the cancer immunosurveillance hypothesis was tested in molecularly defined immunodeficiency models and provided strong and convincing data. Further experiments revealed that the immune system exerts both host-protecting and tumor-sculpting effects on developing tumors. Therefore, the initial theory of cancer immunosurveillance was no more appropriate to describe the interaction between tumor and immune system, so Robert Schreiber and collaborators proposed to use the broader term “Cancer immunoediting” to describe more appropriately the dual role of the immune system that not only prevents, but also shapes neoplastic disease (reviewed in<sup>6</sup>). Cancer immunoediting can be considered as a result of three processes: elimination, equilibrium and escape (Figure 1), defined as the three “Es” of cancer immunoediting. The first phase, elimination, is the moment in which immunosurveillance occurs and the immune system is able to recognize and eliminate newly formed cancer cells. In the second phase, equilibrium, the Darwinian selection of tumor variants leads to the survival of the cancer cells endowed with low immunogenicity, that therefore have a better

chance to survive in the immunocompetent host. The alterations that occur during the immunologic sculpting of a developing tumor are probably facilitated by genetic instability of cancer cells. In this phase the tumor is not yet clinically apparent because the immune system is still able to control the growth of transformed cells. During the third phase of immunoediting, tumors become able to escape the immune control, to create an immunosuppressive tumor microenvironment and to grow in an uncontrolled manner becoming clinically relevant (reviewed in <sup>6</sup>). Work in the field of cancer immunoediting is now focusing on the study of the molecular mechanisms that drive the three processes and on the determination of the quality and quantity of tumor antigens expressed in newly transformed cells and that drive immune-mediated elimination and/or sculpting. This, in turn, should allow the development of new therapeutic strategies to facilitate the recognition and elimination of tumor cells by the immune system (reviewed in <sup>7</sup>).

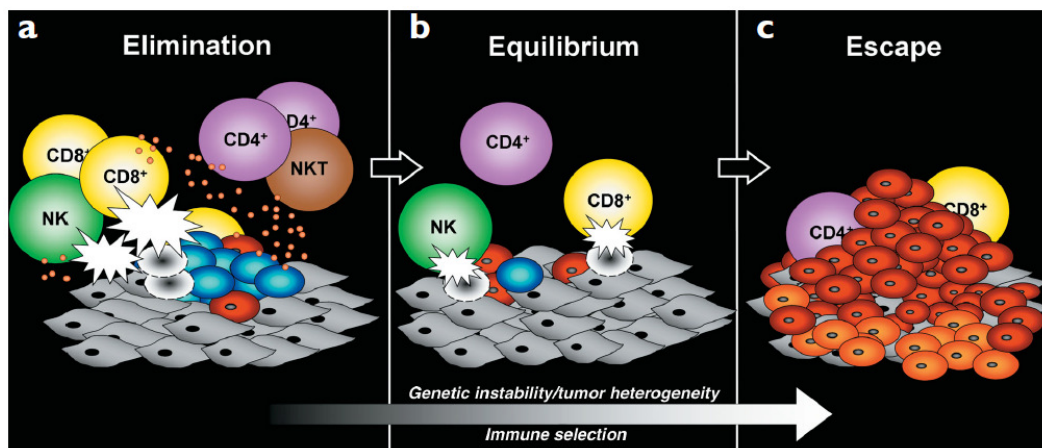


**Figure 1: The three phases of cancer immunoediting.**

The theory of cancer immunoediting comprises three processes. (a) Elimination corresponds to immunosurveillance. (b) Equilibrium is the phase in which immune system contains but not fully extinguishes tumor cells. During this process tumor variants with increased capacity to survive are selected. (c) Escape is the phase where selected tumor cells expand in an uncontrolled manner, avoiding the control of the immune system. In blue are represented developing tumor cells, in red tumor cell variants, in grey the stroma and nontransformed cells, in orange additional tumor variants. Taken from “Cancer immunoediting: from immuno-surveillance to tumor escape” (Dunn *et al*, Nature Immunology, 2002).

## 1.2 Tumor immune tolerance

In the last phase of cancer immunoediting, tumor cells are able to outgrow because they evade the control of the immune system. This is possible because during the equilibrium phase less immunogenic tumor variants are selected, but

also because tumor promotes a number of strategies that allow immune escape. One of these is represented by an impaired antigen presentation that can be due to down-regulation of the expression of tumor antigens<sup>8-10</sup>, or to reduced MHC-I expression that prevents recognition of tumor cells by the immune system<sup>11,12</sup>. Moreover, in some tumors, mutations of the antigen lead to an heterogeneity of tumor lesions that hinder the establishment of an efficient specific anti-tumor immune response<sup>13</sup>. Another strategy triggered by tumors is the production of immunosuppressive factors<sup>14,15</sup> that can be secreted by the malignant cells themselves or by other cells of the tumor microenvironment such as immune, epithelial or stromal cells. Among these factors there are TGF- $\beta$ , VEGF, prostaglandins, IL-10, macrophage-colony stimulating factor (M-CSF) and soluble tumor gangliosides (reviewed in<sup>16</sup>). IL-10 and TGF- $\beta$  can contribute, together with presentation of the tumor antigens by B cells to CD4<sup>+</sup> T lymphocytes, to the deviation from a Th1 response, that is required for efficient tumor rejection, toward a Th2 humoral response<sup>17,18</sup>. Also the production of indoleamine 2,3- dioxigenase (IDO), an enzyme that catalyzes the rate-limiting first step in tryptophan catabolism and overexpressed in response to IFN- $\gamma$  in a variety of different malignancies, has immunosuppressive properties; in fact, the depletion of tryptophan from the tumor microenvironment has been shown to inactivate effector T cells and to promote the conversion of dendritic cells to immunosuppressive (reviewed in<sup>19</sup>). Another strategy used by tumor to evade immune response concerns the change in expression of molecules that mediate apoptosis signalling, in order to avoid the killing mechanisms of the immune system. Moreover, tumors can adopt killing mechanisms proper of cytotoxic immune cells to delete the anti-tumor lymphocytes, a phenomenon called “tumor counter-attack” (reviewed in<sup>16</sup>). T cells can be neutralized by tumor cells because tumors express molecules with inhibitory effect on T lymphocytes, such as B7-H1 (reviewed in<sup>20</sup>), HLA-G<sup>21</sup> and HLA-E<sup>22</sup>, or through the induction of T cell anergy, a process that is induced when a T lymphocyte binds via its TCR to a peptide-MHC complex on the target cell without sufficient co-stimulation. Moreover, many tumors do not express costimulatory molecules and this may anergize anti-tumor T cells because of a lack of a proper co-stimulation signal (reviewed in<sup>16</sup>).

Through all these mechanisms tumor can modify its microenvironment, creating an immunosuppressive milieu where many cell types are present and whose phenotype and function can be changed in order to favor tumor growth. Among these cells there are tumor-associated macrophages (TAMs) that mostly resemble M2 macrophages because M2 polarizing cytokines, such as IL-4 and IL-13, are common in tumors, but have properties that do not fit in a rigid classification of M1 and M2 macrophages<sup>23</sup>. Their accumulation is associated with poor prognosis as they promote tumor growth, invasion, metastasis and angiogenesis through the release of cytokines, growth factors, extracellular-matrix (ECM) -degrading enzymes and angiogenic factors (reviewed in<sup>24</sup>). EGF or RANKL (receptor activator of NF- $\kappa$ B ligand) secreted by tumors are the major mechanisms by which TAMs stimulate tumor dissemination (reviewed in<sup>24</sup>). Similar to macrophages, tumor-associated neutrophils can be divided into N1 and N2 phenotypes able to respectively inhibit or promote cancer development. TGF- $\beta$  polarizes neutrophils towards a N2 phenotype<sup>25</sup> and these cells promote cancer by producing angiogenic factors and ECM-degrading enzymes<sup>26,27</sup> and by suppressing the antitumor immune response<sup>28</sup>. Mast cells infiltrate hyperplastic lesions in the skin of K14-HPV16 transgenic mice and invasive fronts of carcinomas where they release proteinases that stimulate fibroblast proliferation and induce angiogenesis via MMP9 activation<sup>29</sup>.

Moreover, tumor secreted VEGF can stimulate immature dendritic cells (iDCs) which are recruited from the bone marrow to the tumor site<sup>30</sup> where they are functionally modulated and referred to as tumor associated-iDC (TiDCs) that are resistant to apoptosis and express the immunosuppressive enzyme IDO<sup>31</sup>. Although TiDCs may capture tumour antigens derived from apoptotic cells and migrate to tumor-draining lymph nodes, they cannot present these antigens to naive T cells without amplification of co-stimulatory signals, resulting in immune tolerance<sup>32</sup>. TiDCs, together with other immune cells and tumor-derived factors, can also induce a population of regulatory T cells (Treg)<sup>33</sup>. Tregs are cells that normally play an indispensable role in the immune system as they are involved in the prevention of autoimmune diseases, allergies, infection-induced organ pathology, transplant rejection as well as graft versus host disease (GvHD) by suppression of effector T cells<sup>34</sup>, however they can also dampen immune responses against tumors<sup>35</sup>. Treg cells, together with myeloid-derived suppressor

cells (MDSCs), constitute one of the major player in tumor-induced immunosuppression.

### **1.3 Myeloid derived suppressor cells (MDSCs)**

Myeloid –derived suppressor cells (MDSCs) are an immature myeloid population that originates from myeloid precursors present in the bone marrow, but unable to develop into terminally differentiated subsets, such as macrophages, granulocytes and dendritic cells, therefore retaining an immature phenotype, and acquiring the ability to suppress innate and adaptive immunity<sup>36-38</sup>. The current hypothesis is that MDSC expansion in peripheral lymphoid organs and recruitment to the tumor site depend on tumor-derived factors (TDFs), which comprise a variety of biologically active compounds, including growth factors, cytokines and chemokines, structured in a complex pattern of expression and reciprocal crosstalk<sup>39</sup>. MDSCs, recruited during neoplastic growth, sustain tumor progression by providing a favourable microenvironment in which transformed cells can proliferate, acquire new mutations, expand and evade immunosurveillance. Moreover, MDSC subsets can take part in neoangiogenesis and metastatic spread<sup>39</sup>.

#### **1.3.1 Factors involved in MDSC expansion**

Tumor cells can induce the expansion of MDSCs by means of different TDFs, that not only mobilize MDSCs, but may also limit their maturation and differentiation, thereby contributing to their accumulation<sup>40</sup>. The difficulty in defining the crucial factors involved in MDSC recruitment is due to the fact that plasma cytokines and chemokines are different depending on the tumor type, resulting in tumor-dependent MDSC proliferation, sites of accumulation and infiltration (reviewed in<sup>41</sup>).

IL-6, IL-1 $\beta$ , granulocyte macrophage-colony stimulating factor (GM-CSF) and granulocyte-colony stimulating factor (G-CSF) found in the microenvironment of many tumors have been shown to significantly increase MDSC accumulation and T cell suppression (reviewed in<sup>42</sup>). Prostaglandin E2 (PGE2) induces differentiation of c-kit<sup>+</sup> hematopoietic stem cells into MDSCs, contributing to T

cell immunosuppression<sup>43,44</sup>. In addition, the pro-inflammatory proteins S100A8/A9 induce MDSC accumulation<sup>45</sup>. An autocrine positive feedback loop is created by MDSC secreting pro-inflammatory factors, including IL-6 and S100A8/A9, thus further sustaining themselves in the tumor microenvironment<sup>45,46</sup>. Tumor necrosis factor (TNF) impairs MDSC maturation by regulating the receptor for advanced glycation end products (RAGE) and its ligands (S100A8/A9)<sup>47</sup>. Other factors, such as VEGFA (reviewed in<sup>41</sup>), stem cell factor (SCF, also known as KIT ligand)<sup>48</sup>, FMS-like tyrosine kinase 3 ligand (FLT3L)<sup>49</sup> and M-CSF<sup>50</sup> have been shown to be secreted by tumors that stimulate MDSC proliferation. Also the complement system, in particular C5a, has been shown to be involved in MDSC expansion by attracting them or increasing their activity<sup>51</sup>. Among all these factors, on three of them there is strong evidence about their involvement in MDSC recruitment and expansion: GM-CSF, G-CSF and IL-6. In fact, it has been demonstrated that silencing GM-CSF in a mammary carcinoma model determined a reduction in the accumulation of MDSCs and in the systemic immunosuppression induced by this tumor<sup>52</sup>. GM-CSF also appears to assume a key role in MDSC expansion in cancer patients, since melanoma patients who received GM-CSF as an adjuvant, together with a vaccine, expanded an MDSC population which suppressed PBMC proliferation in a TGF- $\beta$  dependent fashion<sup>53</sup>.

The key role of G-CSF in regulating MDSC expansion is proved by the fact that it is present at high level in the sera of mice implanted with AT-3 and 4T1 mammary cancer and the treatment with anti-G-CSF mAb or down-regulation of G-CSF expression by RNA interference led to a significant reduction of MDSCs<sup>54</sup>.

Another group showed instead that IL-6 promoted tumor progression by enhancing the accumulation of MDSCs acting as downstream mediator of the IL-1 $\beta$  signaling, an established TDF that triggers MDSC generation<sup>55</sup>.

### **1.3.2 Murine MDSCs**

From the early observations in tumor-bearing mice, MDSC phenotype has been defined on the basis of the co-expression of CD11b and Gr-1 markers<sup>56,57</sup> and later as CD11b<sup>+</sup>/Gr-1<sup>+</sup>/IL4R $\alpha$ <sup>+</sup>/CD11c<sup>-</sup>/F4/80<sup>+/-58</sup>. However, such cells are not a

homogeneous cell population, and in fact, more recently, on the basis of Gr-1, Ly-6G, Ly-6C and CD49d expression, two main subsets were described: granulocytic, CD11b<sup>+</sup>/Gr-1<sup>hi</sup>/Ly-6C<sup>low</sup>/Ly-6G<sup>+</sup>/CD49d<sup>-</sup> MDSCs (G-MDSCs or PMN-MDSCs) and CD11b<sup>+</sup>/Gr-1<sup>int</sup>/Ly-6C<sup>hi</sup>/Ly-6G<sup>-</sup>/CD49d<sup>+</sup>, monocytic MDSCs (Mo-MDSCs) <sup>52,59,60</sup>. G-MDSCs suppress antigen (Ag)-specific CD8<sup>+</sup> T cells mainly by producing reactive oxygen species (ROS), while Mo-MDSCs act primarily by expressing nitric oxide synthase (NOS)2 and arginase (ARG)1 enzymes and generating reactive nitrogen species (RNS) <sup>61</sup>. The proportion of G-MDSCs and Mo-MDSCs is highly variable in different tumor models but the factors regulating their distribution are not entirely known. However, in most tumor models the majority of MDSCs in peripheral lymphoid organs are G-MDSCs but the ratio between G-MDSCs and Mo-MDSCs is much lower at tumor sites <sup>62</sup>.

### 1.3.3 Human MDSCs

MDSCs have been extensively studied in the last years given their role in breaking down the immune responses under many pathological conditions, including cancer. However, the fact that MDSC expansion in cancer patients can be induced by many different factors, depending on the tumor type but also on individual factors, and the lack of a cognate Gr-1 antigen in humans has led to the definition of many different MDSC subsets leading to a great heterogeneity (Table 1). However, three major subsets of MDSCs can be distinguished in cancer patients: monocytic MDSCs (Mo-MDSCs), granulocytic MDSCs (G-MDSCs), and immature MDSCs, although other myeloid subpopulations have been described <sup>63 41</sup>. Monocytic MDSCs are CD14<sup>+</sup> and granulocytic MDSCs express CD15, while both subsets express the common myeloid markers CD11b and CD33 <sup>64</sup>. Our group demonstrated the expansion of two MDSC subsets, one belonging to CD14<sup>+</sup> monocytes, the other to CD15<sup>+</sup> PMN, in the peripheral blood of melanoma and colorectal cancer patients. These subsets expressed the alpha chain of IL-4 receptor (IL4R $\alpha$ ) at higher levels as compared to the same cells isolated from healthy donors, but the presence of this marker positively correlated only with the immunosuppressive activity of monocytes, but not of granulocytes

<sup>65</sup>. These data are in agreement with a previous study in which it was demonstrated that IL4R $\alpha$  is a marker for murine MDSCs <sup>66</sup>.

Immature MDSCs are mainly defined as Lin<sup>-</sup>/HLA-DR<sup>-</sup>/CD33<sup>+</sup>/CD11b<sup>+</sup> <sup>67</sup>. Lineage (Lin) cocktail is a mixture of antibodies that contains markers progressively up-regulated during hematopoietic commitment. Lin thus allows the distinction of uncommitted cells (Lin<sup>-</sup>) from their more mature counterparts (Lin<sup>+</sup>).

More recently, a novel subset was added to MDSC family, documented in metastatic cancer patients. These cells were named F2 fibrocytes, because they bore the phenotypical and functional hallmarks of fibrocytes but were able to inhibit T cell response *via* indolamine 2,3 oxygenase (IDO) <sup>68</sup>.

Phenotype	Cancer Type	References
CD34 <sup>+</sup>	HNSCC	Pak et al (1995)
Lin <sup>-</sup> /HLA-DR <sup>+</sup>	Breast HNSCC	Almand et al (2001)
CD15 <sup>+</sup> granulocytes	NSCLC Breast Colon Pancreatic	Schielaue and Finn (2001)
CD11b <sup>+</sup> /CD14 <sup>-</sup> /CD15 <sup>-</sup>	Renal cell	Zea et al (2005)
CD14 <sup>+</sup> /Arginase <sup>+</sup>	HNSCC	Serafini et al (2006)
CD14 <sup>+</sup> /HLA-DR <sup>-</sup>	MM Melanoma	Filipazzi et al (2007)
CD11b <sup>+</sup> /CD33 <sup>+</sup>	NSCLC	Srivastava et al (2008)
Lin <sup>-</sup> /HLA-DR <sup>-</sup> /CD33 <sup>+</sup> /CD11b <sup>+</sup> §	Multiple solid tumors (Breast, esophageal, gastric, colorectal and other solid malignancies)	Solito et al (2011) Diaz-Montero et al (2009) Gabliss et al (2011)
Lin <sup>-</sup> /HLA-DR <sup>-</sup> /CD33 <sup>+</sup> †	Melanoma	Daud et al (2008)
CD11b <sup>+</sup> /CD14 <sup>-</sup> /CD33 <sup>+</sup> /CD15 <sup>-</sup>	NSCLC	Wang et al (2008) Liu et al (2010)
CD14 <sup>+</sup> /IL4R $\alpha$ <sup>+</sup>	Colon Melanoma	Mandruzzato et al (2008)
CD14 <sup>+</sup> /HLA-DR <sup>-</sup> /B7-H <sup>+</sup>	Melanoma	Wilcox et al (2008)
CD11b <sup>+</sup> /CD14 <sup>-</sup> /CD33 <sup>+</sup>	HNSCC	Corzo et al (2008)
CD11b <sup>+</sup> /CD13 <sup>-</sup> /CD34 <sup>+</sup> /CD14 <sup>-</sup> /CD45 <sup>-</sup>	Hodgkin lymphoma	Paninello et al (2009)
CD14 <sup>+</sup> /HLA-DR <sup>-</sup>	Melanoma	Poschke et al (2010)
DC-Sign <sup>+</sup> /CD80 <sup>+</sup> /CD83 <sup>+</sup>		
CD11b <sup>+</sup> /CD13 <sup>-</sup> /CD14 <sup>-</sup> /CD34 <sup>+</sup> /CD45 <sup>-</sup>	MM MGUS	Paninello et al (2009)
Lin <sup>-</sup> /HLA-DR <sup>-</sup> /CD33 <sup>+</sup> ‡	MDS	Wei et al (2009)
CD11b <sup>+</sup> /CD16 <sup>+</sup> /CD62L <sup>+</sup> /CD66b <sup>+</sup> /VEGFR1 <sup>+</sup>	Renal cell	Rodriguez et al (2009)
CD14 <sup>+</sup> /CD15 <sup>-</sup> /CD33 <sup>+</sup> /HLA-DR <sup>-</sup>	Bladder	Shepard et al (2010)
CD14 <sup>+</sup> /HLA-DR <sup>-</sup>	MM NHL	Brimnes et al (2010) Lin et al (2011)
SSC <sup>+</sup> /CD66b <sup>+</sup> /CD125 <sup>+</sup> /CD33 <sup>+</sup> /HLA-DR <sup>-</sup>	HCC Urothelial tract	Hochst et al (2008, 2009) Brandau et al (2011)
CD34 <sup>+</sup> /CD45 <sup>-</sup> /CD116 <sup>+</sup> /CD13 <sup>+</sup> /CD14 <sup>-</sup>	HNSCC NSCLC NHL	Pitini et al (2011)
CD11b <sup>+</sup> /CD15 <sup>+</sup> /CD33 <sup>+</sup>	Bladder	Eruslanov et al (2011)

<sup>\*</sup> -CD3, -CD4, -CD19 and -CD57.  
<sup>†</sup> -CD8, -CD14, -CD19, and -CD56.  
<sup>‡</sup> Lin not defined in the paper.  
<sup>§</sup> -CD3, -CD14, -CD16, -CD19, -CD20, and -CD56.  
 HCC indicates hepatocellular carcinoma; HNSCC, head and neck squamous cell carcinoma; MDS, myelodysplastic syndrome; MGUS, monoclonal gammopathy of undetermined significance; MM, multiple myeloma; NHL, non-Hodgkin lymphoma; NSCLC, non-small-cell lung cancer.

**Table 1.** Phenotype of MDSCs in human malignancies. Modified from “Myeloid-derived suppressor cells in cancer patients: a clinical perspective” (Montero et al., Journal of immunotherapy, 2012)

MDSC levels have been shown to correlate negatively with prognosis and overall survival (OS) in cancer patients and the accumulation of this population appears to contribute to tumor progression. Recently, human MDSCs have also been proposed as biomarkers associated to either survival or disease progression. However, the main difficulty of these studies depends on a lack of consensus on MDSC phenotype or, rather, on the increasing number of different phenotypes documented in several tumors of different origins <sup>63</sup>. Recently, by taking into account all the reported myeloid subsets endowed with suppressive activity, a recent study identified six human MDSC phenotypes (MDSC1-MDSC6) using a single multicolor staining: MDSC1 (CD14<sup>+</sup>/IL4R $\alpha$ <sup>+</sup>), MDSC2 (CD15<sup>+</sup>/IL4R $\alpha$ <sup>+</sup>), MDSC3 (Lineage<sup>-</sup>/HLA-DR<sup>-</sup>/CD33<sup>+</sup>), MDSC4 (CD14<sup>+</sup>/HLA-DR<sup>low/-</sup>), MDSC5 (CD11b<sup>+</sup>/CD14<sup>-</sup>/CD15<sup>+</sup>) and MDSC6 (CD15<sup>+</sup>/FSC<sup>low</sup>/SSC<sup>high</sup>) <sup>69</sup>. With the exception of MDSC1, all other MDSC subsets were significantly higher in RCC patients than in healthy controls. Furthermore, MDSC4 and MDSC5 subsets were negatively associated with overall survival of RCC patients treated with cyclophosphamide and IMA901, a multipeptide vaccine designed for RCC immunotherapy <sup>69</sup>.

Given the clear discrepancies in documenting human MDSC phenotype, a phenotyping proficiency panel, to which our group is actively participating, is ongoing under the guidance of the association of Cancer Immunotherapy Immunoguiding Program (CIP) in order to reach the harmonization of MDSC immunophenotyping across different groups. This will help to rearrange all the knowledge in the field and will also facilitate clinical application of MDSC screening.

#### **1.3.4 Mechanisms of action of MDSCs**

Over the years, several mechanisms have been described by which MDSCs are able to suppress T-cell responses. One of these involves the depletion of aminoacids such as L-arginine (L-Arg), L-cysteine and L-phenylalanine. The two major catabolic enzymes through which MDSCs metabolize L-Arg are arginase, that converts L-Arg into urea and L-ornithine, and NOS that which oxidizes L-Arg generating NO and citrulline. ARG1 and NOS isoforms were reported to be expressed by MDSCs (reviewed in <sup>70</sup>) and ARG1 was found up-regulated also in

plasma of cancer patients <sup>71</sup>. MDSCs were shown to play a role as L-cysteine consumers/sequesters since these cells import the aminoacid but do not express the transporter to release it in the extracellular milieu <sup>72</sup>. Moreover, human and mouse MDSCs can express IL4 induced 1 (IL4I1), a secreted L-phenylalanine oxidase that produces hydrogen peroxide (H<sub>2</sub>O<sub>2</sub>) and phenylpyruvate following oxidative deamination of phenylalanine <sup>66,73</sup>. Depletion of these aminoacids from the microenvironment is involved in immunoregulation since the lack of L-Arg causes an arrest of T cells in G0-G1 phase and the sequestration of L-cysteine inhibit T cell activation, proliferation and differentiation (reviewed in <sup>42</sup>). Both depletion of L-Arg and the metabolism of phenylalanine can lead to the production of H<sub>2</sub>O<sub>2</sub> that can inhibit CD3ζ chain expression and T cell proliferation <sup>73</sup>, effects mediated also by deprivation of L-arginine <sup>74</sup>. Production of reactive oxygen species (ROS), such as H<sub>2</sub>O<sub>2</sub>, is a mechanism that greatly affects immune regulation by inhibiting T cell proliferation. MDSCs can increase the presence of ROS in tumor microenvironment by the expression of NOX2, the catalytic subunit (also known as gp91phox) of NADPH oxidase <sup>75</sup> that reduces oxygen to superoxide anion using electrons supplied by NADPH <sup>76</sup>. Another mechanism involved in generation of ROS by MDSCs implies the co-expression of ARG and NOS2, in fact the limited availability of L-Arg produced by ARG induce NOS2 to produce superoxide anion. When superoxide anion interacts with NO, reactive nitrogen species (RNS) can be generated <sup>77</sup>. The latter are able to nitrate tyrosine residues in the TCR and CD8 receptors, thus resulting in a decreased recognition of peptide-MHC complexes by the TCR <sup>78</sup>. The importance of RNS in the tumor context was highlighted by a study in which it was demonstrated that CCL2, an inflammatory chemokine involved in the recruitment of both CTLs and myeloid cells to tumors, can be modified in the tumor microenvironment by RNS. Such alteration is a stable posttranslational modification, that changes CCL2 functional properties resulting in an impaired capacity of T cells to bind the modified chemokine. As a result, nitrated CCL2 loses its ability to recruit tumor-specific CTLs, while retaining its ability to attract myeloid cells to the tumor <sup>79</sup>. Concerning the role of transcription factors, our group demonstrated that the immunosuppression exerted by MDSCs depends on CCAAT-enhancer binding protein-β (C/EBP-β). In fact, silencing of this transcription factor by short-hairpin RNA allowed to restore the proliferation of activated T cells co-cultured with

silenced MDSCs<sup>80</sup>. Moreover, studies in murine models performed by our group recently demonstrated that the expression of LAP\*, one of the 3 isoforms of C/EBP- $\beta$ , can be regulated by miR-142-3p, by non-canonical binding to its 5' mRNA coding sequence. MiR-142-3p up-regulation decreased LAP\* expression, but also reduced the activation of STAT3. In fact, the canonical binding of the miRNA to the 3' UTR of IL6st decreased the expression of this protein, that is one of the subunits of the IL-6 cytokine receptor upstream of STAT3. Through the described mechanisms, miR-142-3p up-regulation reduced the immunosuppressive activity of MDSCs, by impairing their differentiation toward the monocytic-macrophage subset, that in mice is endowed with the strongest immunosuppressive activity<sup>81</sup>.

MDSCs can induce immunosuppression also by releasing IL-10. This cytokine, exerts several immunosuppressive effects: it drives the development of a Th2 response, can enhance Treg cell activity, inhibits TLR-induced IL-12 production by DCs and reduces DC-mediated activation of T cells<sup>58</sup>.

MDSCs isolated from gastric cancer patients were reported to secrete S100A8/A9 molecules, when cultured with activated T cells. Interestingly, addition in the culture of agents inhibiting the S100A8/A9 molecules and their receptor RAGE restored T cell function and proliferation in the cultures<sup>82</sup>.

Moreover, a recent work reported the expansion of CD14<sup>+</sup>/HLA-DR<sup>low/-</sup> MDSCs in patients who underwent allo-hematopoietic stem cell transplantation after hematological malignancies and the immunosuppression mediated by these cells depended on IDO expression, since IDO inhibition significantly enhanced T cell proliferation *in vitro*<sup>83</sup>.

Moreover MDSCs can indirectly induce immunosuppression through induction of Tregs expansion<sup>84</sup> and by converting anti-tumor M1 cells into tumor-promoting M2 cells by producing IL-10 and reducing macrophage production of IL-12 (reviewed in<sup>58</sup>).

### **1.3.5 MDSCs as a therapeutic target**

Given their clinical relevance in cancer patients, MDSCs become an interesting therapeutic target. MDSC inhibitors used so far in clinical studies for cancer patients can be divided into three classes according to their ability to: i) promote

MDSC differentiation into mature non-suppressive cells, ii) decrease MDSC levels, iii) functionally inhibit MDSCs (reviewed in <sup>42</sup>).

Promoting differentiation of suppressive MDSCs into mature, non-suppressive cells has been considered a way to neutralize immunosuppressive properties of MDSCs and enhance anti-tumor immune responses. All trans retinoic acid (ATRA), a derivative of vitamin A, has been shown to induce MDSC differentiation by a glutathione synthase dependent mechanism <sup>85</sup>. ATRA induced differentiation of MDSC into myeloid dendritic cells *in vitro* and *in vivo*, but it did not decrease tumor burden <sup>37</sup>. Better results were instead obtained combining ATRA with antigen specific peptide vaccines in two different tumor models <sup>86</sup>. In metastatic RCC patients with elevated MDSC levels, treatment with ATRA was effective in reducing MDSC number only when it reached a high plasma concentration (>150 ng/ml) <sup>87</sup>. Also treatment with vitamin D3 was shown to reduce the number of immunosuppressive CD34<sup>+</sup> cells in patients with HNSCC <sup>88</sup>. Sunitinib, an oral receptor tyrosine kinase inhibitor that targets signaling by PDGFRs, VEGFRs and c-kit and that was approved for the treatment of advanced RCC was shown to reduce MDSCs levels. In fact, sunitinib treatment of RCC patients augmented T cell response in association with a decrease in MDSC levels, including a reduction in the dominant population, G-MDSCs <sup>89</sup>. Additional studies in a mouse tumor model (4T1) indicate that sunitinib treatment may induce apoptosis in the granulocytic MDSC subset <sup>90</sup>. Other studies on a murine kidney cancer model (RENCA) showed that it may act through inhibition of STAT3 and of STAT3 regulated pro-angiogenic genes in MDSCs <sup>91,92</sup>.

Gemcitabine, a cytidine nucleoside analog, has been shown to decrease splenic MDSCs in murine models of five advanced lung cancer cell lines. An increase in the anti-tumor activity of CD8<sup>+</sup> T cells and in the activation of NK cells was noted, making this a promising MDSC targeting agent. Moreover, at specific time points after treatment, gemcitabine was shown to selectively induce MDSC's apoptosis <sup>93</sup>.

5-FU, a pyrimidine analog, is another chemotherapeutic agent that has shown selective anti-MDSC activity. In mouse tumor models, 5-FU showed efficacy in MDSC depletion by induction of apoptosis, leading to increased IFN- $\gamma$  production by tumor-specific CD8<sup>+</sup> T cells infiltrating the tumor and promoting T cell-dependent anti-tumor responses *in vivo* <sup>94</sup>.

Moreover VEGF over-production was reported in RCC cancer patients, so treatment of tumor bearing mice with anti-VEGF-1 mAb was performed and it was observed that it caused a reduction of MDSC levels. Unfortunately, the same effect was not reported in RCC patients treated with the antibody alone or in combination with IL-2<sup>95,96</sup>.

Phosphodiesterase type 5 (PDE-5) inhibitors, COX-2 inhibitors, CDDO-Me and nitroaspirin have been evaluated as functional inhibitors of MDSCs. In multiple murine tumor models treatment with PDE-5 inhibitors not only increased CD8<sup>+</sup> T cell intratumoral infiltration, but also dampened MDSC suppressive pathways through the down-regulation of ARG1, NOS2 and IL4R $\alpha$ . Interestingly, PDE-5 inhibitors restored T cell proliferation also in cancer patients<sup>97</sup>.

The enzyme cyclooxygenase 2 (COX-2) plays a role in the production of PGE-2, which induces MDSC expansion<sup>44</sup>. In a murine glioma model, treatment with COX-2 inhibitors inhibited systemic PGE-2 production and decreased MDSC level both in the bone marrow and the tumor microenvironment<sup>98</sup>. Moreover it was shown that PGE-2 attracts MDSC into the ascites microenvironment of ovarian cancer patients by inducing expression of CXCR4 in MDSCs and playing a role in the production of its ligand CXCL12, thus ensuring MDSC migration. In fact, MDSC frequencies closely correlated with CXCL12 and PGE-2 levels in ascitic fluid<sup>99</sup>.

CDDO-Me belongs to the class of synthetic triterpenoids and has been shown to up-regulate several antioxidant genes. Since production of ROS is a mechanism used by MDSCs, it was expected that this drug could have an effect on their activity. In fact, treatment of mice with this agent eliminated MDSC-mediated immunosuppression and CDDO-Me added *in vitro* to MDSCs isolated from RCC patients was able to inhibit their activity<sup>100</sup>.

Another compound able to interfere with the mechanisms of action of MDSCs is nitroaspirin, developed by coupling a NO-releasing moiety to aspirin. This drug is able to inhibit both NOS and ARG activity and to reduce the nitration of proteins within the tumor microenvironment. The immune stimulating effect of nitroaspirin however was evident only when it was combined with active immunotherapy<sup>101</sup>. As for nitroaspirin, other drugs showed enhanced activity when used in combination. The current strategies of cancer therapy in fact are

aimed to combine approaches that reduce MDSCs as an adjuvant to different forms of immunotherapy (reviewed in <sup>42</sup>).

### **1.3.6 *In vitro* induction of MDSCs from BM cells**

Our group demonstrated that MDSCs can be induced *in vitro* from human and murine bone marrow (BM) cells cultured with the combination of cytokines G-CSF+ GM-CSF and GM-CSF+ IL-6 <sup>80</sup>. CD11b and CD16 markers were used to evaluate the phenotypes of the cultures as they allow to distinguish the differentiation stages of myeloid cells because the expression of these two molecules increases with the progressive commitment of BM cells. The treatment of BM with the above mentioned cytokines, in particular with the combination G-CSF+GM-CSF, gave rise to a cell population with an heterogeneous pattern of maturation ranging from promyelocytes to mature granulocytes, but with a significant increase in more immature CD11b<sup>+</sup>CD16<sup>-</sup> cells as compared to other combinations of cytokines or untreated BM <sup>80</sup>. Moreover, BM cells treated with G-CSF+GM-CSF had the highest expression of IL4R $\alpha$ , that we demonstrated to be a marker of human MDSCs. We also evaluated the immunosuppressive activity of these cells and, as they were able to inhibit both mitogen-activated and alloantigen-stimulated T cells, we named them BM-derived MDSCs (BM-MDSCs) <sup>80</sup>. Our group also demonstrated that the immunosuppressive activity of BM-MDSCs is due to CCAAT-enhancer binding protein beta (C/EBP $\beta$ ) <sup>80</sup>, a transcription factor that controls emergency granulopoiesis induced by cytokines and infection <sup>102</sup>. Further characterization of the mechanisms of action of these cells revealed that BM-MDSCs can induce a significant reduction in the intracellular levels of CD3 $\zeta$  chain in co-cultured CD8<sup>+</sup> T cells <sup>103</sup>, moreover, the inhibitory effect on T cell proliferation was evident only in the presence of a cell-to-cell contact and the immunosuppressive capacity of BM-MDSCs is enhanced in the presence of strongly activated T lymphocytes <sup>103</sup>.

Since BM-MDSCs are a very heterogeneous population, we further characterized them by separating, through FACS sorting, three subsets at different stages of maturation, based on the expression levels of CD11b and CD16 antigens. Testing the immunosuppressive activity of these subsets, we observed that only the most

immature CD11b<sup>low/-</sup>/CD16<sup>-</sup> cell population (iBM-MDSCs) was able to block lymphocyte proliferation and to affect IFN- $\gamma$  production, while the other two subsets of BM-MDSCs were completely devoid of suppressive activity<sup>103</sup>. iBM-MDSCs had a morphology similar to that of promyelocytes, however, the same population isolated from fresh BM cells completely lacked suppressive activity. Flow cytometry analysis revealed that iBM-MDSCs did not express the monocytic marker CD14 while such cells expressed the CD15 granulocytic antigen<sup>103</sup>. Moreover, they were negative for lineage markers and expressed the myeloid marker CD33. Two discrete populations with different expression of HLA-DR (low or negative) were noted<sup>103</sup>. This phenotype was similar to that of MDSCs previously described in tumor-bearing patients<sup>67 104</sup>. Indeed, in the blood of patients with stage IV breast or colorectal cancer we could identify a Lin<sup>-</sup>/HLA-DR<sup>-</sup>/CD33<sup>+</sup>/CD11b<sup>+</sup> MDSC population resembling *in vitro*-generated BM-MDSCs and increased levels of these cells correlated with worse prognosis and radiographic progression<sup>103</sup>.

Further analysis of the suppressive subset of BM-MDSCs was performed after co-culture with either resting or activated T cells since the activation level of T lymphocytes appeared to be critical to drive the suppressive activity of BM-MDSCs. We observed that the presence of activated T cells was able to increase the proliferation of iBM-MDSCs and also to maintain their immature phenotype, as shown by the levels of expression of CD11b and CD16 markers (Figure 7). We also observed that the expression of the markers HLA-DR and CD34 were maintained or even increased, in the presence of activated T cells, while CD66b was down-regulated. Control cultures of immature BM-MDSCs alone or in the presence of resting T cells followed instead the default maturation program, thus highlighting that only the presence of activated T cells is able to block the differentiation process of iBM-MDSCs and suggesting the existence of an interplay between MDSCs and activated T cells (Figure 2)<sup>103</sup>.

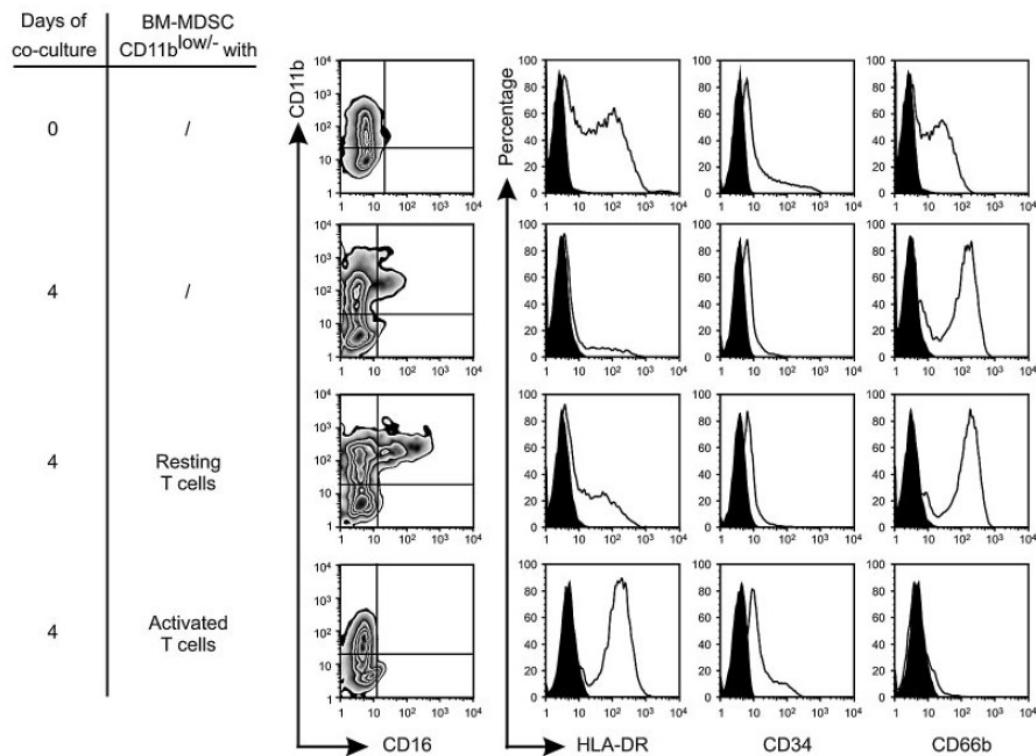


**Figure 2: T lymphocyte activation maintains the immature phenotype of iBM-MDSCs**

Flow cytometric evaluation of CD11b, CD16, HLA-DR, CD34 and CD66b markers in the immature subset of BM-MDSCs. Analysis was performed before and after the co-culture of iBM-MDSCs with either resting or anti-CD3/CD28-activated T cells. The expression of the markers was compared to the autofluorescence signal (black histogram). Taken from “A human promyelocytic-like population is responsible for the immune suppression mediated by myeloid-derived suppressor cells” (Solito et al, Blood, 2011).

#### 1.4 Signal Transducer and Activator of Transcription 3 (STAT3): a key factor in promoting tumor growth

STAT3 is implicated in a series of processes that favor tumor growth, as it is involved in cell proliferation and transformation, it suppresses apoptosis and can mediate cellular invasion, angiogenesis and metastasis and has a role in chemoresistance and radioresistance (reviewed in <sup>105</sup>). Moreover, it mediates tumor-induced immunosuppression at different levels, since STAT3 activity in tumor cells can negatively influence the expression of pro-inflammatory cytokines and chemokines <sup>106</sup> and inversely correlates with immune-cell migration *in vitro* and infiltration into tumours *in vivo* <sup>107</sup>. STAT3 activation in tumor cells negatively affects DC functional maturation by suppressing the expression of MHC-II and of co-stimulatory molecules and IL-12 secretion through the

production of IL-10 and VEGF that in turn activate STAT3 in DCs, leading to an arrest in their maturation <sup>106</sup>. Moreover, STAT3 signalling can inhibit immune stimulation in macrophages <sup>108</sup> and anti-tumor cytotoxic activity in NK and neutrophils <sup>109</sup>, while its activation in Treg cells is important for their proliferation and for the suppression of tumour-specific CD8<sup>+</sup> effector T cells <sup>109</sup>. A role for STAT3 was reported also in MDSCs expansion and activity. In fact, it was demonstrated that MDSCs isolated from tumor bearing mice have increased levels of phosphorylated STAT3, as compared to immature myeloid cells from healthy mice,<sup>110</sup> and that the expansion of MDSCs is abrogated when STAT3 is inhibited in hematopoietic progenitor cells <sup>111</sup>. Moreover, STAT3 can also induce the expression of S100A8/A9 in murine myeloid cells, molecules that induce MDSC accumulation and prevent their differentiation <sup>47</sup>. All these data highlight the importance of STAT3 signalling in tumor progression since it is activated in both tumors and tumor-infiltrating immune cells.

From the molecular point of view, STAT3 is a 92-kDa protein, 770 amino acids long with sequential N-terminal coiled-coil domain, DNA-binding domain, a linker, SH2 domain and C-terminal transactivation domain. The latter contains a tyrosine residue at position 705 and a serine residue at position 727, which undergoes phosphorylation when activated (Figure 3). STAT3 activation is driven by: i) many cytokines, such as IL-6 and IL-10; ii) growth factors, including G-CSF and GM-CSF; iii) oncogenic proteins such as Src and Ras (reviewed in <sup>105</sup>). The activation of STAT3 is regulated by receptor and non-receptor protein tyrosine kinases, such as epidermal growth factor receptor (EGFR) kinase, Src, Janus-activated kinases (JAK) and extracellular signal-regulated kinase (ERK) (reviewed in <sup>105</sup>), that phosphorylate STAT3 at Tyr705 in the cytoplasm leading to its dimerization, translocation into the nucleus, and DNA binding <sup>112</sup>; this, in turn, leads to the expression of genes that regulate cell proliferation, differentiation and apoptosis. Other serine kinases, including protein kinase C (PKC) and mitogen-activated protein kinases, have been implicated in the phosphorylation of STAT3 at serine 727, which maximizes its transcriptional activity <sup>105,113</sup>. Besides phosphorylation at sites within the carboxyl-terminal region, STAT3 is also acetylated on a single lysine residue 685 by histone acetyltransferase p300, a modification that can be reversed by type I histone deacetylase (HDAC) <sup>114</sup>. The acetylation of STAT3 is critical to form stable

dimers, which are required for cytokine-stimulated DNA binding and transcriptional regulation. STAT3 activation is instead negatively regulated through numerous mechanisms that include the suppressors of cytokine signaling (SOCS), protein inhibitor of activated STAT (PIAS), protein phosphatases and ubiquitination-dependent proteosomal degradation (reviewed in <sup>105</sup>).

STAT3 exists in two isoforms, the full length STAT3 $\alpha$  (92 kDa) and the truncated STAT3 $\beta$  (86 kDa), generated by alternative mRNA splicing in exon 23 <sup>115</sup>. STAT3 $\beta$  lacks the 55-residue C-terminal trans-activation domain, containing Ser727, that is substituted by a unique 7 residue sequence (CT7) whose function is still unknown <sup>116</sup>. However, it was demonstrated that, although STAT3 $\alpha$  has a greater transcriptional activity, STAT3 $\beta$  binds more efficiently to DNA, forms more stable dimers, due to the lack of the C-terminal acidic region, and has a more prolonged nuclear retention, likely due to its unique C-terminal domain, in addition to a reduced intranuclear mobility, especially upon cytokine stimulation <sup>116,117</sup>.

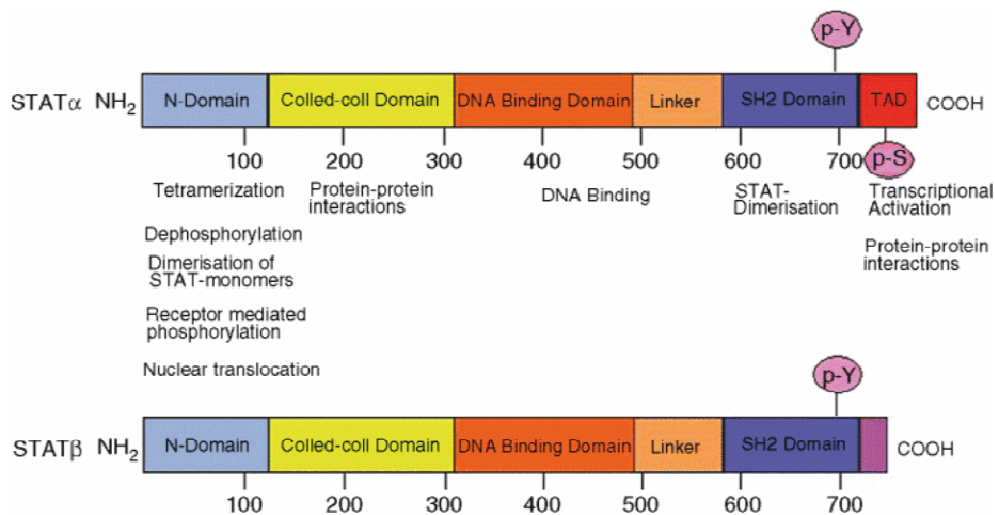


**Figure 3: Structure of STAT3  $\alpha$  and  $\beta$  isoforms.**

Modified from “Signal transducer and activator of transcription (STAT) signalling and T-cell lymphomas” (Mitchell and John, Immunology, 2005)

## 1.5 The B7- family of proteins: surface molecules involved in the modulation of immune response

The B7-family consists of structurally related, cell-surface proteins that regulate immune responses by interacting with their ligands expressed on the surface of T cells (Figure 4). Until today, nine family members have been identified that include CD80 (B7-1), CD86 (B7-2), CD274 (programmed cell death-1 ligand (PD-L1)/B7-H1), CD273 (programmed cell death-2 ligand (PD-L2)/B7-DC), CD275 (inducible costimulator ligand (ICOS-L)/B7-H2/B7RP-1/B7h), CD276 (B7-H3), B7-H4 (B7-S1/B7x) and B7-H6 (reviewed in <sup>118 119</sup>). The importance of B7- family members in regulating immune responses is due to their capacity to deliver co-stimulatory or co-inhibitory signals to T cells. In fact, the activation of T cells is induced upon the interaction of the TCR with the specific peptide/MHC, but requires also a second signal given by the antigen presenting cell (APC) (co-stimulation). When co-stimulation is not engaged and signaling occurs through TCR alone, a state of anergy or apoptosis is induced <sup>120</sup>. Besides these activatory signals, inhibitory co-stimulatory receptors promote negative stimuli and their balance influences T lymphocyte activation and the maintenance of peripheral tolerance <sup>121,122</sup>. If such balance is impaired, autoimmune conditions may arise <sup>123</sup>. Classically, CD80 and CD86 expressed on the surface of APC interact with the co-receptor CD28 that is constitutively expressed on the surface of T cells. The effect of CD28 ligation is to increase the level of proliferation and cytokine production, promote cell survival and enhance expression of CD40 ligand (CD40L) and adhesion molecules necessary for trafficking (reviewed in <sup>119</sup>). Limited expression of CD80 and CD86 on APCs is a mechanism for maintenance of peripheral T cell tolerance, ensuring that T cells activation can only be stimulated by appropriate cells <sup>124</sup>. After activation, T cells express CTLA-4, a close homologue to CD28, but with a higher affinity of binding to members of the B7 family <sup>125</sup>. CTLA-4 is an inhibitory membrane receptor expressed exclusively on T cells, where it primarily regulates the amplitude of the early stages of T cell activation, by competing with CD28 for binding to CD80 and CD86 (reviewed in <sup>126</sup>).

Another inhibitory receptor expressed by T cells is PD-1, a type 1 transmembrane glycoprotein of the Ig superfamily, with an extracellular domain showing 21-33%

sequence identity with CTLA-4, CD28 and ICOS molecule, but with distinct function and ligand specificity. Two ligands for PD-1 have been identified on the basis of similarity to other B7 superfamilies: PD-L1 and PD-L2, two type 1 transmembrane glycoproteins composed of IgC and IgV-type extracellular domains that present 40% amino acid identity (reviewed in <sup>127</sup>). PD-L1 is more broadly expressed on immune and non-hematopoietic cells, specifically it is constitutively expressed on T and B cells, macrophages and dendritic cells and it is upregulated upon stimulation by proinflammatory cytokines such as IFN. In contrast, PD-L2 expression is limited to the medullary region of the thymus and, at low level, on fetal myocardium and endothelial cells, while it is strongly expressed in placental endothelial cells <sup>128</sup>. PD-L2 can be induced on several cell types, such as DCs, peritoneal B1 B cells, macrophages, BM-derived mast cells and memory B cells (reviewed in <sup>129</sup>). Although PD-L1 expression is wider than that of PD-L2, PD-L2 can bind PD-1 with a higher affinity than PD-L1 and appears to have an additional, but yet unidentified receptor (reviewed in <sup>119</sup>). The concomitant binding of PD-1 by PD-L1 or PD-L2 during TCR activation induces blockade of B and T cell proliferation, secretion of cytokines, inhibition of cytolytic function and influences T cell survival (reviewed in <sup>129</sup>).

Another couple of receptor-ligand that can give co-stimulatory signals to T cells is constituted by ICOS, a CD28-like molecule expressed only on activated T cells, and ICOSL (also called B7-H2/B7RP-1/B7h), a protein with structural similarities to CD80/CD86 that, in fact, signals by binding to its receptor, but also *via* CD28. ICOSL is constitutively expressed by APCs and in non-haematologic tissues and is down-regulated with ongoing inflammation, in contrast to the activation-induced CD28 ligands (reviewed in <sup>118</sup>). Although involved in maintaining durable immune reactions, ICOS has a controversial role in T cell regulation, because it favours IL4/IL10/IL13 and humoral responses at the expense of IFN- $\gamma$ -mediated cytotoxic/Th1 responses. Moreover, it plays a role in maintaining immunosuppressive CD4<sup>+</sup> T cell subsets secreting more IL-10, and is an essential factor, together with FOXP3, for proper Treg development (reviewed in <sup>118</sup>).

B7-H3 protein can be expressed by dendritic cells and in several normal lymphoid and peripheral tissues <sup>130</sup>, but its expression was reported to be elevated also in numerous types of cancer <sup>131</sup>. However, the physiological and pathological role of B7-H3 is largely unknown. It was reported to be a co-stimulator of T cells,

promoting T cell proliferation and cytokine production<sup>132</sup>, but more recently B7-H3 was described as a potent inhibitor of T cell activity<sup>133</sup>. In contrast to these studies, Steinberg and colleagues suggested that B7-H3 has no characteristics of a co-signaling molecule and does not act as a regulator of immune responses<sup>134</sup>. Conflicting findings may be due to the existence of two isoforms of B7-H3: one with four Ig-like domains in the extracellular domain and one with two Ig-like domains in the extracellular domain due to alternative splicing<sup>135 136</sup>. The expression patterns of each isoform in tumors and the mechanism by which the two isoforms affect cancer progression remain unknown. However, Sun and colleagues recently reported a negative correlation both between the expression levels of B7-H3 and the survival time of patients with non-small cell lung cancer and (NSCLC) and between B7-H3 expression and the levels of tumor-infiltrating macrophages, suggesting a role in immunosuppression in cancer patients<sup>137</sup>.

B7-H4 was identified as a co-inhibitory member of the B7 family. In humans, B7-H4 mRNA is found in many organs, with little protein expression that can be induced in monocytes, macrophages and dendritic cells upon IL-6 and IL-10 stimulation<sup>138-140</sup>. B7-H4 transcripts and proteins are overexpressed in many solid tumors to varying extent (reviewed in<sup>20</sup>) and there is evidence that B7-H4 can promote tumor growth, although the mechanism of action and its receptor on T cells are still unknown<sup>141 142</sup>. A study revealed a dual role of B7-H4, because they confirmed the negative regulation on Th1- mediated antitumor immunity, but they also reported an inhibition of MDSCs, underlying the opposite effects of this molecule on immune system<sup>143</sup>.

A recent study has described HERV-H LTR-associating protein 2 (HHLA2) as a member of the B7 family that shares 10-18% amino acid identity and 23-33% similarity to other human B7 proteins and phylogenetically forms a subfamily with B7-H3 and B7-H4<sup>144</sup>. It is the only molecule that is expressed in humans, but not in mice, in particular it is constitutively present on the surface of monocytes and it is induced on B cells after stimulation with LPS and IFN- $\gamma$ . HHLA2 does not interact with other members of the family, but binds a putative receptor expressed on T cells and APCs, inhibiting T cell proliferation and cytokine production.

Another member of the family is B7-H6, a PD-L1/B7-H3 homologue that specifically binds the NK-effector molecule Nkp30, leading to NK activation. B7-H6 is not expressed in any normal tissue, but it is present in a variety of

primary tumors and cell lines <sup>145</sup> and its expression was reported to be dependent on histone deacetylase 3 (HDAC3), thus suggesting a new potential strategy for cancer treatment <sup>146</sup>.

Besides the molecules listed before, there are also newer potential members of the B7 family, that have been identified *via in silico* screening over the last few years. One of these is V-domain Ig suppressor of T-cell activation (VISTA) that is primarily expressed on hematopoietic cells and highly upregulated on APCs and CD4<sup>+</sup> T cells. Data show that a soluble VISTA-Ig fusion protein or VISTA expression on APCs inhibits T cell proliferation and cytokine production. Moreover, overexpression of this molecule on tumor cells interferes with protective antitumor immunity *in vivo* in mice, thus suggesting that it could have a role in immune suppression in cancer <sup>147</sup>.

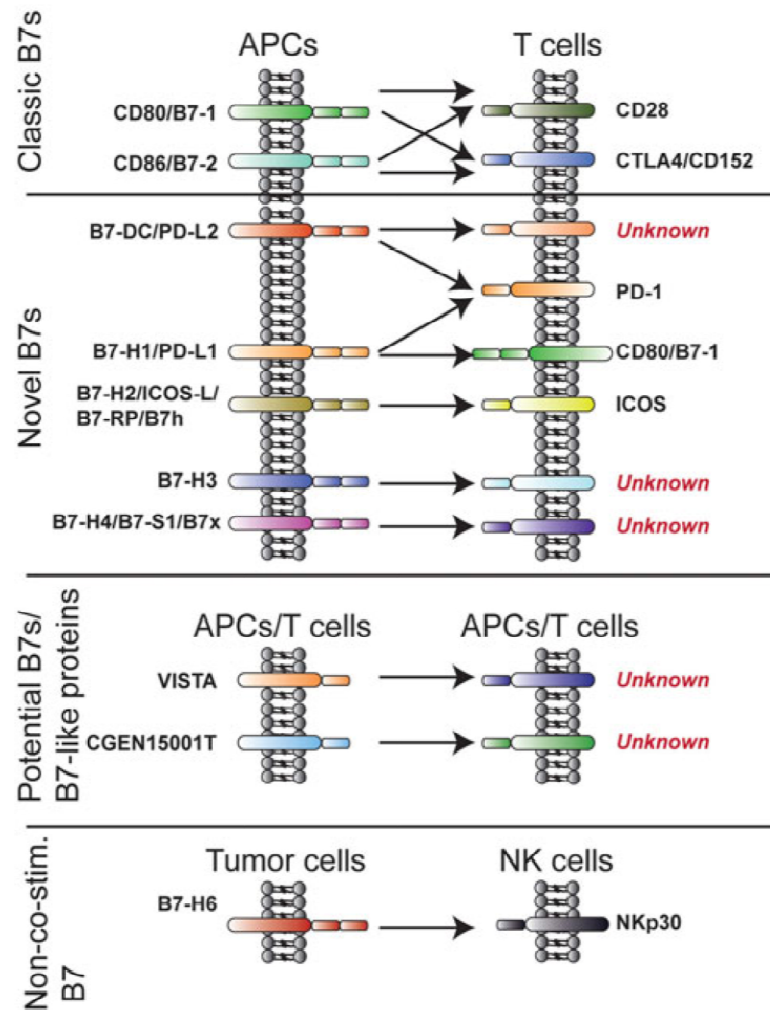


**Figure 4: B7/CD28 family members**

B7 family proteins provide co-stimulatory and co-inhibitory signals to T cells. This is classically illustrated by CD80/CD86-CD28 interaction, that delivers a co-stimulatory signal, in comparison to CD80/CD86-CTLA-4 interaction that instead delivers a co-inhibitory signal. Other B7 family members have been identified that are PD-L1, PD-L2, ICOSL, B7-H3 and B7-H4 with activating or inhibiting functions on T cells. Besides these molecules, there are also newly described potential family members like V-domain IG suppressor of T-cell activation (VISTA) and Cgen-1500T. B7-H6 is expressed by tumor cells and interacts with NKp30 on NK cells. Taken from “Targeting the B7 Family of Co-Stimulatory Molecules: successes and challenges” (Podojil and Miller, BioDrugs, 2013).

## 1.6 Functional role of PD-1/PD-L1 interaction in tumors

The discoveries that PD-L1 is constitutively expressed in many human cancers and that PD-1 is expressed in TILs (reviewed in <sup>127</sup>) have highlighted the possible role that these molecules could have in the induction of tumour tolerance. In fact, the interaction of PD-L1 with its receptor PD-1 on T cells causes an impairment of T cell function through induction of apoptosis, anergy or exhaustion (reviewed

in <sup>20</sup>), inhibition of T-cell cytokine release, such as IFN- $\gamma$ , IL-4, and IL-2 (reviewed in <sup>129</sup>), thereby inducing the production of the immunosuppressive cytokine IL-10. PD-1/PD-L1 interaction can also influence Treg generation and their suppressive properties <sup>148</sup>. Moreover, PD-L1 was reported to be involved in MDSC mechanism of action and in their crosstalk with T reg cells <sup>149</sup>. All these mechanisms favour the formation of an immunosuppressive milieu that thus facilitates tumor progression. In fact, PD-L1 expression on TILs was significantly associated with poor prognosis in renal cell carcinoma patients <sup>150</sup>, a result confirmed also in patients with oesophageal, gastric and ovarian cancers (reviewed in <sup>20</sup>) and some reports have shown that PD-L1 expression on tumour cells can be associated with decreased numbers of TILs in cancer patients. These observations opened the possibility to interfere with PD-L1 signalling by blocking the interaction with its receptor. Two large clinical trials of anti-PD-1<sup>151</sup> and anti-PD-L1 neutralizing antibodies <sup>152</sup> showed that blocking these immunoregulatory proteins induced durable tumor regression and prolonged disease stabilization in patients with selected advanced cancers, including NSCLC, a tumor considered to be non-responsive to immunotherapy.

## **1.7 T cell anergy, exhaustion and senescence in tumor microenvironment**

The phenotype and functional profile of effector T cells in cancer are dramatically altered by the tumor microenvironment. Three different processes of T cell impairment can be distinguished on the basis of functional state of the cell: T cell anergy, exhaustion and senescence.

T cell anergy is generally described as the induced hyporesponsive state with low IL-2 production and cell cycle arrest at the G<sub>1</sub>/S phase, to which naïve T cells fall upon low co-stimulatory and/or high co-inhibitory stimulation. Under physiological conditions T cell anergy functions to induce tolerance in the periphery and protects the host from developing autoimmune disease, however there are evidences that this mechanism plays an important role also in the context of tumor microenvironment (reviewed in <sup>153</sup>). One of the mechanisms is due to the expression of B7-family members by tumor cells and immune cells, accompanied

by a low or absent expression of B7-1 and B7-2, thus indicating a poor co-stimulatory and high co-inhibitory signals. However, cellular and molecular mechanisms controlling T cell anergy are still insufficiently understood. Early growth response gene 2 (Egr2) may be a central transcription factor that regulates T cell anergic state <sup>154</sup> and it has been suggested that the anergy program is initiated by improper mTOR and Ras/MAPK signalling, a pathway that lies directly downstream of TCR/CD28 engagement <sup>155,156</sup>. Moreover, the E3 ubiquitinating ligase family can affect PI3K, mTOR and Ras/MAPK pathways actively maintaining anergy and epigenetic factors such as IKAROS and Sirt1 are involved in histone modifications that promote T cell anergy (reviewed in <sup>153</sup>). Thus, anergy is the combined result of negative regulation of TCR-coupled signal transduction and of a program of active transcriptional silencing reinforced through epigenetic mechanisms <sup>157</sup>. The incomplete knowledge of the molecular mechanisms involved in the process has hindered also the definition of specific markers for anergic T cells, that are thus difficult to characterize.

T cell exhaustion occurs when T cells are chronically activated at sites of chronic inflammation, such as cancer, autoimmunity and chronic infection. One of main features of T cell exhaustion, is the loss of function of CD8<sup>+</sup> and CD4<sup>+</sup> T cells, that gradually leads to dysfunctional T cells. Exhausted T cells are described as effector T cells with decreased cytokine expression, decreased effector functionality and resistant to reactivation <sup>158</sup>. Exhausted T cells are marked by the expression of inhibitory receptors that have a key role in this process. Initial mouse studies have proposed that B7-H1/PD-1 signalling pathway mediates CD8<sup>+</sup> T cell functional exhaustion in the context of chronic infection and PD-1 was proposed as marker for exhausted T cells <sup>159</sup>. The observation that tumoral cells and APCs in tumor microenvironment express B7-H1 and that TILs express PD-1 has revealed that the axis B7-H1/PD-1 can be involved in T cell exhaustion also in tumor context. The detailed molecular mechanism of T cell exhaustion is still incompletely defined but it was suggested that recruitment of protein tyrosine phosphatases, such as SHP-1 and SHP-2, to the immunoreceptor tyrosine-based switch motif (ITSM) within the PD-1 cytoplasmic tail inhibits signalling events downstream of the TCR <sup>160</sup>. Other studies done with the aim to better characterize PD-1<sup>+</sup> T lymphocytes have revealed that these cells express on their surface T cell immunoglobulin and mucin-domain-containing molecule-3 (Tim-3), lymphocyte-

activation gene (LAG)-3, and the Band T-cell lymphocyte attenuator (BTLA, CD272), 2B4 (CD244), CTLA-4, CD160 (reviewed in <sup>153</sup>). However, it is still controversial if the co-expression of these inhibitory molecules is functionally important to determine T cell functional state (reviewed in <sup>153</sup>).

Another mechanism of T cell functional impairment is T cell senescence. Senescent T cells are characterized by telomere shortenings, phenotypic change (loss of CD28 expression) and cell cycle arrest <sup>161</sup>. Senescent T cells manifest defective killing abilities and the development of negative regulatory functions <sup>162</sup>. Senescence is naturally associated with physiological ageing, however it was demonstrated that it can be induced *in vitro* by tumor cells <sup>163</sup>. Phenotypically, senescent CD28<sup>dim/-</sup> CD8<sup>+</sup> T cells are observed in patients with lung cancer <sup>164</sup> and head and neck cancer <sup>165</sup>. In addition to low expression of CD28, high expression of Tim-3, CD57, killer cell lectin-like receptor subfamily G, member 1 (KLRG-1) are thought to be associated with T cell senescence (reviewed in <sup>153</sup>). Concerning the molecular mechanisms, it is known that Tim-3 interacts with its ligand Galectin-9 that, in turn, induces intracellular calcium flux, aggregation and death of Th1 cells <sup>166</sup>. An involvement of human leukocyte antigen (HLA)-B-associated transcript 3 (BAT3) was also postulated, but how the interaction between TIM-3 and Bat3 leads to T cell senescence remains to be elucidated <sup>167</sup>.

## 2. AIM OF THE PROJECT

Among the mechanisms carried out by tumor cells to evade immune response, a key role is played by the expansion of MDSCs, an heterogeneous population of immature myeloid cells able to inhibit both innate and adaptive immunity in mouse tumor models and in cancer patients. Of note, it was demonstrated that MDSC's levels correlate with tumor burden and are associated to poor efficacy of immunotherapy strategies in cancer patients. However, the molecular mechanisms involved in MDSC activity are still poorly understood.

We previously demonstrated that MDSCs can be derived *in vitro* by treating fresh BM cells with the cytokines G-CSF and GM-CSF and we observed that the activation state of T lymphocytes is able to influence the phenotype and proliferation of MDSCs, thus suggesting the existence of a crosstalk between MDSCs and T cells. We therefore evaluated the molecules potentially involved in the interaction with activated T cells.

In particular, we focused our attention on the role of IL-10, a cytokine known to have immunosuppressive properties, studying if this cytokine is increased in the process of immunosuppression mediated by MDSC.

We also studied the role of the transcription factor STAT3, since it can be activated by G-CSF, GM-CSF and IL-10 and it is involved in MDSC expansion.

Since immunosuppression mediated by MDSCs is dependent on cell-to cell contact with activated T cells, we investigated the expression on MDSCs and on T cells of ligands and receptors that can mediate inhibitory pathways leading to an impairment of T cell function.

Finally, we started to evaluate the findings obtained with our *in vitro* model of immune suppression, by analysing the presence of MDSCs and T lymphocytes in liver metastases from colorectal cancer patients to determine if the molecular mechanisms discovered *in vitro* are active also *in vivo*.



### **3. MATERIALS AND METHODS**

#### **3.1 BM samples**

Fresh BM aspirate samples were received from the Department of Woman and Child Health, University of Padua. These samples were obtained from patients with suspected leukemia or lymphomas, patients with lymphatic leukemia after 78 days without recurrences, and patients with lymphatic leukemia after BM transplantation as a part of the diagnostic follow-up. For this study only samples with normal cytological characteristics were used. The project was approved by Ethics Committee and all patients gave their informed consent.

#### **3.2 BM-MDSC generation and separation of BM-MDSC subsets**

Red blood cells present in BM aspirates were lysed with a hypotonic solution containing  $\text{NH}_4\text{Cl}$  0.15 M (Sigma-Aldrich),  $\text{KHCO}_3$  0,01 mM (Analytical Carlo Erba), Ethylenediaminetetraacetic acid (EDTA) 0,1 mM (Sigma-Aldrich) at room temperature (RT) for 5 minutes. The obtained cells were washed, counted and labeled with immunomagnetic beads anti-CD3 $\epsilon$ , CD19 and CD56 (Miltenyi Biotec) in order to deplete T, B and NK lymphocytes, respectively. Immunomagnetic beads were added to the cell pellet in a quantity of  $20\mu\text{l}/10^7$  cells, in a total volume of  $100\mu\text{l}/10^7$  cells of cold Buffer Sorting, composed of phosphate buffered saline (PBS) (LONZA) additioned with 0, 5% Bovine Serum Albumin (BSA, SIGMA) and 2mM EDTA (Sigma-Aldrich). Cells were then incubated for 15 minutes at 4°C, stirring a few times. Cells were then washed and subjected to immunomagnetic negative separation with LD column (Miltenyi Biotec) following manufacturer's instructions. Negative fraction was subsequently washed and resuspended in Iscove's Modified Dulbecco's Medium (IMDM, GIBCO, Life Technologies) supplemented with 10% Fetal Bovine Serum (FBS, GIBCO, Life Technologies), 0.01M HEPES (LONZA), 10 U/ml penicillin/streptomycin (LONZA), Arginine 0,55 mM (Sigma-Aldrich), Asparagine 0,24 mM (Sigma-Aldrich) and Glutamine 1,5 mM (Sigma-Aldrich) and  $\beta$ -mercaptoethanol (Sigma-Aldrich). Cell purity was checked by FACS analysis on forward scatter/side scatter parameters with a FACSCalibur cytometer (BD Biosciences).

Lymphocyte-depleted BM cells were cultured in 24-multiwell plates at a concentration of  $1 \times 10^6$  cells/ml with 40 ng/mL of recombinant human (rh) G-CSF (Miltenyi Biotech) and rh-GM-CSF (Miltenyi Biotech) for 4 days at 37°C, 8% CO<sub>2</sub>, in order to expand BM-MDSCs, following the protocol previously published<sup>80</sup>. After the treatment with rh G-CSF+GM-CSF, BM-MDSCs were harvested, washed and depleted of the mature CD11b<sup>+</sup> fraction with immunomagnetic anti-human CD11b beads (Miltenyi Biotec), using LD columns (Miltenyi Biotech). The purity of CD11b<sup>low/-</sup> (iBM-MDSCs) and of CD11b<sup>+</sup> (mBM-MDSCs) cells obtained from BM-MDSCs was checked by staining both fractions with anti-CD16 FITC (BD Pharmingen) and anti-CD11b PE (Beckman Coulter) antibodies.

### **3.3 Proliferation assay**

Peripheral Blood Mononuclear cells (PBMCs) were isolated from peripheral blood of healthy donors by density gradient centrifugation on Ficoll-Paque PLUS (GE Healthcare-Amersham). Peripheral blood was diluted 1:3 in PBS, stratified on Ficoll-Paque PLUS and centrifuged 30 minutes at 1800 rpm at 20°C. After centrifugation, PBMCs were aspirated, washed 3 times with PBS 1% human serum type AB (HS) (LONZA), and stored in liquid nitrogen. At the moment of the experiment, PBMCs were thawed and stained with CellTrace Violet Cell Proliferation Kit (Molecular Probes). For the staining, PBMCs were resuspended in PBS at  $2 \times 10^7$  cells/ml and incubated with CellTrace at a final concentration of 1 μM for 5 minutes at 37°C. Then FBS was added at a dilution of 1:5 of the total volume. Cells were washed and then plated for 30 minutes at 37°C, 8% CO<sub>2</sub> in a 24 well plate. CellTrace-labelled PBMCs were then washed again and plated in a 96-well flat-bottom plate previously coated with 0,5 μg/ml anti-CD3; 5 μg/ml soluble anti-CD28 (BioLegend) were added to the culture as co-stimulus. i-BM-MDSCs and mBM-MDSCs were co-cultured with stimulated PBMCs at 1:1 ratio for 4 days at 37°C and 5% CO<sub>2</sub> in arginine-free Roswell Park Memorial Institute medium (RPMI, Biological Industries), supplemented with 150μM arginine, 10% FBS (Biowhittaker), 10 U/ml penicillin/streptomycin, and HEPES. Anti-IL-10 (Biolegend), anti-PD-1 (Miltenyi Biotech) and anti-B7-H1 (eBioscience) blocking antibodies were added to the co-cultures of activated T cells and iBM-MDSCs in

a concentration of respectively 10 µg/ml, 1 µg/ml and 1 µg/ml. Stattic, the inhibitor of the Tyr-705 phosphorylation of STAT3, was used at the concentration of 5 µM to pre-treat iBM-MDSCs for 30 minutes at room temperature before adding them to the co-culture with activated T cells.

At the end of the cultures, cells were harvested and stained with anti-CD3 PE-Cy7 (Beckman Coulter) antibody. Before acquisition, cell suspensions were transferred into TruCount™ tubes (BD Biosciences), in order to determine the absolute cell number of CD3<sup>+</sup> cells in the samples. Data acquisitions were performed on LSRII flow cytometer (BD Bioscience). Proliferation of CD3<sup>+</sup> CellTrace<sup>+</sup> T cells was evaluated both qualitatively and quantitatively, by assessing the signal of CellTrace on CD3<sup>+</sup> cells. The extent of T cell proliferation was quantified, analyzing the percentage of proliferating cells from generation 3 to generation 10, assumed to be 100% without BM-MDSCs. In addition, it was evaluated the ratio between the absolute number of CD3<sup>+</sup>CellTrace<sup>+</sup> cells co-cultured with BM-MDSCs and the number of the same cells stimulated in the absence of BM-MDSCs.

### **3.4 Flow cytometric analysis of BM-MDSCs and activated T cells**

The phenotype of BM-MDSCs and activated T cells alone or in co-culture was evaluated by flow cytometry using anti-B7-H1 PE (eBioscience), anti-B7-H2 PE (BioLegend), anti-B7-H3 PE (BioLegend), anti-CD33 APC (BD Bioscience), anti-CD3 PE-Cy7 (Beckman Coulter), anti-CD8 APC-H7 (BD Bioscience), anti-LAG3 FITC (AdipoGen), anti-PD1 PE (Miltenyi Biotec). For the staining, approximately 10<sup>5</sup> cells were washed and incubated with Fc Receptor (FcR) Blocking Reagent (Miltenyi Biotec) for 15 minutes and then labelled with monoclonal antibodies (mAbs) for 20 minutes on ice. Cells were then washed and resuspended in 250 µl of cold HCF(137 mM NaCl, 5 mM KCl, 0.3 mM Na<sub>2</sub>HPO<sub>4</sub>, 0.7 mM KH<sub>2</sub>PO<sub>4</sub>, 0.4 mM MgSO<sub>4</sub>, 0.3 mM MgCl<sub>2</sub>, 5 mM glucose, 4 mM NaHCO<sub>3</sub>, 1mM EDTA) supplemented with 1% FBS and then analysed on either a FACSCalibur (BD Bioscience) or LSRII cytometer (BD Bioscience). To determine the percentage of apoptotic and early apoptotic cells, after the staining with anti-CD3 PE-Cy7, cells were washed with HCF, resuspended in 100 µl of Annexin V binding buffer (BioLegend) and incubated with Annexin V Alexa 647

(BioLegend) plus 7AAD (eBioscience) for 15 minutes at RT. Samples were then supplemented with additional 200 µl of Annexin V binding buffer and immediately analysed by FACSCalibur. Data were elaborated using FlowJo software (Tree Star Inc.) version 7.2.5

### **3.5 Analysis of IL-10 production**

The supernatants of cell cultures of BM-MDSCs and activated T cells were harvested after 4 days of culture, centrifuged at 2000 rpm for 6 minutes at 4°C and stored at -80°C. The concentration of IL-10 was determined by ELISA Ready-SET-Go (eBioscience), following manufacturer's instruction. Briefly, 96-well plates were coated over-night with 100 µl/well of anti-IL10 capture antibody, then washed 3 times with a washing buffer composed of PBS 0,05% Tween20 (Sigma-Aldrich) and incubated for 1 hour with a saturating solution. After 3 washes, properly diluted supernatants and IL-10 standards were added to the plate and incubated for 2 hours at RT. The plate was then washed 3 times and 100 µl/well of anti-IL10 biotinylated antibody were added for 1 hour. Other 3 washes were performed and then wells were filled with 100 µl of avidin-horseradish peroxidase (HRP) and plate was incubated for 30 minutes at RT. After 3 washes, 100 µl/well of HRP substrate were added. The enzymatic activity of HRP was stopped after 15 minutes by adding sulphuric acid. The plate was then analysed by Victor X4 plate reader (Perkin Elmer).

To determine which cells were responsible of IL10 production, we performed IL-10 secretion assay (Miltenyi Biotech) on activated T cells alone or in the presence of iBM-MDSCs. PBMCs cultured with or without 100 ng/ml of LPS for 14 hours were used as positive and negative control, respectively. Cells were harvested, washed with a buffer containing PBS 0.5% BSA, 2mM EDTA and incubated 5 minutes on ice in a mixture of catch reagent and FcR blocking solution. A large amount of warm RPMI 3% HS was added to dilute cells that were incubated for 45 minutes at 37°C stirring the tubes every 5 minutes to prevent contact of cells which would lead to cross contamination with cytokines. At the end of incubation, the cells were washed twice by filling up the tubes with cold buffer, and centrifuging them at 1700 rpm for 10 minutes at 4°C. LPS-stimulated or unstimulated PBMCs were subsequently incubated with IL-10 Detection

Antibody PE, anti-CD14 APC (BioLegend), anti-CD3 PECy7 (Beckman Coulter) for 10 minutes on ice, while MDSC/T cell co-culture were labelled with anti-IL-10 Detection Antibody PE, anti-CD33 APC (BD Bioscience), anti-CD3 PECy7 (Beckman Coulter). Cells were washed and immediately analysed by LSRII flow cytometer.

### **3.6 Protein extraction and Western Blot analysis**

After immunomagnetic sorting, iBM-MDSCs and mBM-MDSC fractions were stored for Western Blot analysis. About  $10^6$  cells were washed with PBS, resuspended in 500 $\mu$ l of PBS plus 1% Protease Inhibitor Cocktail (Calbiochem) and centrifuged for 6 minutes, at 4°C, 2000 rpm. The supernatant was discarded and pellet was stored at -80°C.

Nuclear and cytoplasmic protein fractions were obtained using NE-PER Nuclear and Cytoplasmic Extraction Reagents (Thermo Scientific). The frozen pellet was thawed in the presence of 50  $\mu$ l of ice-cold CERI reagent, supplemented with 1:10 Protease Inhibitor Cocktail, 50 mM NaF, 1 mM Na<sub>3</sub>VO<sub>4</sub>, 5mM EDTA pH 8,00, 2 mM PMSF (SIGMA), vortexed vigorously to resuspend the pellet and incubated on ice for 10 minutes. Then 2,5  $\mu$ l of CERII reagent were added to the sample which was vortexed and incubated on ice for one minute. After centrifugation, the supernatant, containing the cytoplasmic protein fraction, was withdrawn and the remaining pellet was then resuspended in 12  $\mu$ l of ice-cold NER reagent, supplemented with the same protease inhibitors of CERI. The sample was incubated on ice for 40 minutes, vortexing every 10 minutes. After centrifugation, the supernatant, containing the nuclear protein fraction, was withdrawn.

Protein fractions were quantified with Bradford Method. Calibration curve was created using different quantities of BSA (Ultrapure BSA Non-Acetylated, Applied Biosystem). Absorbance was determined using a DU530 UV/Vis spectrophotometer (Beckman) at a wave length of 595 nm.

To evaluate P-STAT3 and STAT3 protein expression, nuclear and cytoplasmic protein extracts were separated on a 10% sodium dodecyl sulphate (SDS) polyacrylamide gel in denaturing conditions. Electrophoresis was performed with a XCell II™ SureLock (Life Technologies) at a voltage of 90 V until the samples entered the resolving gel and subsequently at 120 V. Proteins were transferred on

a Polyvinylidene fluoride (PVDF) membrane (Millipore) by electric transfer, carried out with a Mini Trans-Blot® cell (BioRad) at 350 mA for 2 hours. Membrane was stained with Ponceau Red dye (Fluka) to test protein transfer efficiency, then briefly washed with PBS supplemented with 0,05% Tween 20 (SIGMA) and saturated with PBS, 0,05% Tween 20, 5% BSA (SIGMA Aldrich) for 1 hour at room temperature. After a rapid wash, the membrane was hybridized with rabbit anti-human STAT3 mAb (Cell Signalling Technology) and anti-P-STAT3 (Tyr705) mAb (Cell Signalling Technology) diluted 1:1000 in PBS 0,05% Tween 20, 5% BSA shaking overnight at 4°C. After three more washes of 10 minutes, the membrane was hybridized with the secondary HRP-conjugated donkey anti-rabbit IgG antibody (NA934V, GE Healthcare) diluted 1:5000 in PBS with 0,05% Tween 20 and 5% BSA, shaking for 1h at 4°C. After 3 more washes, chemiluminescence was developed incubating the membrane with SuperSignal West Pico Chemiluminescent Substrate (Thermo Scientific) reagent for 5 minutes in the dark and then the signal was acquired with ChemiDoc XRS (Bio-Rad). Subsequently, hybridization with mouse anti-human Nucleoporin p62 mAb (BD Transduction Laboratories) and mouse anti-human  $\beta$ -actin mAb (Santa Cruz Biotechnology Inc.), both diluted in PBS, 0,05% Tween 20, 5% BSA, was performed. For these two antibodies a secondary HRP-conjugated, sheep anti-mouse IgG antibody (GE Healthcare) was used, diluted 1:5000 in PBS, 0,05% Tween 20, 5% BSA.

### **3.7 Intracellular staining for P-STAT3**

iBM-MDSCs before and after 20 hours of co-culture with T cells were analyzed by flow cytometry for the expression of P-STAT3. The staining was performed also after the addition in the co-culture of anti-IL10 blocking antibody and after the pre-treatment of iBM-MDSCs with Stattic, as previously described.  $2 \times 10^5$  cells were washed with staining buffer, composed of PBS + 4% FBS, then 50  $\mu$ l of PBS with 1% formaldehyde were added and tubes were incubated for 10 minutes at 37°C. After 2 washes with staining buffer, 450  $\mu$ l of cold methanol were added and cells were fixed for 15 minutes at -20°C. After 2 more washes, cells were incubated for 30 minutes at RT with 50  $\mu$ l of rabbit anti-human P-STAT3 (Tyr705) mAb (Cell Signalling Technology) diluted 1:100 in PBS + 4%

FBS. Next, cells were washed and incubated for 30 minutes at RT with 50 µl of DyLight488-donkey anti-rabbit IgG antibody (BioLegend) diluted 1:700 in PBS + 4% FBS. After a wash, cells were resuspended in 250 µl of staining buffer. As positive control for the staining, HepG2 (liver hepatocellular) cells treated with rh IL-6 (PeproTech) were fixed and permeabilized as previously described and frozen at -20°C in RPMI medium containing 10% glycerol and 20% FBS. For each experimental run, the positive control was stained with mAb together with the samples. For all samples data acquisition was performed on LSRII flow cytometer.

### **3.8 FACS sorting to separate B7-H1<sup>+</sup> and B7-H1<sup>-</sup> subsets**

iBM-MDSCs and CellTrace-labelled PBMCs stimulated with anti-CD3/CD28 were harvested after 20 hours of co-culture and collected in polypropylene tubes previously rinsed with FBS. Cells were washed with a sorting buffer composed of HCF 2% FBS, 0.5 mM EDTA (SIGMA), 1% PenStrep (LONZA), and then incubated on ice for 15 minutes with FcR blocking. Anti-B7-H1 PE (eBioscience) mAb was added and cells were incubated on ice for 20 minutes. After a wash, cells were resuspended in 1 ml of sorting buffer and B7-H1<sup>+</sup> and B7-H1<sup>-</sup> subsets, within CellTrace- cells, were separated by FACS ARIA (BD Bioscience). On both subsets, an intracellular staining for P-STAT3 was performed as previously described.

### **3.9 Analysis of STAT3 target genes by TRANSFAC database**

Genes already validated as targets of STAT3 in Homo sapiens were retrieved by means of the TRANSFAC Professional database (release 2013.3), containing published data on eukaryotic transcription factors, their experimentally-proven binding sites and regulated genes. Both direct targets of STAT3 and of complexes in which STAT3 takes part were considered for the analysis.

### **3.10 Colon cancer patients cohort**

Biopsies from liver metastases of stage IV colorectal cancer patients were received from the biobank of the Department of Surgery, Oncology and

Gastroenterology of the University of Padova. The project was approved by Ethics Committee and all patients gave their informed consent.

### **3.11 Enzymatic digestion of biopsies and flow cytometric analysis**

Biopsies were collected in 0.9% NaCl solution and processed immediately after the withdrawal. They were dissected into small pieces and resuspended in an enzymatic mix composed of collagenase 1 g/l, (Sigma-Aldrich), hyaluronidase 100 mg/l (Sigma-Aldrich), DNase 30 U/ml. The enzymatic digestion was performed at 37°C, shaking for 40-60 minutes. At the end of the incubation, the remaining aggregates were broken up and cell solution was filtered through a 100 µm cell strainer. Cells were washed with IMDM supplemented with 10% FBS, 1% PenStrep, 1% HEPES and, if necessary, red blood cells were lysed as described for BM samples.  $5 \times 10^5$  cells were aliquoted in each tube for flow cytometry analysis. Cells were washed with HCF 1% FBS, incubated with FcR blocking solution for 15 minutes on ice and then stained with two mix of mAbs, one for myeloid cells and one for the characterization of T lymphocytes. The first mix contained: LiveDead Aqua (Life Technologies), anti-CD45 Vioblue (Miltenyi Biotec), anti-CD33 PE-Cy7 (eBioscience), anti-HLA-DR PerCP-Cy5.5 (BioLegend), Lineage cocktail 1 FITC (BD Bioscience), anti-CD11b Alexa700 (BD Pharmingen), anti-B7-H1 PE (eBioscience). The second mix contained: LiveDead Aqua, anti-CD45 Vioblue, anti-CD33 PE-Cy7, anti-HLA-DR PerCP-Cy5.5, anti-CD3 ECD (Beckman Coulter), anti-CD8 APC-H7 (BD Bioscience), anti-LAG-3 FITC (AdipoGen), anti-PD1 PE (Miltenyi Biotec). After incubation with mAbs, cells were stained with Annexin V Alexa 647 and samples were immediately analysed by LSRII flow cytometer.

### **3.12 Statistical analysis**

Data were analyzed using SigmaPlot (Systat Software). When data distribution passed the normality test, Student's t test was applied, otherwise Mann-Whitney U test was performed. The results were considered statistically significant with  $P < 0,05$ .

## 4. RESULTS

### 4.1 Role of IL-10 in the immune suppression induced by MDSCs expanded *in vitro*

We recently demonstrated that the *in vitro* treatment of freshly isolated BM cells with the addition of the cytokines G-CSF and GM-CSF induces the expansion of MDSCs from cell precursors present in BM samples, and we named these cells BM-MDSCs<sup>80</sup>. Further characterization of these cells revealed that BM-MDSCs are a heterogeneous immature myeloid cell population and that the immunosuppressive activity is retained by the most immature subset (immature BM-MDSCs, iBM-MDSCs). This cell population shares the morphology and the markers of promyelocytes and is equivalent to MDSCs present in the peripheral blood of breast and colorectal cancer patients<sup>103</sup>. To understand which molecular mechanisms are involved in the immunosuppression mediated by iBM-MDSCs, we focused our attention on soluble factors, and in particular on IL-10, a cytokine known to have inhibitory effects on the immune system. We therefore performed an ELISA assay to test the production of this cytokine on the supernatants of the cultures of T cells and iBM-MDSCs (Figure 1). T cells were labeled with CellTrace and cultured in the absence of stimuli or with anti-CD3/CD28 antibodies for 4 days. Unfractionated BM-MDSCs and iBM-MDSCs were cultured alone or in the presence of activated T cells for 4 days. As control, the most mature subset isolated from BM-MDSCs (mature BM-MDSC, mBM-MDSC) was also used. At the end of the culture, IL-10 concentration was quantified on the supernatants. As shown in figure 1, the highest level of IL-10 release was reached when activated T cells were cultured in the presence of iBM-MDSCs, while cultures between activated T lymphocytes and unfractionated BM-MDSCs or the mBM-MDSC had lower levels of IL-10 production. Activated T cells alone produced IL-10, but the concentration increased more than two fold in the presence of iBM-MDSCs. A negligible concentration of IL-10 was detected in the supernatants of resting T cells and of BM-MDSC subsets cultured alone. These data indicate that the co-culture between activated T lymphocytes and immunosuppressive cells induces a significant increase in the release of IL-10, although this assay does not allow to discriminate if myeloid or lymphoid cells are responsible for IL-10 secretion.

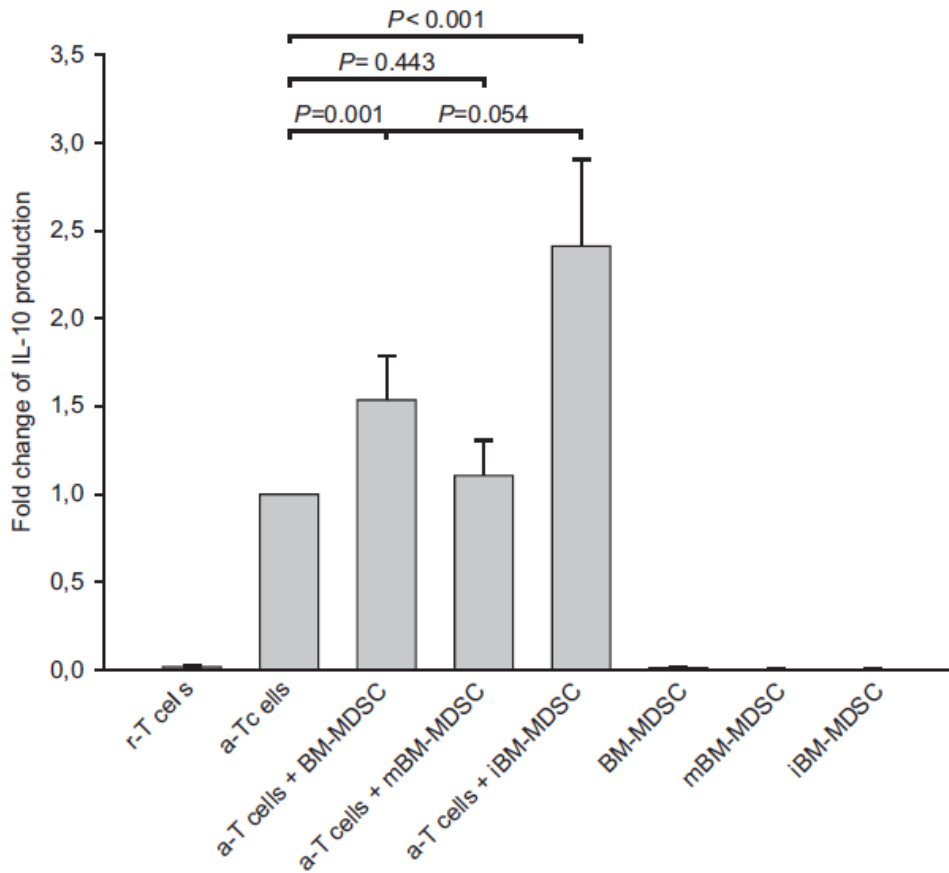


**Figure 1: IL-10 release is increased in the co-culture between activated T cells and iBM-MDSCs.**

ELISA assay performed on the supernatant of cell cultures of CellTrace labelled-PBMCs stimulated with anti-CD3 and anti-CD28 antibodies for 4 days, alone or in the presence of BM-MDSCs, mBM-MDSCs and iBM-MDSCs. Cultures of different BM-MDSC subsets alone and of unstimulated PBMCs were performed as control (r-T cells= resting T cells, a-T cells= activated T cells). In each experiment, IL-10 concentration was normalized on activated T cells and expressed as fold change. The histogram shows the mean  $\pm$  standard error (SE) of 10 independent experiments. Mann-Whitney U test was applied.

We therefore performed a flow cytometry-based IL-10 secretion assay, that allows to identify which cells are secreting the cytokine. We cultured activated T cells alone and in the presence of iBM-MDSCs and we checked for IL-10 production by T and myeloid cells, by gating respectively on CD3<sup>+</sup> and on CD33<sup>+</sup> cells during the 4 days of culture. Our results demonstrate that activated T cells are mainly responsible of IL-10 secretion in the co-culture with iBM-MDSCs, while the contribution of myeloid cells is very low (Figure 2A). The percentage of T cells producing IL-10 is increased when activated T lymphocytes are cultured in

the presence of iBM-MDSCs as compared to activated T cells alone. Concerning the kinetics of IL-10 release, we observed that the cytokine is rapidly released after one day of culture, and that its secretion increases up to the third day, reaching a plateau after 4 days (Figure 2C). At each time point IL-10 release by T cells in the presence of iBM-MDSCs was always higher as compared to unstimulated T cells cultured in the presence of iBM-MDSCs. Taken together, these results indicate that the presence of iBM-MDSCs induces IL-10 production by activated T cells and that IL-10 secretion is an early event among the molecular mechanisms of MDSC-mediated inhibitory activity.

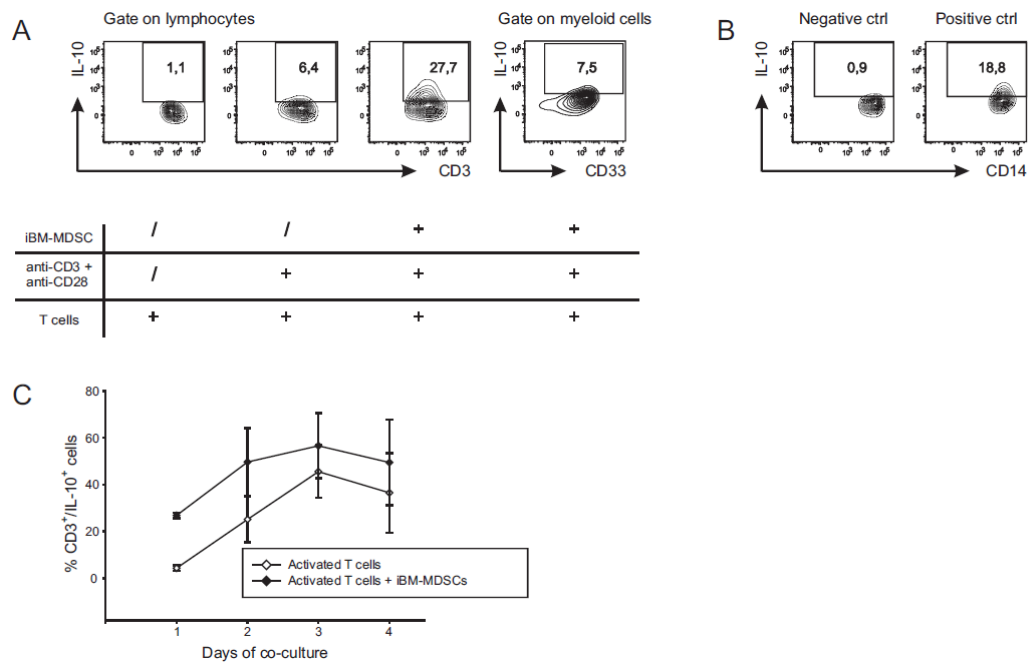


**Figure 2: IL-10 is secreted by activated T cells following contact with iBM-MDSCs.** (A) IL-10 secretion assay was performed on CellTrace-labelled PBMCs stimulated with anti-CD3 and anti-CD28 for one day, alone or in the presence of iBM-MDSCs. Cell cultures were stained with mAbs anti-CD3 and anti-CD33 in order to discriminate between T cells and myeloid cells. Gating of IL-10<sup>+</sup> cells was set on the basis of a fluorescence minus one (FMO) control. (B) Panel B shows the results of IL-10 secretion assay performed on monocytes cultured with or without 100 ng/ml of LPS for 14 hours. (C) Kinetics of IL-10 secretion assay in 4 days cell cultures of activated T cells with (upper line) or without (lower line) iBM-MDSCs. These results are representative of 3 independent experiments.

## 4.2 Role of STAT3 phosphorylation in MDSC-mediated immune suppression

Since our results show that iBM-MDSCs increase the release of IL-10 by co-cultured T cells, we asked which signalling pathways can be activated by this

cytokine. We focused our attention on STAT3, a transcription factor known to be activated by IL-10<sup>168</sup> and that is involved in immunosuppression<sup>47</sup>. To this aim, we performed a Western Blot analysis of the nuclear and cytoplasmic fractions of proteins extracted from mBM-MDSCs and iBM-MDSCs. We used mAbs directed against STAT3 protein and recognizing its phosphorylated form at Tyr705, a modification responsible of the translocation of the transcription factor into the nucleus. STAT3 consists of two isoforms, named  $\alpha$  and  $\beta$ , of respectively 86 and 79 kDa that differ because the  $\beta$  isoform lacks 55 residues in its C terminal. We observed that STAT3 is phosphorylated on the nuclear and cytoplasmic fractions of the iBM-MDSCs (Figure 3, lanes 1) on both isoforms. Only a faint phosphorylation could be detected in the mBM-MDSCs in the nuclear fraction, but not in the cytoplasmic fraction (Figure 3, lanes 2). No significant differences between the two BM-MDSC subsets were detected when considering total STAT3 expression. In line with the literature, these results demonstrate STAT3 phosphorylation in the suppressive subset of BM-MDSCs.



**Figure 3: P-STA3 is expressed mainly in iBM-MDSCs.**

Western blot analysis of P-STAT3 and STAT3 isoforms' expression in the nuclear (NF, left panel) and cytoplasmic (CF, right panel) protein fractions of BM-MDSCs. Nucleoporin 62 (Np62) and  $\beta$ -actin were used as endogenous controls respectively for nuclear and cytoplasmic fractions. Molecular weight of the proteins was determined on the basis of a chemiluminescent marker (M).

Since these results demonstrate STAT3 activation in iBM-MDSCs, we decided to investigate if the phosphorylation of STAT3 in these cells is influenced by the co-culture with T lymphocytes. To this aim, we optimized a flow cytometry intracellular staining to detect if the phosphorylation of STAT3 at Tyr705 changes

in different culture conditions. Flow cytometry analysis revealed that among iBM-MDSCs two cell populations can be distinguished on the basis of their different morphology, one presenting a high side-scatter (SSC) and one with a low SSC. These two populations differ in terms of STAT3 phosphorylation, since the SSC<sup>high</sup> cells are partially phosphorylated, while SSC<sup>low</sup> cells are completely negative (Figure 4).

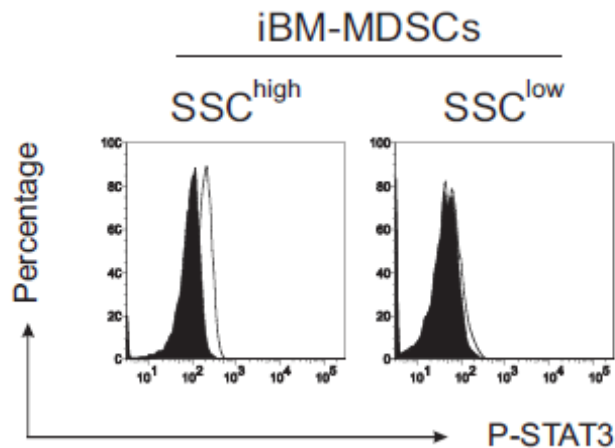


**Figure 4: P-STAT3 analysis by flow cytometry on iBM-MDSCs.**

Intracellular staining for P-STAT3 was performed on iBM-MDSCs. Side-scatter high (SSC<sup>high</sup>) and side-scatter low (SSC<sup>low</sup>) cells were gated. Black histograms show the signal of secondary antibody alone. These results are representative of 4 independent experiments.

We thus evaluated P-STAT3 mean fluorescence intensity (MFI) in the SSC<sup>high</sup> subset of iBM-MDSCs before and after 20 hours of culture alone or in the presence of either resting or activated T lymphocytes (Figure 5A). The staining of T cells with CellTrace allowed us to discriminate myeloid cells (CellTrace<sup>-</sup>) from T lymphocytes (CellTrace<sup>+</sup>) in the co-culture.  $\Delta$ MFI was calculated by subtracting the MFI of secondary antibody from the MFI of P-STAT3 and then the values obtained were normalized on iBM-MDSCs cultured alone. This analysis revealed that P-STAT3 expression was up-regulated in myeloid cells when they were cultured with activated T cells, while in the presence of resting T lymphocytes this phosphorylation decreased, becoming almost negligible when iBM-MDSCs were cultured alone (Figure 5A). By flow cytometry we also analyzed the expression of P-STAT3 in T cells cultured alone or in the presence of MDSCs (Figure 5B). The  $\Delta$ MFI of P-STAT3 was calculated as previously described and then the values were normalized on the  $\Delta$ MFI of activated T cells. Activated T cells expressed P-

STAT3 but in the presence of iBM-MDSCs the extent of phosphorylation was significantly increased. Resting T cells also expressed P-STAT3 but at a low level and in the presence of MDSCs significantly increased the level of phosphorylation. These results suggest the existence of an interplay between activated T cells and MDSCs that leads to the activation of STAT-3 signalling pathway in both cell types. Since it is known that STAT3 activation is driven by IL-10 and our results show that the production of IL-10 is increased when iBM-MDSCs are co-cultured with activated T cells, we tested if a neutralizing anti-IL-10 mAb had any effect on the activation of STAT3. We therefore added the anti-IL-10 blocking Ab at the beginning of the co-culture between iBM-MDSCs and activated T cells, and we noticed that its presence caused a decrease of STAT3 phosphorylation on both myeloid cells (Figure 5A) and activated T cells (Figure 5B), thus confirming that IL-10 is involved in STAT3 activation.

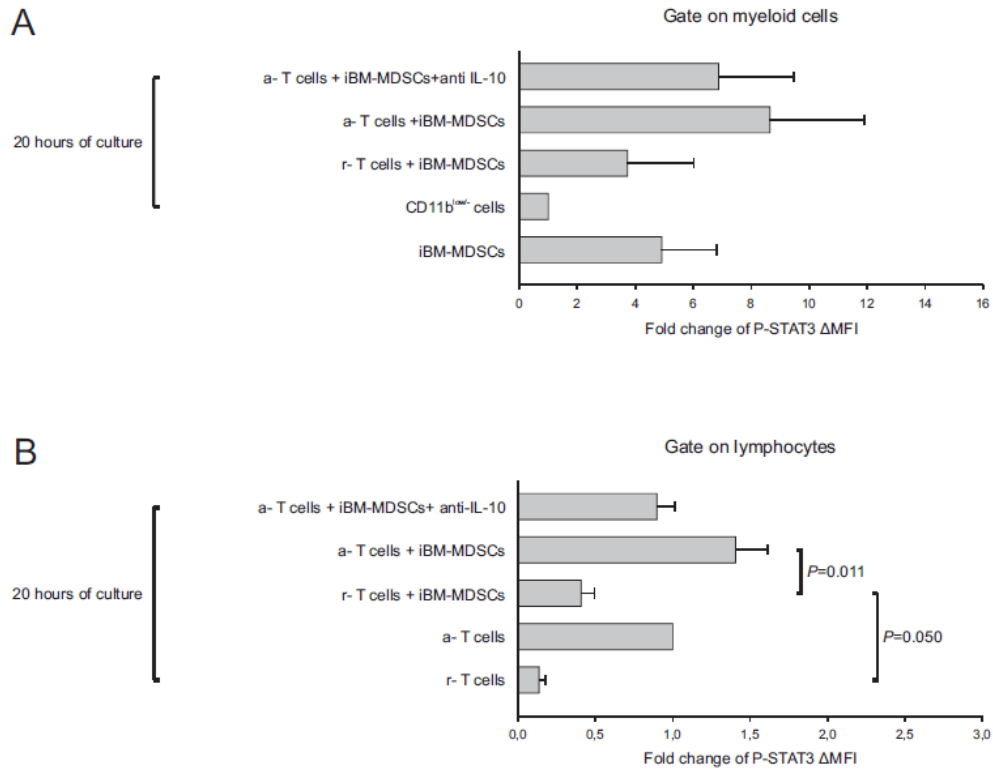


**Figure 5: Analysis of P-STAT3 expression in iBM-MDSCs and activated T cells.**

Intracellular staining for P-STAT3 was performed on iBM-MDSCs and T cells in different culture conditions. iBM-MDSCs were cultured for 20 hours in the presence of resting (r-T cells) or anti-CD3/anti-CD28 activated T cells (a-T cells), previously stained with CellTrace. To discriminate between myeloid cells and T cells in co-culture, cells were gated respectively on CellTrace<sup>-</sup> and CellTrace<sup>+</sup> cells and the difference in mean fluorescence intensity ( $\Delta$ MFI) of P-STAT3 was evaluated by subtracting the MFI of secondary antibody to that of P-STAT3 antibody. Values obtained were then normalized on the  $\Delta$ MFI of iBM-MDSCs cultured alone for 20 hours, when considering myeloid cells (A), and on the  $\Delta$ MFI of activated T cells, when evaluating P-STAT3 expression on T lymphocytes. (B) Anti-IL-10 mAb (10  $\mu$ g/ml) was added to the co-culture between a-T cells and iBM-MDSCs. The values reported are the mean  $\pm$  standard error (SE) of 4 independent experiments. Student's t test was applied.

### **4.3 Analysis of the expression of B7-family members on iBM-MDSCs under different experimental conditions**

Our results clearly indicate that STAT3 activation is increased both on iBM-MDSCs and activated T cells when they are co-cultured. STAT3 can induce the expression of B7-H1 by binding to its promoter leading to the transcription of the gene <sup>169</sup>. We thus decided to test the expression of B7-H1 on iBM-MDSCs and also to enlarge this study to other members of the B7-family, in particular B7-H2 and B7-H3. B7-H2 is the ligand of ICOS on T lymphocytes and is known to have a co-stimulatory effect, while B7-H3 has an inhibitory effect but its ligand is still unknown. We tested the expression of these molecules by flow cytometry on iBM-MDSCs before and after 4 days of culture alone or in the presence of either resting or activated T cells (Figure 6). We noticed that iBM-MDSCs did not express B7-H1, and showed a partial expression of B7-H2 and B7-H3. Upon contact with activated T cells, B7-H1 and B7-H3 were highly up-regulated on iBM-MDSCs, while in the presence of resting T cells B7-H1 expression was very low, and B7-H3 expression was increased but at a lower intensity. The co-stimulatory molecule B7-H2 had instead a different pattern of expression since it was present at low level in iBM-MDSCs, but after culture, either alone or with T lymphocytes, its expression decreased even further. Taken together, our results suggest that the presence of activated T cells induces on MDSCs the expression of surface molecules, such as B7-H1 and B7-H3, that are known to be involved in a negative regulation of immune responses.

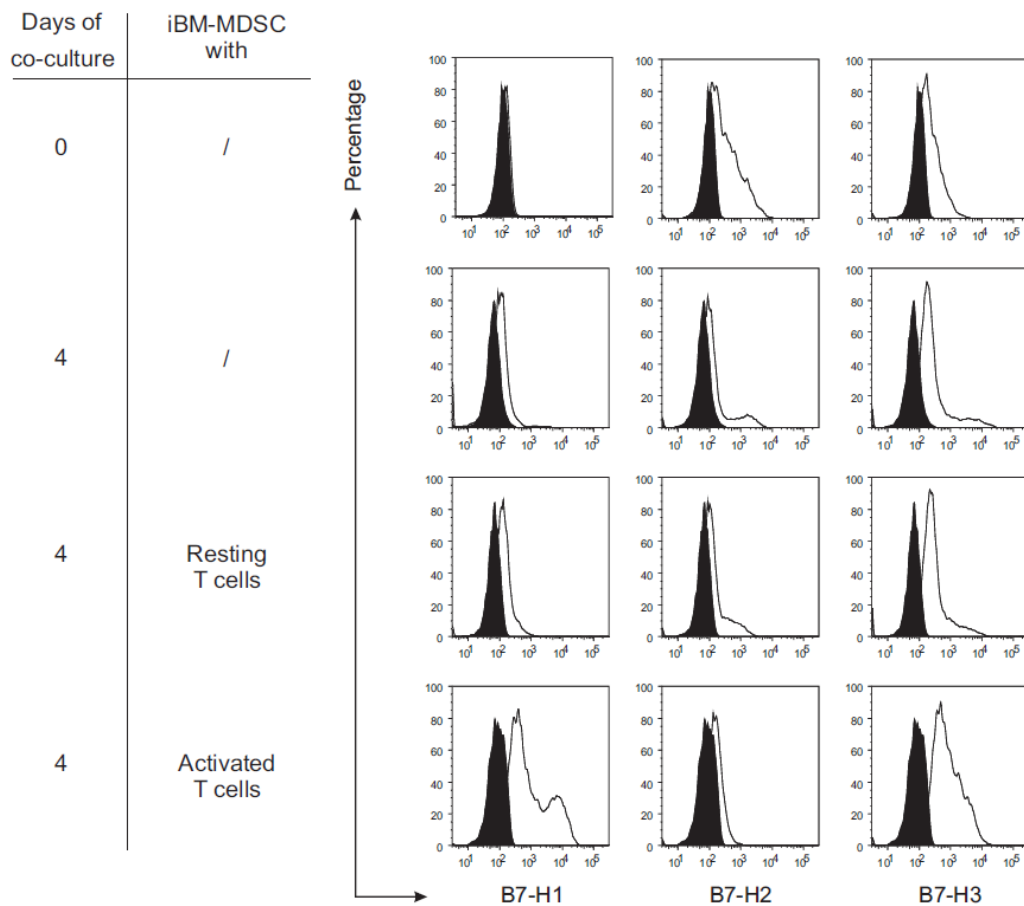


**Figure 6: Analysis of the expression of B7 family members on iBM-MDSCs in different culture conditions.**

iBM-MDSCs were isolated by immunomagnetic sorting and cultured for 4 days alone or in the presence of resting or activated T cells, previously labelled with CellTrace. After 4 days, cells were harvested and labelled with CD3 and B7-H1/B7-H2/B7-H3 mAbs. Myeloid cells were identified by gating on CellTrace<sup>-</sup>/CD3<sup>-</sup> cells and the negative signal (black histogram) was evaluated using a fluorescence minus one (FMO) control. The data are representative of 3 independent experiments.

We next quantified the percentage of B7-H1<sup>+</sup> cells in different culture conditions, and Figure 7 shows that there is a statistically significant increase in the level of B7-H1<sup>+</sup> cells among iBM-MDSCs co-cultured with activated T cells, as compared to control cultures. Although not statistically significant, we observed a lower percentage of B7-H1<sup>+</sup> cells in the presence of resting T cells, as compared to activated T lymphocytes, thus confirming our previous results.

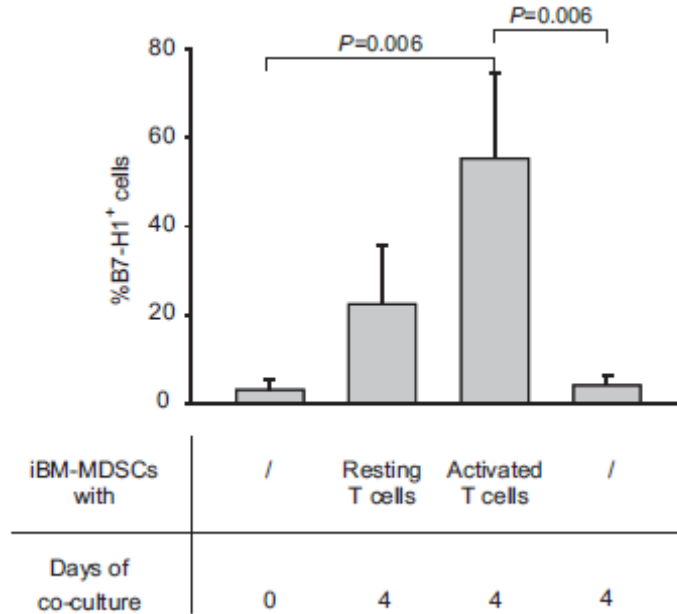


**Figure 7: Expression of B7-H1<sup>+</sup> cells among iBM-MDSCs in the presence of T cells.**

Staining with anti-B7-H1 mAb was performed on iBM-MDSCs and on the same cells cultured for 4 days alone or in the presence of resting or anti-CD3/CD28 activated T cells, labelled with CellTrace. Myeloid cells were discriminated gating on CellTrace<sup>+</sup>/CD3<sup>-</sup> cells and the percentage of B7-H1<sup>+</sup> cells was obtained using an FMO as negative control. The histogram reports the mean  $\pm$  SE of 4 independent experiments. Mann-Whitney U test was applied.

We decided to analyse the kinetics of B7-H1 expression during the 4 days of culture with activated T cells because we observed that STAT3 phosphorylation is an early event occurring after 20 hours of co-culture and from literature we know that STAT3 can activate the transcription of B7-H1. We observed that the maximum percentage of B7-H1<sup>+</sup> cells among MDSCs was reached after the first day of culture, then decreased between the first and the second day and was maintained almost unchanged until the end of the culture (Figure 8). Moreover, we observed that iBM-MDSCs that up-regulate B7-H1 after 20 hours of co-culture with activated T cells, also present a high SSC, in analogy with the P-STAT3<sup>+</sup> cell subset of iBM-MDSCs. These observations prompted us to investigate the link between the expression of these two markers and their involvement in the BM-MDSC-mediated immunosuppression.

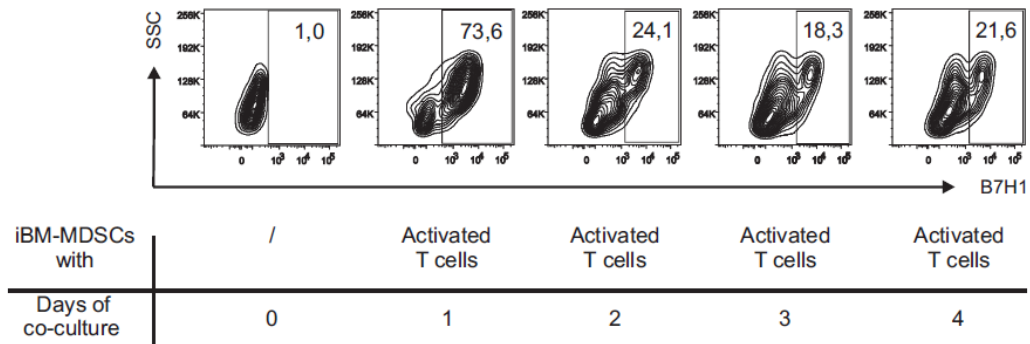


**Figure 8: Kinetics of B7-H1 expression on myeloid cells cultured with activated T cells.**

Cell surface staining with B7-H1 mAb at different time points of co-culture of iBM-MDSCs with CellTrace-labelled T cells activated by anti-CD3/CD28. Myeloid cells were defined by gating CellTrace<sup>-</sup>/CD3<sup>-</sup> and then the percentage of B7-H1<sup>+</sup> cells was evaluated. Results shown are representative of 4 independent experiments.

#### **4.4 Evaluation of the relationship between STAT3 activation and B7-H1 expression**

To evaluate the link between P-STAT3 and B7-H1, we investigated whether these two markers were co-expressed in the same cells. To this aim, we cultured for 20 hours iBM-MDSCs with activated T cells and then we separated B7-H1<sup>+</sup> and B7-H1<sup>-</sup> myeloid cells by FACS sorting by gating CellTrace<sup>-</sup> cells. We performed an intracellular staining on sorted cells to detect STAT3 phosphorylation and the  $\Delta$ MFI of P-STAT3 was calculated as previously described. As shown in figure 9, B7-H1<sup>+</sup> cells had a higher intensity of expression of P-STAT3, as compared to B7-H1<sup>-</sup>.

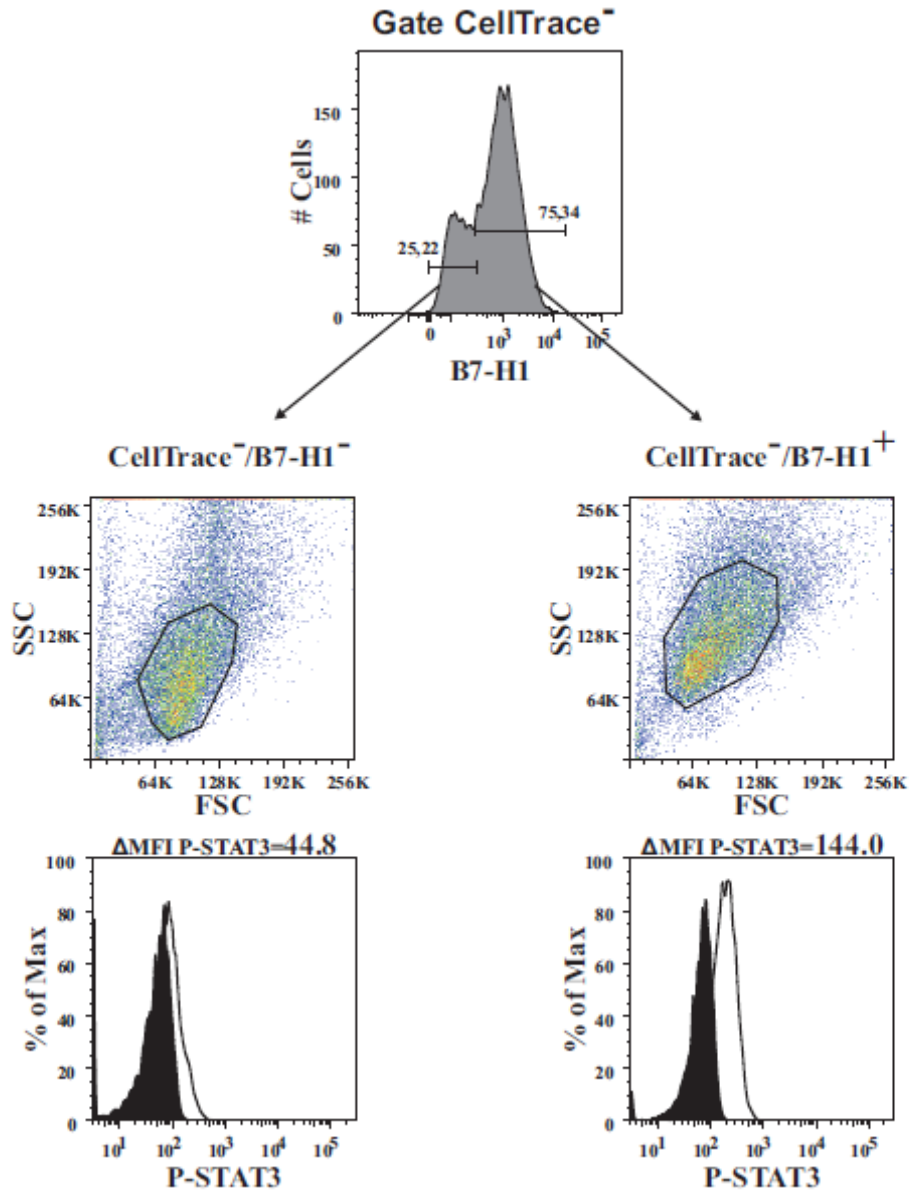


**Figure 9: P-STAT3 expression in B7-H1<sup>+</sup> and B7-H1<sup>-</sup> cells.**

iBM-MDSCs were cultured with CellTrace-labelled T cells. After 20 hours, B7-H1<sup>+</sup> and B7-H1<sup>-</sup> myeloid cells were separated by FACS sorting and an intracellular staining for P-STAT3 was performed. The  $\Delta$ MFI for P-STAT3 was calculated by subtracting the MFI of the secondary antibody from the MFI of P-STAT3. Black histograms show the signal of secondary antibody. The results are representative of 3 independent experiments.

On the basis of this result, we decided to investigate whether the inhibition of STAT3 phosphorylation and therefore of its activation had an effect on the expression of B7-H1. To this aim, we analyzed B7-H1 phenotype in iBM-MDSCs pretreated with 5  $\mu$ M Stattic, an inhibitor of STAT3 phosphorylation at Tyr705, after 20 hours of co-culture with activated T cells. B7-H1 expression was

compared to that of untreated iBM-MDSCs in the same culture conditions. We observed that the percentage of cells expressing B7-H1 was significantly reduced in the presence of Stattic, thus supporting the notion that STAT3 induces B7-H1 expression (Figure 10).

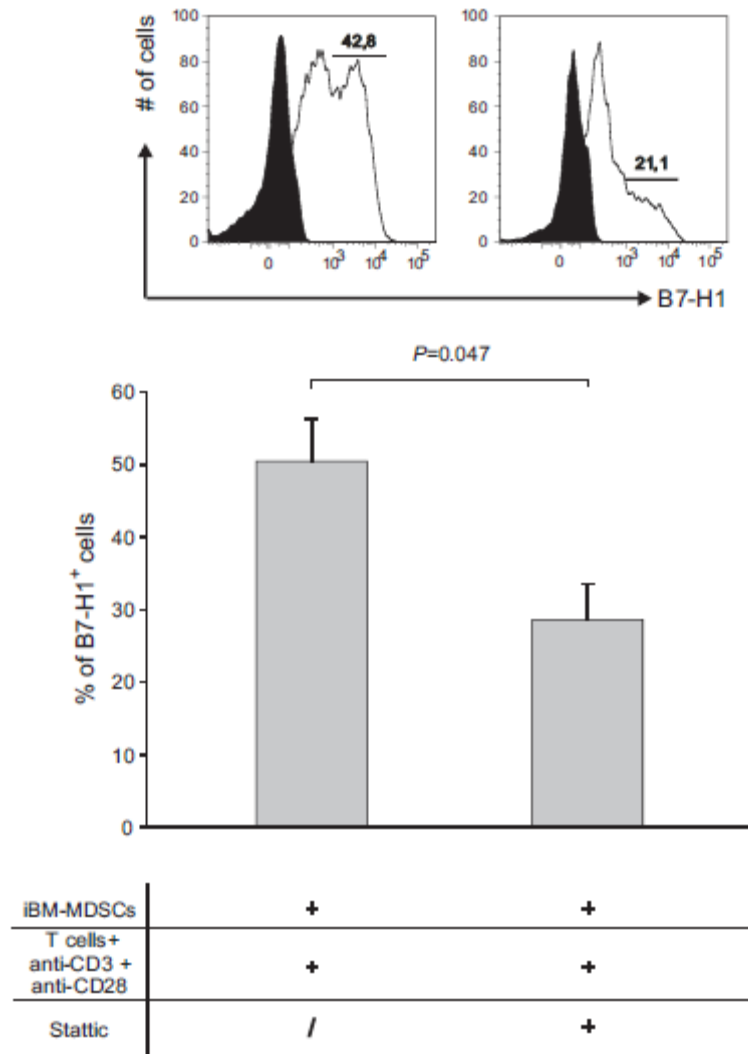


**Figure 10: Stattic reduces the expression of B7-H1 on iBM-MDSCs.**

iBM-MDSCs untreated or pre-treated with 5  $\mu$ M Stattic for 30 minutes were cultured for 20 hours with T cells labelled with CellTrace and activated with anti-CD3/CD28. The percentage of B7-H1<sup>+</sup> cells among CellTrace<sup>-</sup> myeloid cells was quantified as shown in the upper panel. Black histograms represent the FMO control for B7-H1. The histograms below represent the mean  $\pm$  SE of 3 independent experiments. Student's t test was applied.

When we quantified the extent of inhibition of STAT3 phosphorylation induced by Stattic, we observed that the treatment caused a marked reduction of P-STAT3 expression in iBM-MDSCs (Figure 11), although it did not completely abolish P-STAT3 expression and this could explain why more than 20% of cells still

expressed B7-H1 after STAT3 inhibition (Figure 10 upper panel). On the other hand, the concentration of the inhibitor could not be increased, since higher concentrations were toxic on BM cells, causing a marked reduction in cell number (data not shown).

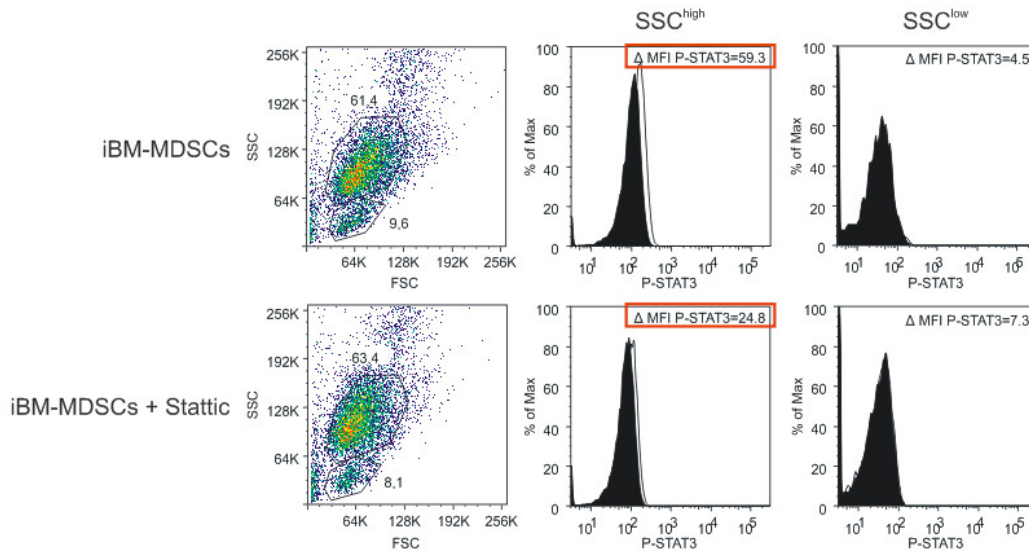


**Figure 11: Effect of Stattic on P-STAT3 expression on iBM-MDSCs.**

iBM-MDSCs were pre-treated with 5  $\mu$ M Stattic for 30 minutes and then stained for P-STAT3.  $\Delta$ MFI for P-STAT3 was calculated subtracting the MFI of secondary antibody from the MFI of P-STAT3 in both subsets present among iBM-MDSCs, characterized by a different morphology (SSC<sup>high</sup> and SSC<sup>low</sup>).

#### 4.5 Inhibition of STAT-3 phosphorylation in iBM-MDSCs restores the immune response

We demonstrated that IL-10, STAT3 and B7-H1 are inter-connected in a loop that is active in immunosuppressive cells after that they come in contact with activated T lymphocytes. We therefore asked if inhibitors of IL-10, STAT3 and B7-H1 were able to rescue the proliferation of T cells suppressed by MDSCs. To this aim, we tested an anti-IL-10 blocking mAb to neutralize IL-10 produced in the co-culture and anti-B7-H1 plus anti-PD-1 to block the interaction of B7-H1, expressed by myeloid cells, with its receptor PD-1 on activated T cells. We chose the antibodies' concentration that was not toxic on activated T cells to avoid side-effects unrelated to immunosuppression. Instead, Stattic, the inhibitor of STAT3 phosphorylation at Tyr 705, could not be added directly in the culture because it was toxic on T cells even at very low concentration and inhibited their proliferation. We therefore chose to pre-treat iBM-MDSCs for 30 minutes and

then add them to the culture after having washed away the inhibitor. Under this condition, we verified that, at least after 24 hours, cell death of Stattic-treated iBM-MDSCs was increased only of 3,7%, as compared to untreated cells (data not shown). We quantified immunosuppression both in a quantitative manner (Figure 12, black bars), considering the absolute number of CD3<sup>+</sup> lymphocytes, and in a qualitative way (Figure 12, grey bars), evaluating the percentage of proliferating T cells following the generations of T cell divisions by CellTrace dilution. In both types of quantification, the values obtained were then normalized on the activated T cells cultured alone, whose proliferation was considered as 100%. As shown in figure 12, among the tested molecules, only Stattic was able to rescue the proliferation of T cells both quantitatively and qualitatively, although statistical significance was reached only when calculating proliferation in a qualitative manner. To exclude the possibility that this rescue in T cell proliferation was due to a reduction in the percentage of myeloid cells as a consequence of Stattic treatment, we evaluated the change in the percentage of myeloid cells and observed a non-significant decrease (Figure 13). Taken together, these results indicate that Stattic interferes with the mechanisms that lead to iBM-MDSC-mediated immunosuppression. Instead, no relevant differences were observed when anti-IL-10 and anti-PD-1 with anti-B7-H1 were added to the culture, possibly because the inhibition of a single molecule is not sufficient to block the immunosuppressive activity of MDSCs that is most likely caused by several signalling pathways acting together. The inhibition of the transcription factor STAT3 has instead a wider effect in MDSC signaling since it rebounds on all STAT3 targets.

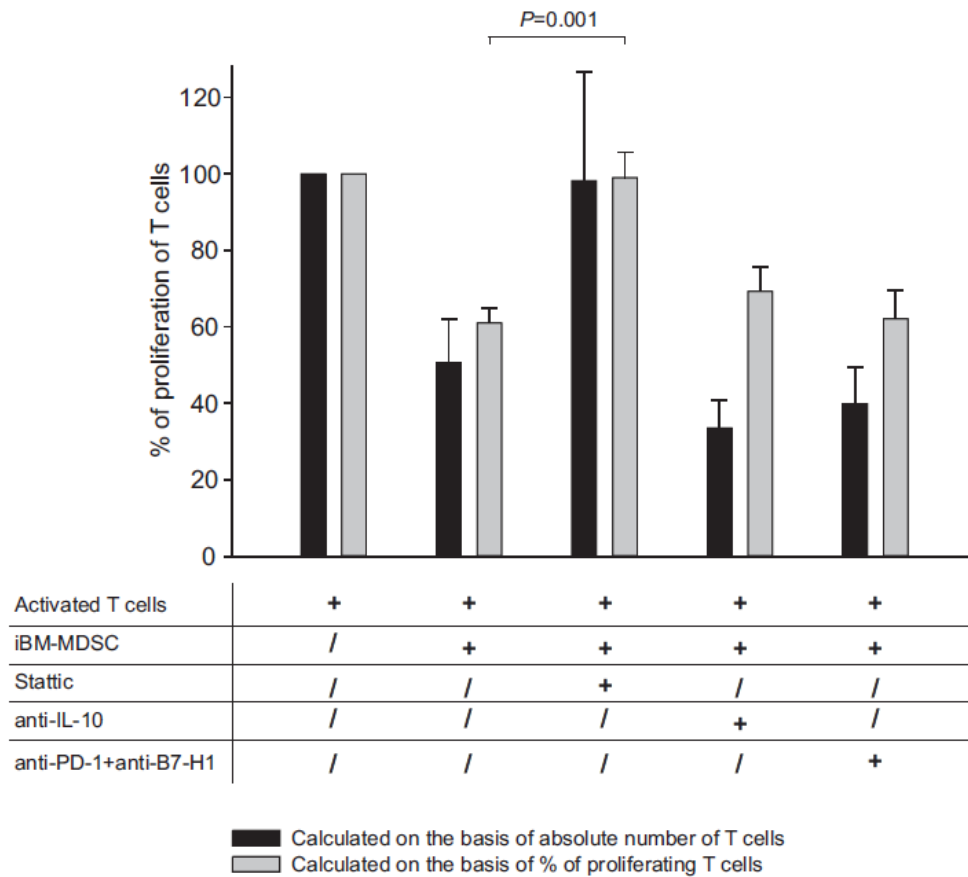


**Figure 12: Proliferation of T cells in the presence of inhibitors for P-STAT3, IL-10, PD-1 and B7-H1.**

CellTrace-labelled PBMCs were cultured for 4 days alone and in the presence of iBM-MDSCs, pre-treated for 30 minutes with 5  $\mu$ M Stattic, while mAbs anti-IL-10 (10  $\mu$ g/ml), anti-PD-1 and anti-B7-H1 (1  $\mu$ g/ml) were added at the beginning of the culture. After 4 days, cell cultures were harvested and T cells were stained with anti-CD3 antibody. Immunosuppressive activity of iBM-MDSCs was evaluated either quantitatively (black bars), considering the absolute number of CD3<sup>+</sup> T cells, as assessed by TrueCount tubes, and qualitatively, evaluating the percentage of proliferating CD3<sup>+</sup> T cells (grey bars). For each experiment, the values were normalized on the proliferation of activated T cells alone. The histograms report the mean of 4 independent experiments  $\pm$  SE. Student's t test was applied.

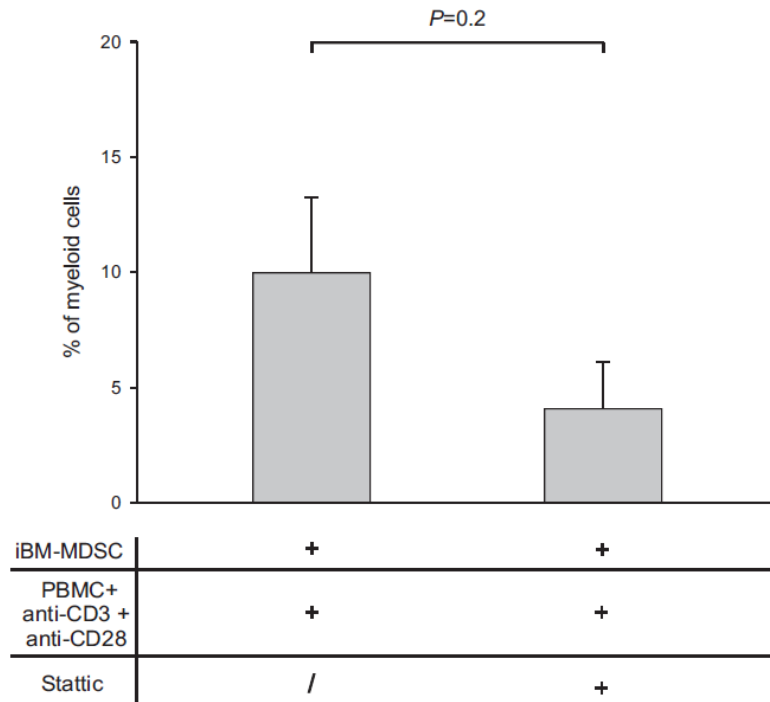


**Figure 13: Effect of Stattic on iBM-MDSCs.**

iBM-MDSCs were pre-treated with 5  $\mu$ M Stattic for 30 minutes and then cultured with CellTrace-labelled T cells activated for 4 days with anti-CD3/CD28. At the end of the culture, cells were harvested and stained with anti-CD3 mAb. Myeloid cells were identified by gating CD3<sup>+</sup>/CellTrace<sup>-</sup> cells. The histogram shows the mean  $\pm$  SE of 4 independent experiments. Student's t test was applied.

#### 4.6 Analysis of STAT3 target genes

To gain insight into the signalling pathways activated by STAT3, we checked for human genes already validated as targets of STAT3 by the use of the TRANSFAC Professional database (release 2013.3) containing published data on eukaryotic transcription factors, their experimentally-proven binding sites and regulated genes. Table 1 reports the validated target genes and miRNA of STAT3, of the dimer between two molecules (STAT3:STAT3), or of the STAT3 protein phosphorylated at Ser 727 (pS727) or at Tyr 705 (pY705), depending on which of these forms was used for the binding site validation. Interestingly, among the validated target genes we noticed CD274 (B7-H1), already implicated in our results, but also genes such as IL-10 and IL6st (gp130) that can both activate a positive feedback on STAT3. Other interesting STAT3 target genes are nitric oxide synthase (NOS3), an enzyme catalyzing the production of nitric oxide from L-arginine and expressed in granulocytic MDSCs<sup>52</sup>, and CDKN1A, a gene that

encodes for a potent cyclin-dependent kinase inhibitor, blocking the activity of cyclin-CDK2 or –CDK4 complexes and thus functioning as a regulator of cell cycle progression at G1. Moreover, among the targets of STAT3 it is reported miR-155. In this respect, our group recently evaluated microRNAs differentially expressed between sorted ex-vivo promyelocytes versus iBM-MDSCs and between iBM-MDSCs before or after contact with activated T cells (Solito et al., unpublished). Of note, miR-155 is significantly up-regulated in both comparisons, thus suggesting that it has a main role in MDSC-mediated immunosuppression. Moreover, C/EBP $\beta$  is a known target of miR-155<sup>170</sup>, and our group demonstrated that this transcription factor has a main role in the immunosuppression mediated by BM-MDSCs<sup>80</sup> and that the expression of its isoforms in mice was regulated by another miRNA that is miR-142-3p<sup>81</sup>.

<b>TF</b>	<b>target gene</b>	<b>number of validated binding sites</b>
STAT3	SERPINA1	1
STAT3	AGT	1
STAT3	BIRC5	3
STAT3	CCR5	1
STAT3	CD274	2
STAT3	CDKN1A	1
STAT3	CISH	1
STAT3	CRP	1
STAT3	CYP19A1	1
STAT3	DMBT1	1
STAT3	FAAH	1
STAT3	FCGR1C	1
STAT3	FGG	3
STAT3	FOS	5
STAT3	FOXM1	1
STAT3	HBG1	1
STAT3	HP	1
STAT3	ICAM1	1
STAT3	IFNG	2
STAT3	IL10	2
STAT3	IL21	1
STAT3	IL2RA	1
STAT3	IL2RG	2
STAT3	IL6ST	1
STAT3	IRF1	2
STAT3	LBP	1
STAT3	MMP1	1

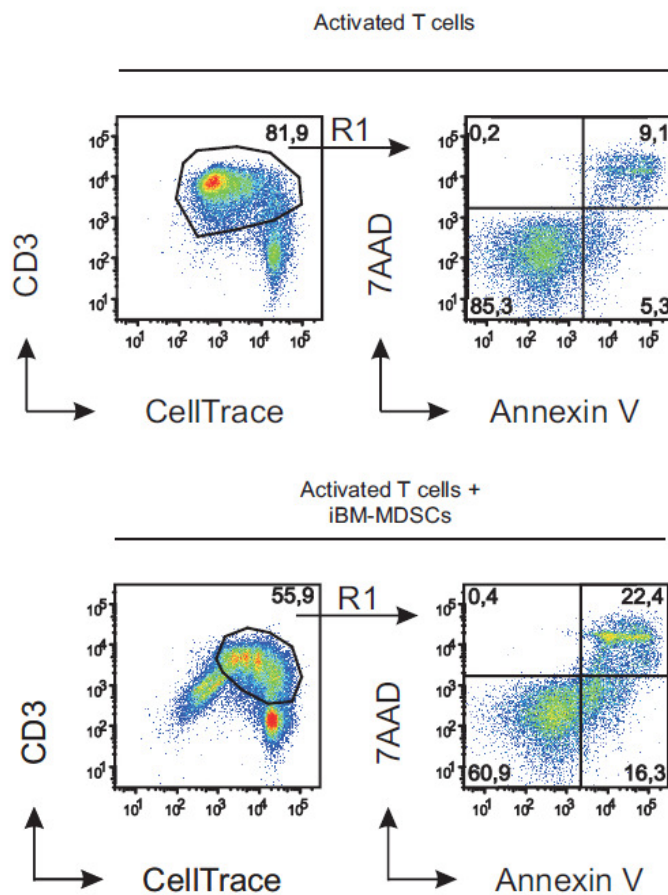
STAT3	MMP7	1
STAT3	MYC	1
STAT3	MYD88	2
STAT3	NOS3	2
STAT3	OPRM1	1
STAT3	PHB	1
STAT3	PIM1	1
STAT3	PML	1
STAT3	PRF1	1
STAT3	REG1A	1
STAT3	ROR1	2
STAT3	TP63	1
STAT3	TRH	1
STAT3	TWIST1	1
STAT3	VEGFA	1
STAT3	VIM	1
STAT3	VIP	1
STAT3	CD46	2
STAT3	MIR155	1
STAT3	SALL4	4
STAT3	VEGFC	1
STAT3:STAT3	FCGR1A	1
STAT3:STAT3	FOS	2
STAT3:STAT3	GBP1	1
STAT3:STAT3	ICAM1	1
STAT3:STAT3	IL10	1
STAT3:STAT3	IRF1	2
STAT3 (pS727)	CRP	1
STAT3(pS727)	FOS	1
STAT3(pY705)	AGT	3
STAT3(pY705)	ICAM1	1
STAT3(pY705)	IRF1	1
STAT3(pY705)	OAS1	1
STAT3(pY705)	FOS	1
STAT3(pY705)	ROR1	2
STAT3(p)	MUC4	1

**Table 1: Validated targets of STAT3 in Homo sapiens.**

Validated target genes of STAT3 in Homo sapiens as reported in TRANSFAC database. The first column reports different forms of STAT3 transcription factor (TF).

## 4.7 Analysis of T cell-suppression induced by iBM-MDSCs

From literature it is still not clear the fate of suppressed T cells. We therefore investigated whether iBM-MDSCs could induce apoptosis on T cells by the use of the two markers 7AAD and Annexin, that allow to discriminate between apoptotic (7AAD<sup>+</sup>/Annexin<sup>+</sup> cells), early apoptotic (7AAD<sup>-</sup>/Annexin<sup>+</sup>) and live (7AAD<sup>-</sup>/Annexin<sup>-</sup>) cells (gating strategy showed in figure 14, upper panel). We compared the percentage of these 3 cell subsets in activated T cells maintained in cell culture with or without iBM-MDSCs. After four days, we observed that the presence of MDSCs (Figure 14, grey bars) induced a significant increase in the percentage of apoptotic and early apoptotic T cells, as compared to T cells cultured alone (black bars) and, accordingly, this result was associated to a reduction in the percentage of live T cells. However, the percentage of live T cells still accounted for the majority of the cells, so we hypothesized that other mechanisms of T cell function impairment could be involved.



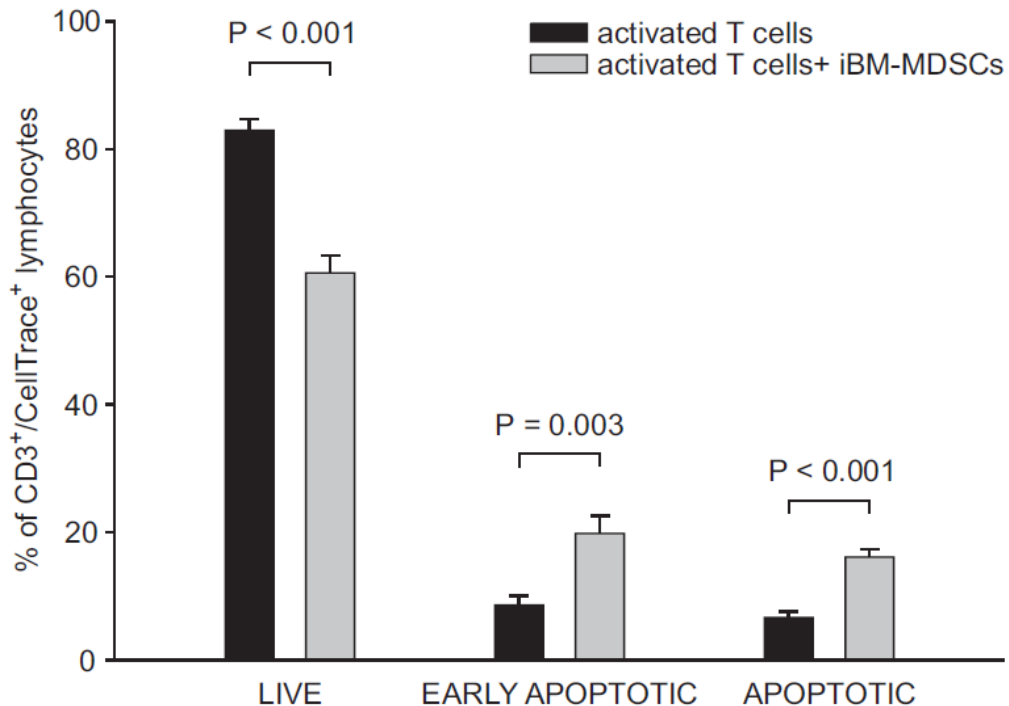


**Figure 14: Analysis of apoptosis induction on T cells cultured with iBM-MDSCs**

CellTrace-labelled PBMCs were cultured alone or in the presence of iBM-MDSCs for 4 days. Cultures were then harvested and cells were stained with anti-CD3, Annexin V and 7AAD, to discriminate among apoptotic, early apoptotic and live T lymphocytes. Gating strategy is shown in the upper panel. The histogram below shows the mean  $\pm$  SE of 8 independent experiments. Black bars refer to activated T cells alone, grey bars to activated T cells in the presence of iBM-MDSCs.

#### 4.8 MDSCs induce markers of cell exhaustion on T cells

We hypothesized that T cell exhaustion could be a mechanism of immune suppression induced by MDSCs. One of main features of T cell exhaustion, is the loss of function of CD8<sup>+</sup> and CD4<sup>+</sup> T cells, that gradually leads to dysfunctional T cells. Exhausted T cells are marked by the expression of inhibitory receptors that have a key role in this process. One of the best characterized pathway of exhaustion is represented by PD-1 and its ligand PD-L1 (also known as B7-H1) that has a critical role for CD8 T cell exhaustion in chronically infected mice <sup>171</sup>. In addition to PD-1, other cell surface inhibitory receptors regulate T cell exhaustion. Among them LAG-3, a CD4-related protein expressed on CD4<sup>+</sup> and CD8<sup>+</sup> T cells, negatively regulates T-cell expansion.

Since our results demonstrated that B7-H1 expression was up-regulated on iBM-MDSCs following culture with activated T cells, we tested the expression of PD-1

on T cell subsets of resting or activated T cells in the presence or absence of iBM-MDSC. This experiment showed that PD-1 was expressed at low level in resting T cells while cell activation caused a high increase in its expression (Figure 15). The addition in the culture of mBM-MDSCs did not change significantly the expression of PD-1 on activated T cells, as compared to activated T lymphocytes cultured alone. Instead, the presence of iBM-MDSCs caused a significant increase of PD-1 expression in CD8<sup>+</sup> T cells (Figure 15). These results show that PD-1 expression is mainly driven by T cell activation, although contact with iBM-MDSC can further up-regulate its expression mainly on CD8<sup>+</sup> T cells.

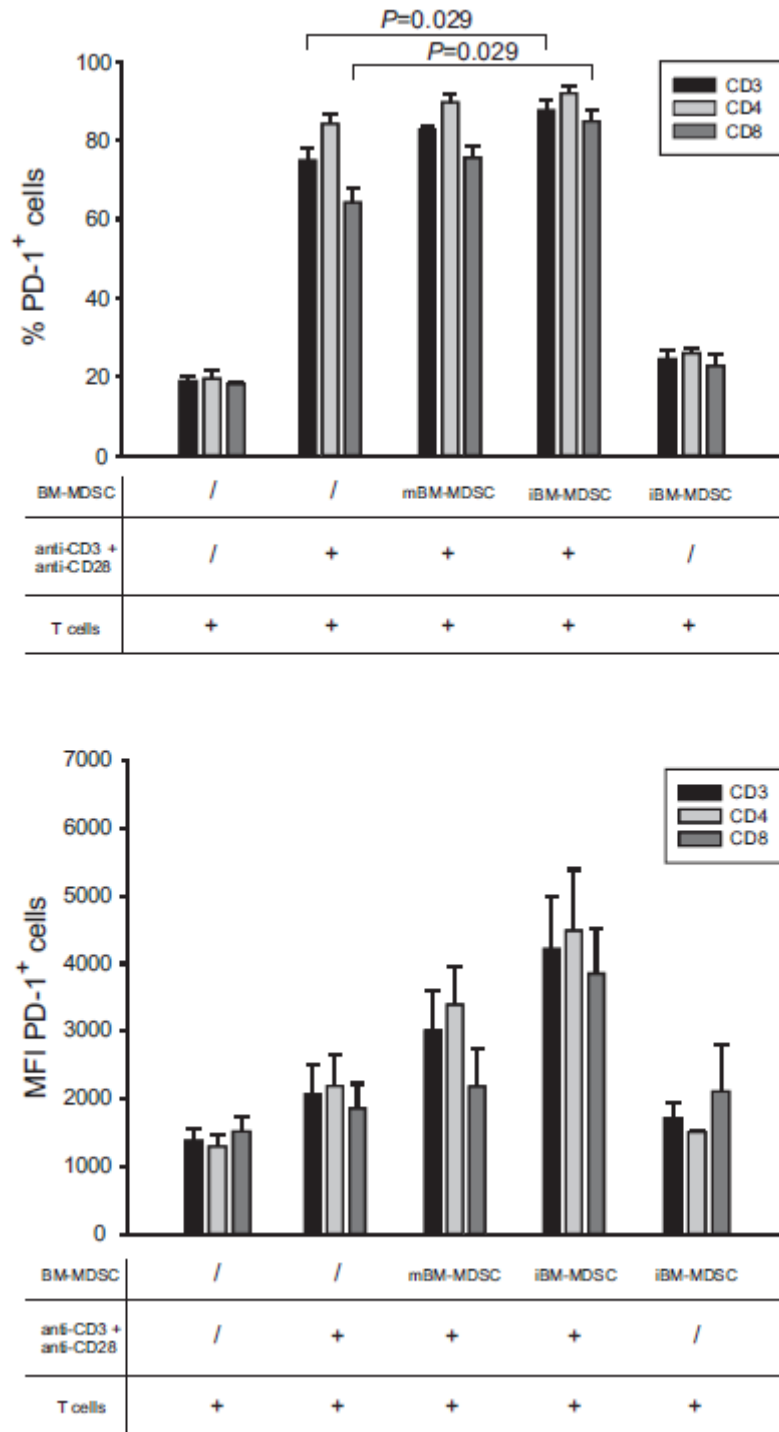


**Figure 15: Evaluation of PD-1 expression in T cell subsets.**

CellTrace-labelled PBMCs were cultured for 4 days alone or in the presence of mBM-MDSCs and iBM-MDSCs. Anti-CD3/CD28 antibodies were used to activate T cells. At the end of the culture, cells were harvested and stained with anti-CD3, anti-CD8 and anti-PD-1 and analyzed gating on CD3<sup>+</sup>/CellTrace<sup>+</sup> cells (CD3), CD3<sup>+</sup>/CellTrace<sup>+</sup>/CD8<sup>-</sup> cells (CD4) and on CD3<sup>+</sup>/CellTrace<sup>+</sup>/CD8<sup>+</sup> cells (CD8). The upper histogram shows the percentage of PD-1<sup>+</sup> cells in the three subsets of T lymphocytes, while the lower graph reports the MFI of PD-1 calculated in the same cells. The values reported are the mean  $\pm$  SE of three independent experiments. Student's t test was applied.

We next evaluated the expression of LAG-3, another marker of T cell exhaustion. This analysis was performed as previously described for PD-1 and in this case T cell activation induced only a slight up-regulation of this marker, while a significant intensity was reached with iBM-MDSCs (Figure 16) and we observed that the strongest increase both of the percentage and in the MFI of LAG-3<sup>+</sup> cells was induced in CD8<sup>+</sup> T cells. The addition of mBM-MDSCs caused only a slight increase of CD8<sup>+</sup> /LAG-3<sup>+</sup> cells, but had no effect on the other two T cell subsets, as compared to activated T cells alone (Figure 16, upper histogram). No statistically significant differences were observed between activated T cells alone and in the presence of mBM-MDSCs when considering the MFI of LAG-3<sup>+</sup> cells. Overall our results indicate that the expression of the markers LAG-3 and PD-1 on T cells suppressed by MDSCs is consistent with the phenotype of exhausted T cells.

Interestingly, it has been reported that LAG-3 is a natural ligand for MHC class II<sup>172</sup> and that it is a negative co-stimulatory receptor<sup>173</sup>. Moreover, recent preclinical studies documented a role for LAG-3 in CD8 T cell exhaustion<sup>171</sup>. We recently demonstrated that HLA-DR expression is increased in iBM-MDSCs co-cultured with activated T cells<sup>103</sup>. Since both LAG3 and HLA-DR expression are increased respectively in T lymphocytes and iBM-MDSCs when they are co-cultured, we speculate that the interaction between these two molecules may mediate the inhibitory signalling that leads to immunosuppression.

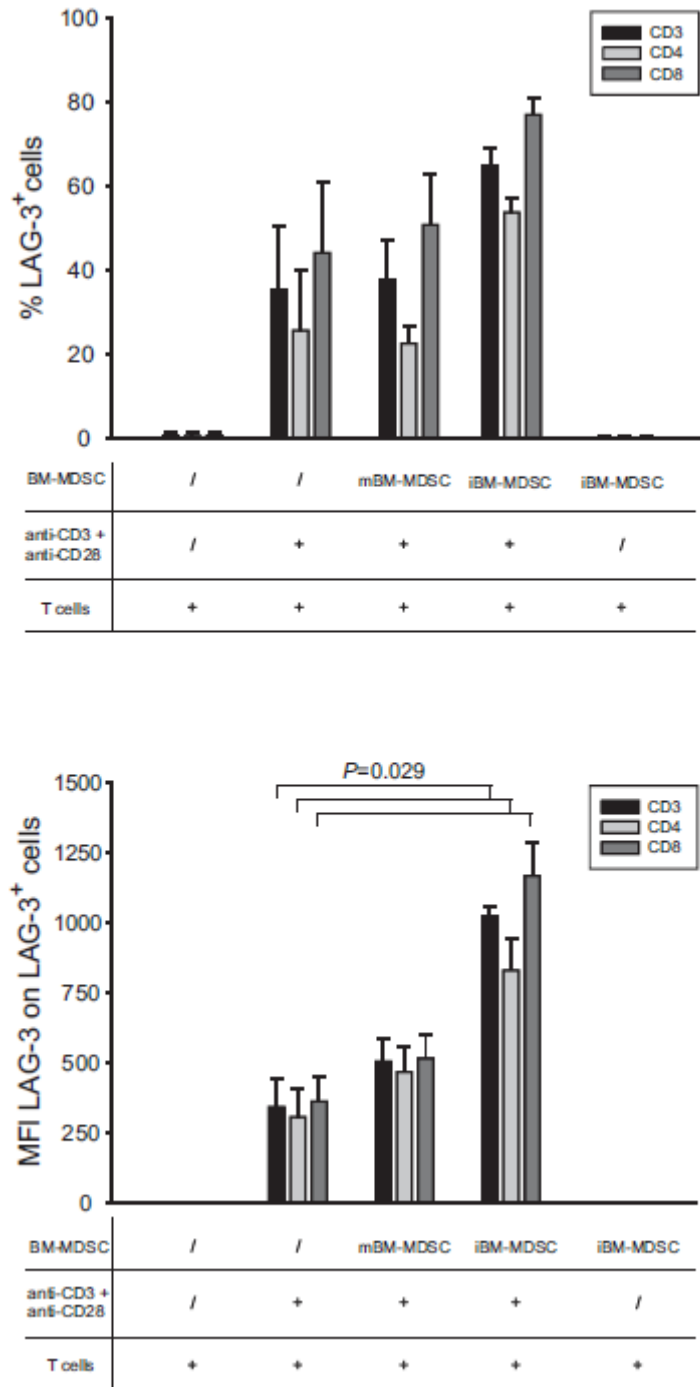


**Figure 16: Evaluation of LAG-3 expression in T cell subsets.**

CellTrace-labeled PBMCs were cultured for 4 days alone or in the presence of mBM-MDSCs and iBM-MDSCs. Anti-CD3/CD28 antibodies were used to activate T cells. At the end of the culture, cells were harvested and stained with anti-CD3, anti-CD8 and anti-LAG-3 and analyzed gating on CD3<sup>+</sup>/CellTrace<sup>+</sup> cells (CD3), CD3<sup>+</sup>/CellTrace<sup>+</sup>/CD8<sup>-</sup> cells (CD4) and on CD3<sup>+</sup>/CellTrace<sup>+</sup>/CD8<sup>+</sup> cells (CD8). The upper histogram shows the percentage of LAG-3<sup>+</sup> cells in the three subsets of T lymphocytes, while the lower graph reports the MFI of LAG-3 calculated in LAG-3<sup>+</sup> cells. The values reported are the mean ± SE of three independent experiments. Student's t test was applied.

#### **4.9 Analysis of myeloid cells present in liver metastases from colorectal cancer patients**

Thus far we have demonstrated that activated T cells induce the activation of signalling pathways in suppressive iBM-MDSCs. This result led us to hypothesize that normal promyelocytes, present in the bone marrow, can be primed with tumor-derived factors to acquire a suppressive phenotype and become MDSCs. We believe that these cells are equivalent to the MDSCs found in the blood stream and we name these cells “*unprimed MDSCs*” as they lack the markers of MDSCs found after contact with activated T cells, which, instead, we call “*effector MDSCs*”, since they activate their full suppressive ability. Our hypothesis relies on the fact that MDSCs are harmless when in contact with resting T cells, but acquire a suppressive phenotype only when required, and that this change in functional activity is driven by the activation state of the T cells. To verify if the mechanisms that we found to be active *in vitro* are the same driving immunosuppression *in vivo*, we studied myeloid and lymphoid cells present in liver metastases of colorectal cancer patients, since at this site “*effector MDSCs*” might be present. As we previously demonstrated that *in vitro*-derived MDSCs are equivalent to Lineage<sup>-</sup>/HLA-DR<sup>-</sup>/CD33<sup>+</sup>/CD11b<sup>+</sup> MDSCs expanded in peripheral blood of stage IV colorectal cancer patients<sup>103</sup>, we used this combination of markers to study myeloid cells in liver metastases from colorectal cancer patients. Thus far we could analyze only 3 samples and therefore this is only a preliminary study, whose results cannot be generalized but that may serve us to plan future directions in a higher cohort of samples. We noticed that in all 3 samples, among live leukocytes, a very small population of Lin<sup>-</sup>/HLA-DR<sup>-</sup>/CD33<sup>+</sup> cells is present and that this subset also expresses B7-H1 (Figure 17). Further studies are needed to verify these findings in a higher number of samples and also to determine if Lin<sup>-</sup>/HLA-DR<sup>-</sup>/CD33<sup>+</sup> cells present in liver metastases are endowed with suppressive activity and if B7-H1 is implied in the induction of immunosuppression. These studies are challenging due to the very low percentage of Lin<sup>-</sup>/HLA-DR<sup>-</sup>/CD33<sup>+</sup> cells present in tumor biopsies, we are therefore optimizing FACS sorting conditions in order to sort a sufficient number of cells that will be essayed in a functional assay.

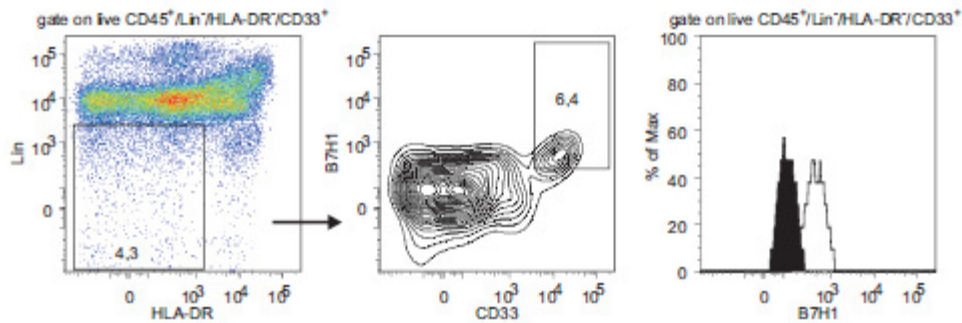


**Figure 17: Analysis of B7-H1 expression in myeloid cells present in liver metastases from colorectal cancer patients**

Cell suspension was obtained with enzymatic digestion from liver metastasis of colorectal cancer patients. Surface staining was performed and live leukocytes were analysed by gating on Live/dead<sup>-</sup>/Annexin<sup>-</sup>/CD45<sup>+</sup> cells, after doublets exclusion. B7-H1 expression was analyzed on Lin<sup>-</sup>/HLA-DR<sup>+</sup>/CD33<sup>+</sup> cells among live leukocytes, setting the gate on the basis of FMO, as negative control. The dotplots are representative of 3 independent experiments.

#### **4.10 Analysis of PD-1 and LAG-3 expression in T cells infiltrating liver metastases from colorectal cancer patients**

Since we demonstrated that T cells in the presence of iBM-MDSCs acquire a phenotype consistent with that of exhausted T cells, we studied the expression of exhaustion markers in the lymphocytic counterpart present in liver metastases from colorectal cancer patients. To this aim, we set up a multicolor flow cytometry staining to analyze PD-1 and LAG-3 expression in CD4<sup>+</sup> and CD8<sup>+</sup> T cell subsets. We noticed that PD-1 was expressed on both CD4<sup>+</sup> and CD8<sup>+</sup> T cells (Figure 18, upper panels), while LAG-3 was absent on both T cell subsets analyzed (Figure 18, lower panels). Albeit the role of LAG-3 and PD-1 in T cell exhaustion has been documented <sup>171</sup>, it was recently demonstrated that their expression can be modulated also by T cell differentiation and from the degree of T cell activation <sup>174</sup>. Therefore we are planning to expand this analysis on a larger number of biopsies in order to perform other phenotypic and functional studies and determine if T cells present in liver metastases of colorectal cancer patients are functionally exhausted.

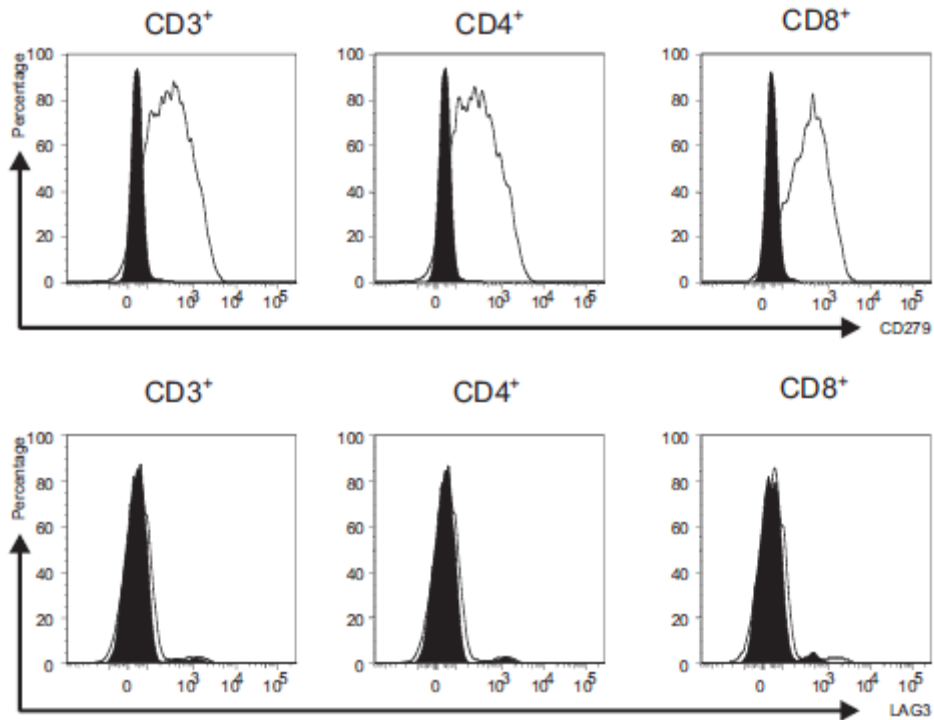


**Figure 18: Analysis of PD-1 and LAG-3 expression in T cells present in liver metastases from colorectal cancer patients.**

Cell suspension was obtained with enzymatic digestion from liver metastases of colorectal cancer patients. If necessary, red blood cell lysis was performed. Surface staining was performed and live leukocytes were analysed by gating on Live/dead<sup>-</sup>/Annexin<sup>-</sup>/CD45<sup>+</sup> cells, after doublets exclusion. PD-1 and LAG-3 expressions were analysed on CD3<sup>+</sup> cells (CD3), on CD3<sup>+</sup>/CD8<sup>-</sup> (CD4) cells and on CD3<sup>+</sup>/CD8<sup>+</sup> (CD8) cells among live leukocytes, setting the gate on the basis of FMO, as negative control (black histogram). The dotplots are representative of 3 independent experiments.

## 5. DISCUSSION

Increasing evidence shows that myeloid-derived suppressor cells play a key role in the inhibition of immune responses of cancer patients and that their expansion is correlated to tumor burden and poor OS. Some of the mechanisms involved in the immunosuppressive activity of MDSCs have been studied in different tumor models, but a clear picture is still lacking.

Our group demonstrated that G-CSF and GM-CSF are growth factors able to induce the expansion of immature myeloid cells from bone marrow precursors and that these *in vitro*-derived cells are endowed with immunosuppressive activity. The inhibition of T cell proliferation was dependent on cell-to-cell contact and C/EBP $\beta$  was shown to be a key transcription factor involved in immunosuppressive activity. Since MDSCs derived from BM cells are a very heterogeneous cell population, a deeper phenotypic and functional characterization was performed and revealed that only the most immature subset, resembling to promyelocytes, was responsible of the inhibition of T cell proliferation. The phenotype and suppressive capability of these cells was influenced by the degree of activation of T lymphocytes, in fact the presence of mitogen-activated T cells enhanced the immunosuppression mediated by MDSCs and maintained their immature phenotype. These results indicated the existence of a cross-talk between MDSCs and activated T cells at the basis of immunosuppression.

On the basis of these results, we investigated at molecular level potential mechanisms involved in the interplay between MDSCs and activated T cells and found that a loop involving surface molecules and a soluble factor is set in motion when the two cells interact.

We found that IL-10 is released by activated T cells and this, in turn, lead to the activation of STAT3 in both cell types. Interestingly, a similar mechanism was reported also for murine macrophages stimulated with CpG interacting with CD4<sup>+</sup> T cells activated by anti-CD3/CD28<sup>175</sup>. Under these conditions the cell-to-cell contact led to an increase in IL-10 production in both cell types. Through the use

of the STAT3 inhibitor NSC 74859 it was demonstrated that the activation of STAT3 in CD4<sup>+</sup> T cells was responsible of the production of IL-10<sup>175</sup>.

We demonstrated that in our model, STAT3 activation was sustained by IL-10 signalling, although a low level of activation was observed also in MDSCs before the contact with activated T cells. This was probably due to the fact that MDSCs were derived by using the combination of G-CSF and GM-CSF and it is known that both cytokines signal through STAT3<sup>105,176</sup>. Studies performed in a murine model with conditional deletion of STAT3 in the bone marrow proved that hematopoietic progenitor cells and myeloid precursors deleted for STAT3 were refractory to G-CSF treatment. These studies also demonstrated that STAT3 directly controls G-CSF-dependent expression of C/EBP $\beta$ <sup>177</sup>, a transcription factor with a crucial role in emergency granulopoiesis and that, as already mentioned, is also critically involved in MDSC immunosuppressive activity<sup>80</sup>. The involvement of STAT3 in MDSC expansion was proved in studies carried out with a mouse model with conditional STAT3 gene disruption in myeloid cells that reported a significant reduction in granulocytic MDSCs<sup>178</sup>. As for the mechanism of action, it is known that STAT3 can modulate MDSC expansion by the up-regulation of the myeloid-related protein S100A9, a member of the large family of S100 proteins that forms a dimer with S100A8. The up-regulation of this protein in hematopoietic progenitor cells of colon carcinoma-bearing mice was associated to the expansion of MDSCs and to the impaired differentiation of DCs<sup>47</sup>. CD14<sup>+</sup>/S100A9<sup>+</sup> MDSCs were reported to be expanded also in NSCLC patients and to suppress T cell proliferation via iNOS, ARG1, IL-10 and the IL-13/IL-4R $\alpha$  pathway<sup>179</sup>. ARG1 was expressed also on CD14<sup>+</sup>/HLA-DR<sup>low/-</sup> MDSCs on HNSCC patients and it was demonstrated that STAT3 activation could lead to ARG1 expression by binding to its promoter<sup>180</sup>. Therefore STAT3 can regulate MDSC expansion and activity by activating different signalling pathways.

In this study we also demonstrated that STAT3 phosphorylation leads to the expression of B7-H1, a molecule that can negatively regulate immune responses by interacting with its receptor PD-1 on lymphocytes. B7-H1 was reported to be expressed on MDSCs obtained from ascites and spleens of mice bearing the 1D8 ovarian carcinoma and caused immunosuppression by interacting with PD-1 on Treg cells<sup>149</sup>. Another work performed on a mouse model of *ret* melanoma

reported the expression of B7-H1, B7-H3 and B7-H4 on MDSCs and demonstrated that the expression of these molecules was dependent on the interaction between MDSCs and Treg cells<sup>181</sup>.

We focused our attention on the B7-H1 molecule since it is known that STAT3 binding sites are present on the promoter of B7-H1 gene<sup>169</sup>. Moreover, studies performed on patients infected with HIV revealed that, during infection, PD-1 is up-regulated on monocytes and that the interaction of PD-1 with B7-H1, expressed on other cell types, induced IL-10 production that in turn led to CD4<sup>+</sup> T cell dysfunction<sup>182</sup>. Moreover, IL-10 can modulate PD-L1 up-regulation on human macrophages during HIV infection<sup>183</sup>. To the best of our knowledge, this is the first characterization in human MDSCs of a signalling pathway driven by IL-10 that, through the activation of STAT3, leads to the expression of B7-H1. A similar loop was described for human monocyte-derived DCs differentiated in the presence of TLR agonists. These DCs acquired a tolerogenic function that was dependent on MAPK-induced IL-6 and IL-10 production, which drives STAT-3 mediated B7-H1 expression<sup>184,185</sup>. We believe that also in MDSCs there is a possible involvement of IL-6 signalling since we have evidence that this cytokine is induced in MDSC, (Pinton, unpublished results)

On the whole these data suggested us that IL-10, STAT3 and B7-H1 were interesting targets to inhibit MDSC activity, but when we tested inhibitors for these molecules in the culture between activated T cells and MDSCs, only the block of STAT3 activation rescued T cell proliferation. Probably, the inhibition of IL-10 alone is not sufficient to block MDSC activity because a residual level of STAT3 activation is still present in the presence of IL-10 blocking Ab. Also the inhibition of B7-H1 interaction with its receptor PD-1 did not rescue T cell proliferation, although we believe that these molecules are critically involved in immunosuppression. In fact, preliminary results obtained in our laboratory demonstrate that, among MDSCs, only the subset expressing B7-H1 is able to inhibit T cell proliferation. Moreover, we have evidence that besides the triggering of PD-1 by B7-H1, also the binding of the co-inhibitory receptor LAG-3 to its ligand MHC-II is involved in the interplay between MDSCs and activated T cells. Therefore, the inhibition of the axis B7-H1/PD-1 alone is probably not sufficient to restore T cell proliferation.

It is known that STAT3 controls a vast array of target genes and thus, in order to understand if there are other signalling pathways that might be activated by STAT3 in MDSCs, we analysed its validated targets. Besides the genes, we found one miRNA that is of particular interest for us. In fact, we recently performed a miRNA expression analysis, in which we compared MDSCs derived after cytokine treatment with *ex vivo* sorted promyelocytes and also MDSCs sorted after contact with activated T cells as compared to MDSCs before contact, and under this condition, miR-155 is always significantly up-regulated. This finding is in line with a recent work in which a miRNA expression analysis was carried out on murine MDSCs derived *in vitro* from BM cells treated with the cytokines GM-CSF and IL-6 as compared to *ex vivo* cells, and they also found that the most up-regulated miRNA was miR-155, together with miR-21. Moreover, this work showed that miR-155 and miR-21 have a synergistic effect on MDSC induction by targeting SHIP-1 and PTEN, respectively, leading to STAT3 activation <sup>186</sup>.

A recent study reported that MDSCs present in breast cancer tissues inhibited T cell proliferation and induced apoptosis in T cells in an IDO-dependent manner. IDO expression was up-regulated in MDSCs induced from healthy donors umbilical cord blood and its expression was dependent on STAT3 activation <sup>187</sup>. In line with these results, we have preliminary data suggesting IDO involvement in the mechanism of action of *in vitro* generated MDSCs. Since IDO is not present among validated targets of STAT3, we are planning new experiments to test the effect of Stattic, the inhibitor of STAT3 phosphorylation, on the expression of IDO in MDSCs induced *in vitro*.

Besides the characterization of the molecular mechanisms active in MDSCs, we also evaluated the fate of suppressed T cells and since the reduction in the T cell viability due to apoptosis was not enough to account by itself for the immunosuppression exerted by MDSCs, we searched for additional mechanisms of T cell impairment. We focused on T cell exhaustion, that was initially studied in chronic viral infections, in particular in LCMV <sup>171</sup>, but that was reported to have a role also in promoting tumor escape. We evaluated the expression of PD-1 and LAG-3 on suppressed T cells, two markers that have been related to T cell exhaustion and indeed we found the up-regulation of PD-1 on suppressed CD8<sup>+</sup> T cells and the increase of LAG-3 expression both on CD4<sup>+</sup> and CD8<sup>+</sup> T

lymphocytes cultured with MDSCs. LAG-3 is a CD4 homologue expressed by many cells of the hematopoietic lineage, such as B, NK,  $\gamma\delta$  T cells, activated T cells, Tregs and TILs<sup>188,189</sup> and its expression negatively regulate proliferation, activation and homeostasis of T cells. LAG-3 is known to interact with MHC-II with high affinity and it was reported that blocking LAG-3/MHC-II interaction by the use of a mAb anti-LAG-3 increased the number of CD4<sup>+</sup> and CD8<sup>+</sup> T cells entering division, after stimulation with APCs and low antigen concentrations<sup>190</sup>. Since our *in vitro*-derived MDSCs express MHC-II and this molecule is further increased by the contact with activated T cells, we speculate that an interaction between HLA class II and LAG-3 could be a critical mechanism that mediate the induction of immunosuppression. This hypothesis is supported by a study performed in mouse models and demonstrating that CD4<sup>+</sup> T cell tolerance depended on MHC-II expression. Interestingly, cell-to-cell contact between CD4<sup>+</sup> T cells and MDSCs could enhance the immunosuppressive activity of MDSCs by cross-linking of MHC-II<sup>191</sup>. Although the exact mechanism of MHC class II regulation in MDSC is not clear, STAT3 might play a role in this effect because several cytokines produced by the tumors trigger STAT3 signalling in myeloid cells and STAT3 up-regulation is a common finding in myeloid cells<sup>109,192,193</sup>. We speculate that the negative effect of MHC-II/LAG-3 interaction on T cell functionality might be enhanced by the binding of B7-H1, expressed on MDSCs, to its receptor PD-1, present on activated T lymphocytes. The synergistic effect of PD-1 and LAG-3 in promoting tumor immune escape was proved by a work analyzing CD8<sup>+</sup> T cells specific for NY-ESO-1 (a “cancer-testis” antigen) present in peripheral blood or tumor site in patients with ovarian cancer. Interestingly, tumor-derived NY-ESO-1-specific CD8<sup>+</sup> T cells demonstrated impaired effector function and enriched co-expression of LAG-3 and PD-1, as compared to peripheral blood CD8<sup>+</sup> T lymphocytes. Expression of LAG-3 and PD-1 was up-regulated by IL-10, IL-6 and tumor-derived APCs. Functional analysis revealed that CD8<sup>+</sup>/LAG-3<sup>+</sup>/PD-1<sup>+</sup> T cells were more impaired in IFN- $\gamma$  and TNF- $\alpha$  production as compared to LAG-3<sup>+</sup>/PD-1<sup>-</sup> or LAG-3<sup>-</sup>/PD-1<sup>-</sup> CD8<sup>+</sup> T cells (Matsuzaki et al). The synergistic effect of PD-1 and LAG-3 in the impairment of immune responses has been demonstrated also in Sa1N- and MC38-inoculated mice. In fact the treatment with the combinatorial anti-LAG-3/anti-PD-1 immunotherapy demonstrated higher efficacy in tumor eradication and in the

enhancement of adaptive immune responses as compared to anti-LAG-3 and anti-PD-1 monotherapy<sup>194</sup>.

Studies related to LAG-3 and PD-1 therefore support our hypothesis that these molecules could be involved in T cell functional impairment mediated by MDSCs, and that their overexpression could be related to IL-10 signalling. However, a very recent study challenged the specificity of these molecules as markers of T cell exhaustion<sup>174</sup>. In fact, it was demonstrated that the expression of LAG-3, PD-1 and other inhibitory receptors changed in different subsets of CD8<sup>+</sup> T cells, on the basis of the degree of differentiation, and that the expression of multiple inhibitory receptors positively correlated to T cell activation<sup>174</sup>. To understand if MDSC-induced LAG-3 and PD-1 expression in activated T cells are really associated to T cell exhaustion, we are planning to perform a gene expression analysis on suppressed T cells to evaluate if they present a gene expression profile of exhausted T cells.

In conclusion, we demonstrated that IL-10 signalling through STAT3 leads to the expression on MDSCs of B7-H1 that, in turn, can interact with its receptor PD-1 on T cells. PD-1/B7-H1 and LAG-3/HLA class II interactions probably mediate T cell function impairment. All these results were obtained using an *in vitro* model of MDSC generation, however we are investigating if the same mechanisms are active also *in vivo* in cancer patients. To this aim, we analyzed both myeloid and lymphoid cells present in liver metastases of colorectal cancer patients. We identified B7-H1 expression on a small subset of cells that had the same phenotype of MDSCs<sup>67</sup>. However, to characterize these cells as MDSCs, we need to perform a functional assay to determine if this population of cells is endowed with suppressive activity and to test if B7-H1 plays a role in immunosuppression. By analysing CD4<sup>+</sup> and CD8<sup>+</sup> T cells present in liver metastases, we observed that PD-1 was expressed on both cell subsets, thus supporting the hypothesis of a possible interaction between B7-H1 and its receptor PD-1, while we did not observe LAG-3 expression on T cells. Since it was demonstrated that the expression of inhibitory receptors was dependent on the differentiation and activation state of T cells<sup>174</sup>, the absence of LAG-3 could be due to the fact that lymphocytes in the tumor microenvironment have a different phenotype and degree of activation compared to the *in vitro* conditions. Therefore,

further studies are needed to elucidate the mechanisms underlying immunosuppression at the tumor site.



## 6. REFERENCES

1. Burnet, M. Cancer: a biological approach. III. Viruses associated with neoplastic conditions. IV. Practical applications. *Br Med J* **1**, 841-847 (1957).
2. Burnet, F.M. The concept of immunological surveillance. *Prog Exp Tumor Res* **13**, 1-27 (1970).
3. Burnet, M. Immunological Factors in the Process of Carcinogenesis. *Br Med Bull* **20**, 154-158 (1964).
4. Stutman, O. Tumor development after 3-methylcholanthrene in immunologically deficient athymic-nude mice. *Science* **183**, 534-536 (1974).
5. Rygaard, J. & Povlsen, C.O. The mouse mutant nude does not develop spontaneous tumours. An argument against immunological surveillance. *Acta Pathol Microbiol Scand B Microbiol Immunol* **82**, 99-106 (1974).
6. Dunn, G.P., Bruce, A.T., Ikeda, H., Old, L.J. & Schreiber, R.D. Cancer immunoediting: from immunosurveillance to tumor escape. *Nat Immunol* **3**, 991-998 (2002).
7. Vesely, M.D. & Schreiber, R.D. Cancer immunoediting: antigens, mechanisms, and implications to cancer immunotherapy. *Ann N Y Acad Sci* **1284**, 1-5 (2013).
8. Maeurer, M.J., *et al.* Tumor escape from immune recognition: lethal recurrent melanoma in a patient associated with downregulation of the peptide transporter protein TAP-1 and loss of expression of the immunodominant MART-1/Melan-A antigen. *J Clin Invest* **98**, 1633-1641 (1996).
9. Kim, U., Baumler, A., Carruthers, C. & Bielat, K. Immunological escape mechanism in spontaneously metastasizing mammary tumors. *Proc Natl Acad Sci U S A* **72**, 1012-1016 (1975).
10. Vasmel, W.L., Sijts, E.J., Leupers, C.J., Matthews, E.A. & Melief, C.J. Primary virus-induced lymphomas evade T cell immunity by failure to express viral antigens. *J Exp Med* **169**, 1233-1254 (1989).
11. Hicklin, D.J., Marincola, F.M. & Ferrone, S. HLA class I antigen downregulation in human cancers: T-cell immunotherapy revives an old story. *Mol Med Today* **5**, 178-186 (1999).
12. Garrido, F., *et al.* Implications for immunosurveillance of altered HLA class I phenotypes in human tumours. *Immunol Today* **18**, 89-95 (1997).
13. Stackpole, C.W., Cremona, P., Leonard, C. & Stremmel, P. Antigenic modulation as a mechanism for tumor escape from immune destruction: identification of modulation-positive and modulation-negative mouse lymphomas with xenoantisera to murine leukemia virus gp70. *J Immunol* **125**, 1715-1723 (1980).
14. Elgert, K.D., Alleva, D.G. & Mullins, D.W. Tumor-induced immune dysfunction: the macrophage connection. *J Leukoc Biol* **64**, 275-290 (1998).
15. Chouaib, S., Asselin-Paturel, C., Mami-Chouaib, F., Caignard, A. & Blay, J.Y. The host-tumor immune conflict: from immunosuppression to resistance and destruction. *Immunol Today* **18**, 493-497 (1997).
16. Igney, F.H. & Krammer, P.H. Immune escape of tumors: apoptosis resistance and tumor counterattack. *J Leukoc Biol* **71**, 907-920 (2002).

17. Maeda, H. & Shiraishi, A. TGF-beta contributes to the shift toward Th2-type responses through direct and IL-10-mediated pathways in tumor-bearing mice. *J Immunol* **156**, 73-78 (1996).
18. Qin, Z., *et al.* B cells inhibit induction of T cell-dependent tumor immunity. *Nat Med* **4**, 627-630 (1998).
19. Soliman, H., Mediavilla-Varela, M. & Antonia, S. Indoleamine 2,3-dioxygenase: is it an immune suppressor? *Cancer J* **16**, 354-359 (2010).
20. Zou, W. & Chen, L. Inhibitory B7-family molecules in the tumour microenvironment. *Nat Rev Immunol* **8**, 467-477 (2008).
21. Nuckel, H., Rebmann, V., Durig, J., Duhrsen, U. & Grosse-Wilde, H. HLA-G expression is associated with an unfavorable outcome and immunodeficiency in chronic lymphocytic leukemia. *Blood* **105**, 1694-1698 (2005).
22. Bossard, C., *et al.* HLA-E/beta2 microglobulin overexpression in colorectal cancer is associated with recruitment of inhibitory immune cells and tumor progression. *Int J Cancer* **131**, 855-863 (2012).
23. Pollard, J.W. Trophic macrophages in development and disease. *Nat Rev Immunol* **9**, 259-270 (2009).
24. Egeblad, M., Nakasone, E.S. & Werb, Z. Tumors as organs: complex tissues that interface with the entire organism. *Dev Cell* **18**, 884-901 (2010).
25. Fridlender, Z.G., *et al.* Polarization of tumor-associated neutrophil phenotype by TGF-beta: "N1" versus "N2" TAN. *Cancer Cell* **16**, 183-194 (2009).
26. Nozawa, H., Chiu, C. & Hanahan, D. Infiltrating neutrophils mediate the initial angiogenic switch in a mouse model of multistage carcinogenesis. *Proc Natl Acad Sci U S A* **103**, 12493-12498 (2006).
27. Shojaei, F., Singh, M., Thompson, J.D. & Ferrara, N. Role of Bv8 in neutrophil-dependent angiogenesis in a transgenic model of cancer progression. *Proc Natl Acad Sci U S A* **105**, 2640-2645 (2008).
28. Schmielau, J. & Finn, O.J. Activated granulocytes and granulocyte-derived hydrogen peroxide are the underlying mechanism of suppression of t-cell function in advanced cancer patients. *Cancer Res* **61**, 4756-4760 (2001).
29. Coussens, L.M., *et al.* Inflammatory mast cells up-regulate angiogenesis during squamous epithelial carcinogenesis. *Genes Dev* **13**, 1382-1397 (1999).
30. Zou, W., *et al.* Stromal-derived factor-1 in human tumors recruits and alters the function of plasmacytoid precursor dendritic cells. *Nat Med* **7**, 1339-1346 (2001).
31. Munn, D.H., *et al.* Potential regulatory function of human dendritic cells expressing indoleamine 2,3-dioxygenase. *Science* **297**, 1867-1870 (2002).
32. Hawiger, D., *et al.* Dendritic cells induce peripheral T cell unresponsiveness under steady state conditions in vivo. *J Exp Med* **194**, 769-779 (2001).
33. Bacchetta, R., Gregori, S. & Roncarolo, M.G. CD4+ regulatory T cells: mechanisms of induction and effector function. *Autoimmun Rev* **4**, 491-496 (2005).
34. Sakaguchi, S. Naturally arising CD4+ regulatory t cells for immunologic self-tolerance and negative control of immune responses. *Annu Rev Immunol* **22**, 531-562 (2004).

35. Curiel, T.J. Regulatory T cells and treatment of cancer. *Curr Opin Immunol* **20**, 241-246 (2008).
36. Chioda, M., *et al.* Myeloid cell diversification and complexity: an old concept with new turns in oncology. *Cancer Metastasis Rev* **30**, 27-43 (2011).
37. Gabrilovich, D.I. & Nagaraj, S. Myeloid-derived suppressor cells as regulators of the immune system. *Nat Rev Immunol* **9**, 162-174 (2009).
38. Peranzoni, E., *et al.* Myeloid-derived suppressor cell heterogeneity and subset definition. *Curr Opin Immunol* **22**, 238-244 (2010).
39. Dolcetti, L., *et al.* Myeloid-derived suppressor cell role in tumor-related inflammation. *Cancer Lett* **267**, 216-225 (2008).
40. Sica, A. & Bronte, V. Altered macrophage differentiation and immune dysfunction in tumor development. *J Clin Invest* **117**, 1155-1166 (2007).
41. Talmadge, J.E. & Gabrilovich, D.I. History of myeloid-derived suppressor cells. *Nat Rev Cancer* **13**, 739-752 (2013).
42. Najjar, Y.G. & Finke, J.H. Clinical perspectives on targeting of myeloid derived suppressor cells in the treatment of cancer. *Front Oncol* **3**, 49 (2013).
43. Rodriguez, P.C., *et al.* Arginase I in myeloid suppressor cells is induced by COX-2 in lung carcinoma. *J Exp Med* **202**, 931-939 (2005).
44. Sinha, P., Clements, V.K., Fulton, A.M. & Ostrand-Rosenberg, S. Prostaglandin E2 promotes tumor progression by inducing myeloid-derived suppressor cells. *Cancer Res* **67**, 4507-4513 (2007).
45. Sinha, P., *et al.* Proinflammatory S100 proteins regulate the accumulation of myeloid-derived suppressor cells. *J Immunol* **181**, 4666-4675 (2008).
46. Ostrand-Rosenberg, S. Myeloid-derived suppressor cells: more mechanisms for inhibiting antitumor immunity. *Cancer Immunol Immunother* **59**, 1593-1600 (2010).
47. Cheng, P., *et al.* Inhibition of dendritic cell differentiation and accumulation of myeloid-derived suppressor cells in cancer is regulated by S100A9 protein. *J Exp Med* **205**, 2235-2249 (2008).
48. Pan, P.Y., *et al.* Reversion of immune tolerance in advanced malignancy: modulation of myeloid-derived suppressor cell development by blockade of stem-cell factor function. *Blood* **111**, 219-228 (2008).
49. Solheim, J.C., *et al.* Spleen but not tumor infiltration by dendritic and T cells is increased by intravenous adenovirus-Flt3 ligand injection. *Cancer Gene Ther* **14**, 364-371 (2007).
50. Sawanobori, Y., *et al.* Chemokine-mediated rapid turnover of myeloid-derived suppressor cells in tumor-bearing mice. *Blood* **111**, 5457-5466 (2008).
51. Markiewski, M.M., *et al.* Modulation of the antitumor immune response by complement. *Nat Immunol* **9**, 1225-1235 (2008).
52. Dolcetti, L., *et al.* Hierarchy of immunosuppressive strength among myeloid-derived suppressor cell subsets is determined by GM-CSF. *Eur J Immunol* **40**, 22-35 (2010).
53. Filipazzi, P., *et al.* Identification of a new subset of myeloid suppressor cells in peripheral blood of melanoma patients with modulation by a granulocyte-macrophage colony-stimulation factor-based antitumor vaccine. *J Clin Oncol* **25**, 2546-2553 (2007).

54. Waight, J.D., Hu, Q., Miller, A., Liu, S. & Abrams, S.I. Tumor-derived G-CSF facilitates neoplastic growth through a granulocytic myeloid-derived suppressor cell-dependent mechanism. *PLoS One* **6**, e27690 (2011).
55. Bunt, S.K., *et al.* Reduced inflammation in the tumor microenvironment delays the accumulation of myeloid-derived suppressor cells and limits tumor progression. *Cancer Res* **67**, 10019-10026 (2007).
56. Bronte, V., *et al.* Apoptotic death of CD8+ T lymphocytes after immunization: induction of a suppressive population of Mac-1+/Gr-1+ cells. *J Immunol* **161**, 5313-5320 (1998).
57. Kusmartsev, S. & Gabrilovich, D.I. Immature myeloid cells and cancer-associated immune suppression. *Cancer Immunol Immunother* **51**, 293-298 (2002).
58. Gabrilovich, D.I., Ostrand-Rosenberg, S. & Bronte, V. Coordinated regulation of myeloid cells by tumours. *Nat Rev Immunol* **12**, 253-268 (2012).
59. Haile, L.A., Gamrekelashvili, J., Manns, M.P., Korangy, F. & Greten, T.F. CD49d is a new marker for distinct myeloid-derived suppressor cell subpopulations in mice. *J Immunol* **185**, 203-210 (2010).
60. Youn, J.I., Nagaraj, S., Collazo, M. & Gabrilovich, D.I. Subsets of myeloid-derived suppressor cells in tumor-bearing mice. *J Immunol* **181**, 5791-5802 (2008).
61. Youn, J.I. & Gabrilovich, D.I. The biology of myeloid-derived suppressor cells: the blessing and the curse of morphological and functional heterogeneity. *Eur J Immunol* **40**, 2969-2975 (2010).
62. Youn, J.I., *et al.* Enhanced delivery efficiency of recombinant adenovirus into tumor and mesenchymal stem cells by a novel PTD. *Cancer Gene Ther* **15**, 703-712 (2008).
63. Montero, A.J., Diaz-Montero, C.M., Kyriakopoulos, C.E., Bronte, V. & Mandruzzato, S. Myeloid-derived suppressor cells in cancer patients: a clinical perspective. *J Immunother* **35**, 107-115 (2012).
64. Greten, T.F., Manns, M.P. & Korangy, F. Myeloid derived suppressor cells in human diseases. *Int Immunopharmacol* **11**, 802-807 (2011).
65. Mandruzzato, S., *et al.* IL4Ralpha+ myeloid-derived suppressor cell expansion in cancer patients. *J Immunol* **182**, 6562-6568 (2009).
66. Gallina, G., *et al.* Tumors induce a subset of inflammatory monocytes with immunosuppressive activity on CD8+ T cells. *J Clin Invest* **116**, 2777-2790 (2006).
67. Diaz-Montero, C.M., *et al.* Increased circulating myeloid-derived suppressor cells correlate with clinical cancer stage, metastatic tumor burden, and doxorubicin-cyclophosphamide chemotherapy. *Cancer Immunol Immunother* **58**, 49-59 (2009).
68. Zhang, H., *et al.* Fibrocytes represent a novel MDSC subset circulating in patients with metastatic cancer. *Blood* **122**, 1105-1113 (2013).
69. Walter, S., *et al.* Multipptide immune response to cancer vaccine IMA901 after single-dose cyclophosphamide associates with longer patient survival. *Nat Med* **18**, 1254-1261 (2012).
70. Grohmann, U. & Bronte, V. Control of immune response by amino acid metabolism. *Immunol Rev* **236**, 243-264 (2010).
71. Sippel, T.R., *et al.* Neutrophil degranulation and immunosuppression in patients with GBM: restoration of cellular immune function by targeting arginase I. *Clin Cancer Res* **17**, 6992-7002 (2011).

72. Srivastava, M.K., Sinha, P., Clements, V.K., Rodriguez, P. & Ostrand-Rosenberg, S. Myeloid-derived suppressor cells inhibit T-cell activation by depleting cystine and cysteine. *Cancer Res* **70**, 68-77 (2010).
73. Boulland, M.L., *et al.* Human IL4I1 is a secreted L-phenylalanine oxidase expressed by mature dendritic cells that inhibits T-lymphocyte proliferation. *Blood* **110**, 220-227 (2007).
74. Rodriguez, P.C. & Ochoa, A.C. Arginine regulation by myeloid derived suppressor cells and tolerance in cancer: mechanisms and therapeutic perspectives. *Immunol Rev* **222**, 180-191 (2008).
75. Lambeth, J.D. NOX enzymes and the biology of reactive oxygen. *Nat Rev Immunol* **4**, 181-189 (2004).
76. Lu, T. & Gabrilovich, D.I. Molecular pathways: tumor-infiltrating myeloid cells and reactive oxygen species in regulation of tumor microenvironment. *Clin Cancer Res* **18**, 4877-4882 (2012).
77. Beckman, J.S. & Koppenol, W.H. Nitric oxide, superoxide, and peroxynitrite: the good, the bad, and ugly. *Am J Physiol* **271**, C1424-1437 (1996).
78. Nagaraj, S., *et al.* Altered recognition of antigen is a mechanism of CD8+ T cell tolerance in cancer. *Nat Med* **13**, 828-835 (2007).
79. Molon, B., *et al.* Chemokine nitration prevents intratumoral infiltration of antigen-specific T cells. *J Exp Med* **208**, 1949-1962 (2011).
80. Marigo, I., *et al.* Tumor-induced tolerance and immune suppression depend on the C/EBPbeta transcription factor. *Immunity* **32**, 790-802 (2010).
81. Sonda, N., *et al.* miR-142-3p prevents macrophage differentiation during cancer-induced myelopoiesis. *Immunity* **38**, 1236-1249 (2013).
82. Wang, L., *et al.* Increased myeloid-derived suppressor cells in gastric cancer correlate with cancer stage and plasma S100A8/A9 proinflammatory proteins. *J Immunol* **190**, 794-804 (2013).
83. Mougiakakos, D., *et al.* Immunosuppressive CD14+HLA-DR<sup>low</sup>/neg IDO+ myeloid cells in patients following allogeneic hematopoietic stem cell transplantation. *Leukemia* **27**, 377-388 (2013).
84. Huang, B., *et al.* Gr-1+CD115+ immature myeloid suppressor cells mediate the development of tumor-induced T regulatory cells and T-cell anergy in tumor-bearing host. *Cancer Res* **66**, 1123-1131 (2006).
85. Nefedova, Y., *et al.* Mechanism of all-trans retinoic acid effect on tumor-associated myeloid-derived suppressor cells. *Cancer Res* **67**, 11021-11028 (2007).
86. Gabrilovich, D.I., Velders, M.P., Sotomayor, E.M. & Kast, W.M. Mechanism of immune dysfunction in cancer mediated by immature Gr-1+ myeloid cells. *J Immunol* **166**, 5398-5406 (2001).
87. Mirza, N., *et al.* All-trans-retinoic acid improves differentiation of myeloid cells and immune response in cancer patients. *Cancer Res* **66**, 9299-9307 (2006).
88. Lathers, D.M., Clark, J.I., Achille, N.J. & Young, M.R. Phase 1B study to improve immune responses in head and neck cancer patients using escalating doses of 25-hydroxyvitamin D3. *Cancer Immunol Immunother* **53**, 422-430 (2004).
89. Ko, J.S., *et al.* Sunitinib mediates reversal of myeloid-derived suppressor cell accumulation in renal cell carcinoma patients. *Clin Cancer Res* **15**, 2148-2157 (2009).

90. Ko, J.S., *et al.* Direct and differential suppression of myeloid-derived suppressor cell subsets by sunitinib is compartmentally constrained. *Cancer Res* **70**, 3526-3536 (2010).
91. Kujawski, M., *et al.* Stat3 mediates myeloid cell-dependent tumor angiogenesis in mice. *J Clin Invest* **118**, 3367-3377 (2008).
92. Xin, H., *et al.* Sunitinib inhibition of Stat3 induces renal cell carcinoma tumor cell apoptosis and reduces immunosuppressive cells. *Cancer Res* **69**, 2506-2513 (2009).
93. Suzuki, E., Kapoor, V., Jassar, A.S., Kaiser, L.R. & Albelda, S.M. Gemcitabine selectively eliminates splenic Gr-1+/CD11b+ myeloid suppressor cells in tumor-bearing animals and enhances antitumor immune activity. *Clin Cancer Res* **11**, 6713-6721 (2005).
94. Vincent, J., *et al.* 5-Fluorouracil selectively kills tumor-associated myeloid-derived suppressor cells resulting in enhanced T cell-dependent antitumor immunity. *Cancer Res* **70**, 3052-3061 (2010).
95. Kusmartsev, S., *et al.* Oxidative stress regulates expression of VEGFR1 in myeloid cells: link to tumor-induced immune suppression in renal cell carcinoma. *J Immunol* **181**, 346-353 (2008).
96. Rodriguez, P.C., *et al.* Arginase I-producing myeloid-derived suppressor cells in renal cell carcinoma are a subpopulation of activated granulocytes. *Cancer Res* **69**, 1553-1560 (2009).
97. Serafini, P., *et al.* Phosphodiesterase-5 inhibition augments endogenous antitumor immunity by reducing myeloid-derived suppressor cell function. *J Exp Med* **203**, 2691-2702 (2006).
98. Fujita, M., *et al.* COX-2 blockade suppresses gliomagenesis by inhibiting myeloid-derived suppressor cells. *Cancer Res* **71**, 2664-2674 (2011).
99. Obermajer, N., Muthuswamy, R., Odunsi, K., Edwards, R.P. & Kalinski, P. PGE(2)-induced CXCL12 production and CXCR4 expression controls the accumulation of human MDSCs in ovarian cancer environment. *Cancer Res* **71**, 7463-7470 (2011).
100. Nagaraj, S., *et al.* Anti-inflammatory triterpenoid blocks immune suppressive function of MDSCs and improves immune response in cancer. *Clin Cancer Res* **16**, 1812-1823 (2010).
101. Ugel, S., *et al.* Therapeutic targeting of myeloid-derived suppressor cells. *Curr Opin Pharmacol* **9**, 470-481 (2009).
102. Hirai, H., *et al.* C/EBPbeta is required for 'emergency' granulopoiesis. *Nat Immunol* **7**, 732-739 (2006).
103. Solito, S., *et al.* A human promyelocytic-like population is responsible for the immune suppression mediated by myeloid-derived suppressor cells. *Blood* **118**, 2254-2265 (2011).
104. Almand, B., *et al.* Increased production of immature myeloid cells in cancer patients: a mechanism of immunosuppression in cancer. *J Immunol* **166**, 678-689 (2001).
105. Aggarwal, B.B., *et al.* Signal transducer and activator of transcription-3, inflammation, and cancer: how intimate is the relationship? *Ann N Y Acad Sci* **1171**, 59-76 (2009).
106. Wang, T., *et al.* Regulation of the innate and adaptive immune responses by Stat-3 signaling in tumor cells. *Nat Med* **10**, 48-54 (2004).
107. Burdelya, L., *et al.* Stat3 activity in melanoma cells affects migration of immune effector cells and nitric oxide-mediated antitumor effects. *J Immunol* **174**, 3925-3931 (2005).

108. Cheng, F., *et al.* A critical role for Stat3 signaling in immune tolerance. *Immunity* **19**, 425-436 (2003).
109. Kortylewski, M., *et al.* Inhibiting Stat3 signaling in the hematopoietic system elicits multicomponent antitumor immunity. *Nat Med* **11**, 1314-1321 (2005).
110. Nefedova, Y., *et al.* Regulation of dendritic cell differentiation and antitumor immune response in cancer by pharmacologic-selective inhibition of the janus-activated kinase 2/signal transducers and activators of transcription 3 pathway. *Cancer Res* **65**, 9525-9535 (2005).
111. Nefedova, Y., *et al.* Hyperactivation of STAT3 is involved in abnormal differentiation of dendritic cells in cancer. *J Immunol* **172**, 464-474 (2004).
112. Darnell, J.E., Jr., Kerr, I.M. & Stark, G.R. Jak-STAT pathways and transcriptional activation in response to IFNs and other extracellular signaling proteins. *Science* **264**, 1415-1421 (1994).
113. Yokogami, K., Wakisaka, S., Avruch, J. & Reeves, S.A. Serine phosphorylation and maximal activation of STAT3 during CNTF signaling is mediated by the rapamycin target mTOR. *Curr Biol* **10**, 47-50 (2000).
114. Yuan, L., Wang, J. & Shen, W.C. Reversible lipidization prolongs the pharmacological effect, plasma duration, and liver retention of octreotide. *Pharm Res* **22**, 220-227 (2005).
115. Caldenhoven, E., *et al.* STAT3beta, a splice variant of transcription factor STAT3, is a dominant negative regulator of transcription. *J Biol Chem* **271**, 13221-13227 (1996).
116. Huang, Y., *et al.* Stat3 isoforms, alpha and beta, demonstrate distinct intracellular dynamics with prolonged nuclear retention of Stat3beta mapping to its unique C-terminal end. *J Biol Chem* **282**, 34958-34967 (2007).
117. Schaefer, T.S., Sanders, L.K., Park, O.K. & Nathans, D. Functional differences between Stat3alpha and Stat3beta. *Mol Cell Biol* **17**, 5307-5316 (1997).
118. Greaves, P. & Gribben, J.G. The role of B7 family molecules in hematologic malignancy. *Blood* **121**, 734-744 (2013).
119. Podojil, J.R. & Miller, S.D. Targeting the B7 family of co-stimulatory molecules: successes and challenges. *BioDrugs* **27**, 1-13 (2013).
120. Mueller, D.L., Jenkins, M.K. & Schwartz, R.H. Clonal expansion versus functional clonal inactivation: a costimulatory signalling pathway determines the outcome of T cell antigen receptor occupancy. *Annu Rev Immunol* **7**, 445-480 (1989).
121. Krummel, M.F. & Allison, J.P. CD28 and CTLA-4 have opposing effects on the response of T cells to stimulation. *J Exp Med* **182**, 459-465 (1995).
122. Parry, R.V., *et al.* CTLA-4 and PD-1 receptors inhibit T-cell activation by distinct mechanisms. *Mol Cell Biol* **25**, 9543-9553 (2005).
123. Nielsen, C., Hansen, D., Husby, S., Jacobsen, B.B. & Lillvang, S.T. Association of a putative regulatory polymorphism in the PD-1 gene with susceptibility to type 1 diabetes. *Tissue Antigens* **62**, 492-497 (2003).
124. Schwartz, R.H. Costimulation of T lymphocytes: the role of CD28, CTLA-4, and B7/BB1 in interleukin-2 production and immunotherapy. *Cell* **71**, 1065-1068 (1992).
125. Linsley, P.S., *et al.* CTLA-4 is a second receptor for the B cell activation antigen B7. *J Exp Med* **174**, 561-569 (1991).

126. Ramsay, A.G. Immune checkpoint blockade immunotherapy to activate anti-tumour T-cell immunity. *Br J Haematol* **162**, 313-325 (2013).
127. Merelli, B., Massi, D., Cattaneo, L. & Mandala, M. Targeting the PD1/PD-L1 axis in melanoma: Biological rationale, clinical challenges and opportunities. *Crit Rev Oncol Hematol* **89**, 140-165 (2014).
128. Brown, J.A., *et al.* Blockade of programmed death-1 ligands on dendritic cells enhances T cell activation and cytokine production. *J Immunol* **170**, 1257-1266 (2003).
129. Gianchecchi, E., Delfino, D.V. & Fierabracci, A. Recent insights into the role of the PD-1/PD-L1 pathway in immunological tolerance and autoimmunity. *Autoimmun Rev* **12**, 1091-1100 (2013).
130. Sun, M., *et al.* Characterization of mouse and human B7-H3 genes. *J Immunol* **168**, 6294-6297 (2002).
131. Nygren, M.K., Tekle, C., Ingebrigtsen, V.A. & Fodstad, O. B7-H3 and its relevance in cancer; immunological and non-immunological perspectives. *Front Biosci (Elite Ed)* **3**, 989-993 (2011).
132. Chapoval, A.I., *et al.* B7-H3: a costimulatory molecule for T cell activation and IFN-gamma production. *Nat Immunol* **2**, 269-274 (2001).
133. Castriconi, R., *et al.* Identification of 4Ig-B7-H3 as a neuroblastoma-associated molecule that exerts a protective role from an NK cell-mediated lysis. *Proc Natl Acad Sci U S A* **101**, 12640-12645 (2004).
134. Steinberger, P., *et al.* Molecular characterization of human 4Ig-B7-H3, a member of the B7 family with four Ig-like domains. *J Immunol* **172**, 2352-2359 (2004).
135. Ling, V., *et al.* Duplication of primate and rodent B7-H3 immunoglobulin V- and C-like domains: divergent history of functional redundancy and exon loss. *Genomics* **82**, 365-377 (2003).
136. Sun, J., *et al.* Origination of new immunological functions in the costimulatory molecule B7-H3: the role of exon duplication in evolution of the immune system. *PLoS One* **6**, e24751 (2011).
137. Sun, J., *et al.* Clinical significance of the induction of macrophage differentiation by the costimulatory molecule B7-H3 in human non-small cell lung cancer. *Oncol Lett* **6**, 1253-1260 (2013).
138. Kryczek, I., *et al.* B7-H4 expression identifies a novel suppressive macrophage population in human ovarian carcinoma. *J Exp Med* **203**, 871-881 (2006).
139. Kryczek, I., *et al.* Cutting edge: induction of B7-H4 on APCs through IL-10: novel suppressive mode for regulatory T cells. *J Immunol* **177**, 40-44 (2006).
140. Choi, I.H., *et al.* Genomic organization and expression analysis of B7-H4, an immune inhibitory molecule of the B7 family. *J Immunol* **171**, 4650-4654 (2003).
141. Krambeck, A.E., *et al.* B7-H4 expression in renal cell carcinoma and tumor vasculature: associations with cancer progression and survival. *Proc Natl Acad Sci U S A* **103**, 10391-10396 (2006).
142. Prasad, D.V., Richards, S., Mai, X.M. & Dong, C. B7S1, a novel B7 family member that negatively regulates T cell activation. *Immunity* **18**, 863-873 (2003).
143. Leung, J. & Suh, W.K. Host B7-H4 regulates antitumor T cell responses through inhibition of myeloid-derived suppressor cells in a 4T1 tumor transplantation model. *J Immunol* **190**, 6651-6661 (2013).

144. Zhao, R., *et al.* HHLA2 is a member of the B7 family and inhibits human CD4 and CD8 T-cell function. *Proc Natl Acad Sci U S A* **110**, 9879-9884 (2013).
145. Zhang, T., Wu, M.R. & Sentman, C.L. An NKp30-based chimeric antigen receptor promotes T cell effector functions and antitumor efficacy in vivo. *J Immunol* **189**, 2290-2299 (2012).
146. Fiegler, N., *et al.* Downregulation of the activating NKp30 ligand B7-H6 by HDAC inhibitors impairs tumor cell recognition by NK cells. *Blood* **122**, 684-693 (2013).
147. Wang, L., *et al.* VISTA, a novel mouse Ig superfamily ligand that negatively regulates T cell responses. *J Exp Med* **208**, 577-592 (2011).
148. Baecher-Allan, C., Brown, J.A., Freeman, G.J. & Hafler, D.A. CD4+CD25+ regulatory cells from human peripheral blood express very high levels of CD25 ex vivo. *Novartis Found Symp* **252**, 67-88; discussion 88-91, 106-114 (2003).
149. Liu, Y., Zeng, B., Zhang, Z., Zhang, Y. & Yang, R. B7-H1 on myeloid-derived suppressor cells in immune suppression by a mouse model of ovarian cancer. *Clin Immunol* **129**, 471-481 (2008).
150. Thompson, R.H., *et al.* Costimulatory B7-H1 in renal cell carcinoma patients: Indicator of tumor aggressiveness and potential therapeutic target. *Proc Natl Acad Sci U S A* **101**, 17174-17179 (2004).
151. Topalian, S.L., *et al.* Safety, activity, and immune correlates of anti-PD-1 antibody in cancer. *N Engl J Med* **366**, 2443-2454 (2012).
152. Brahmer, J.R., *et al.* Safety and activity of anti-PD-L1 antibody in patients with advanced cancer. *N Engl J Med* **366**, 2455-2465 (2012).
153. Crespo, J., Sun, H., Welling, T.H., Tian, Z. & Zou, W. T cell anergy, exhaustion, senescence, and stemness in the tumor microenvironment. *Curr Opin Immunol* **25**, 214-221 (2013).
154. Zheng, Y., Zha, Y., Driessens, G., Locke, F. & Gajewski, T.F. Transcriptional regulator early growth response gene 2 (Egr2) is required for T cell anergy in vitro and in vivo. *J Exp Med* **209**, 2157-2163 (2012).
155. Boussiotis, V.A., Freeman, G.J., Berezovskaya, A., Barber, D.L. & Nadler, L.M. Maintenance of human T cell anergy: blocking of IL-2 gene transcription by activated Rap1. *Science* **278**, 124-128 (1997).
156. Dolmetsch, R.E., Xu, K. & Lewis, R.S. Calcium oscillations increase the efficiency and specificity of gene expression. *Nature* **392**, 933-936 (1998).
157. Wells, A.D. New insights into the molecular basis of T cell anergy: anergy factors, avoidance sensors, and epigenetic imprinting. *J Immunol* **182**, 7331-7341 (2009).
158. Wherry, E.J. T cell exhaustion. *Nat Immunol* **12**, 492-499 (2011).
159. Barber, D.L., *et al.* Restoring function in exhausted CD8 T cells during chronic viral infection. *Nature* **439**, 682-687 (2006).
160. Riley, J.L. PD-1 signaling in primary T cells. *Immunol Rev* **229**, 114-125 (2009).
161. Effros, R.B. Replicative senescence in the immune system: impact of the Hayflick limit on T-cell function in the elderly. *Am J Hum Genet* **62**, 1003-1007 (1998).
162. Appay, V., *et al.* HIV-specific CD8(+) T cells produce antiviral cytokines but are impaired in cytolytic function. *J Exp Med* **192**, 63-75 (2000).

163. Montes, C.L., *et al.* Tumor-induced senescent T cells with suppressor function: a potential form of tumor immune evasion. *Cancer Res* **68**, 870-879 (2008).
164. Meloni, F., *et al.* Foxp3 expressing CD4+ CD25+ and CD8+CD28- T regulatory cells in the peripheral blood of patients with lung cancer and pleural mesothelioma. *Hum Immunol* **67**, 1-12 (2006).
165. Tsukishiro, T., Donnenberg, A.D. & Whiteside, T.L. Rapid turnover of the CD8(+)/CD28(-) T-cell subset of effector cells in the circulation of patients with head and neck cancer. *Cancer Immunol Immunother* **52**, 599-607 (2003).
166. Zhu, C., *et al.* The Tim-3 ligand galectin-9 negatively regulates T helper type 1 immunity. *Nat Immunol* **6**, 1245-1252 (2005).
167. Rangachari, M., *et al.* Bat3 promotes T cell responses and autoimmunity by repressing Tim-3-mediated cell death and exhaustion. *Nat Med* **18**, 1394-1400 (2012).
168. Williams, L., Bradley, L., Smith, A. & Foxwell, B. Signal transducer and activator of transcription 3 is the dominant mediator of the anti-inflammatory effects of IL-10 in human macrophages. *J Immunol* **172**, 567-576 (2004).
169. Marzec, M., *et al.* Oncogenic kinase NPM/ALK induces through STAT3 expression of immunosuppressive protein CD274 (PD-L1, B7-H1). *Proc Natl Acad Sci U S A* **105**, 20852-20857 (2008).
170. He, M., Xu, Z., Ding, T., Kuang, D.M. & Zheng, L. MicroRNA-155 regulates inflammatory cytokine production in tumor-associated macrophages via targeting C/EBPbeta. *Cellular & molecular immunology* **6**, 343-352 (2009).
171. Blackburn, S.D., *et al.* Coregulation of CD8+ T cell exhaustion by multiple inhibitory receptors during chronic viral infection. *Nat Immunol* **10**, 29-37 (2009).
172. Liang, B., *et al.* Regulatory T cells inhibit dendritic cells by lymphocyte activation gene-3 engagement of MHC class II. *J Immunol* **180**, 5916-5926 (2008).
173. Siero, S., Romero, P. & Speiser, D.E. The CD4-like molecule LAG-3, biology and therapeutic applications. *Expert opinion on therapeutic targets* **15**, 91-101 (2011).
174. Legat, A., Speiser, D.E., Pircher, H., Zehn, D. & Fuertes Marraco, S.A. Inhibitory Receptor Expression Depends More Dominantly on Differentiation and Activation than "Exhaustion" of Human CD8 T Cells. *Front Immunol* **4**, 455 (2013).
175. Dibra, D. & Li, S. The cell-to-cell coordination between activated T cells and CpG-stimulated macrophages synergistically induce elevated levels of IL-10 via NF-kappaB1, STAT3, and CD40/CD154. *Cell Commun Signal* **11**, 95 (2013).
176. Panopoulos, A.D., *et al.* STAT3 governs distinct pathways in emergency granulopoiesis and mature neutrophils. *Blood* **108**, 3682-3690 (2006).
177. Zhang, H., *et al.* STAT3 controls myeloid progenitor growth during emergency granulopoiesis. *Blood* **116**, 2462-2471 (2010).
178. Abad, C., *et al.* Targeted STAT3 disruption in myeloid cells alters immunosuppressor cell abundance in a murine model of spontaneous medulloblastoma. *J Leukoc Biol* (2013).

179. Feng, P.H., *et al.* CD14(+)S100A9(+) monocytic myeloid-derived suppressor cells and their clinical relevance in non-small cell lung cancer. *Am J Respir Crit Care Med* **186**, 1025-1036 (2012).
180. Vasquez-Dunddel, D., *et al.* STAT3 regulates arginase-I in myeloid-derived suppressor cells from cancer patients. *J Clin Invest* **123**, 1580-1589 (2013).
181. Fujimura, T., Ring, S., Umansky, V., Mahnke, K. & Enk, A.H. Regulatory T cells stimulate B7-H1 expression in myeloid-derived suppressor cells in ret melanomas. *J Invest Dermatol* **132**, 1239-1246 (2012).
182. Said, E.A., *et al.* Programmed death-1-induced interleukin-10 production by monocytes impairs CD4+ T cell activation during HIV infection. *Nat Med* **16**, 452-459 (2010).
183. Rodriguez-Garcia, M., *et al.* Expression of PD-L1 and PD-L2 on human macrophages is up-regulated by HIV-1 and differentially modulated by IL-10. *J Leukoc Biol* **89**, 507-515 (2011).
184. Sumpter, T.L. & Thomson, A.W. The STATus of PD-L1 (B7-H1) on tolerogenic APCs. *Eur J Immunol* **41**, 286-290 (2011).
185. Wolfle, S.J., *et al.* PD-L1 expression on tolerogenic APCs is controlled by STAT-3. *Eur J Immunol* **41**, 413-424 (2011).
186. Li, L., *et al.* MicroRNA-155 and MicroRNA-21 Promote the Expansion of Functional Myeloid-Derived Suppressor Cells. *J Immunol* **192**, 1034-1043 (2014).
187. Yu, J., *et al.* Myeloid-derived suppressor cells suppress antitumor immune responses through IDO expression and correlate with lymph node metastasis in patients with breast cancer. *J Immunol* **190**, 3783-3797 (2013).
188. Kisielow, M., Kisielow, J., Capoferri-Sollami, G. & Karjalainen, K. Expression of lymphocyte activation gene 3 (LAG-3) on B cells is induced by T cells. *Eur J Immunol* **35**, 2081-2088 (2005).
189. Huang, C.T., *et al.* Role of LAG-3 in regulatory T cells. *Immunity* **21**, 503-513 (2004).
190. Macon-Lemaitre, L. & Triebel, F. The negative regulatory function of the lymphocyte-activation gene-3 co-receptor (CD223) on human T cells. *Immunology* **115**, 170-178 (2005).
191. Nagaraj, S., *et al.* Antigen-specific CD4(+) T cells regulate function of myeloid-derived suppressor cells in cancer via retrograde MHC class II signaling. *Cancer Res* **72**, 928-938 (2012).
192. Gabrilovich, D. Mechanisms and functional significance of tumour-induced dendritic-cell defects. *Nat Rev Immunol* **4**, 941-952 (2004).
193. Nefedova, Y. & Gabrilovich, D.I. Targeting of Jak/STAT pathway in antigen presenting cells in cancer. *Current cancer drug targets* **7**, 71-77 (2007).
194. Woo, S.R., *et al.* Immune inhibitory molecules LAG-3 and PD-1 synergistically regulate T-cell function to promote tumoral immune escape. *Cancer Res* **72**, 917-927 (2012).



## **RINGRAZIAMENTI**

Alla fine di questi tre anni, vorrei ringraziare in particolare la Dott.ssa Mandruzzato per avermi seguita nel mio percorso di dottorato e durante la stesura della tesi, il Dott. Bronte per la discussione critica dei risultati e la Prof.ssa Zanovello che, in qualità di direttrice della scuola di dottorato, si è occupata della mia formazione didattica e mi ha permesso di partecipare ad incontri nazionali ed internazionali tra dottorandi.

Un grazie a tutte le ragazze del laboratorio, in particolare a Samantha che mi ha insegnato molte tecniche di laboratorio e mi ha dato preziosi consigli durante tutto il triennio di dottorato e in quest'ultimo periodo di stesura della tesi, a Vera per il supporto morale, per aver condiviso le lunghe serate di analisi dei dati e per la consulenza farmacologica in caso di malattia, a Lisa per avermi insegnato a fare i Western Blot, per i consigli di biologia molecolare e per aver portato la sua allegria in laboratorio. Un grazie anche ad Angela per l'analisi bioinformatica e la consulenza statistica.

Vorrei ringraziare il gruppo del Prof. Basso, in particolare Samuela, per averci fornito i campioni di midollo osseo, e Chiara per il sorting delle cellule e il gruppo del Dott. Mocellin, in particolare Clara, per averci inviato le biopsie dei pazienti.

Un sincero ringraziamento va ai miei genitori e a mia sorella Lisa, per avermi supportato e sopportato nei numerosi momenti di difficoltà e per tutto il loro aiuto in questi tre anni.



## **APPENDIX I**



# blood

2011 118: 2254-2265  
Prepublished online July 6, 2011;  
doi:10.1182/blood-2010-12-325753

## **A human promyelocytic-like population is responsible for the immune suppression mediated by myeloid-derived suppressor cells**

Samantha Solito, Erika Falisi, Claudia Marcela Diaz-Montero, Andrea Doni, Laura Pinton, Antonio Rosato, Samuela Francescato, Giuseppe Basso, Paola Zanovello, Georgiana Onicescu, Elizabeth Garrett-Mayer, Alberto J. Montero, Vincenzo Bronte and Susanna Mandruzzato

---

Updated information and services can be found at:

<http://bloodjournal.hematologylibrary.org/content/118/8/2254.full.html>

Articles on similar topics can be found in the following Blood collections

[Immunobiology](#) (4651 articles)

[Phagocytes, Granulocytes, and Myelopoiesis](#) (267 articles)

---

Information about reproducing this article in parts or in its entirety may be found online at:

[http://bloodjournal.hematologylibrary.org/site/misc/rights.xhtml#repub\\_requests](http://bloodjournal.hematologylibrary.org/site/misc/rights.xhtml#repub_requests)

Information about ordering reprints may be found online at:

<http://bloodjournal.hematologylibrary.org/site/misc/rights.xhtml#reprints>

Information about subscriptions and ASH membership may be found online at:

<http://bloodjournal.hematologylibrary.org/site/subscriptions/index.xhtml>

Blood (print ISSN 0006-4971, online ISSN 1528-0020), is published weekly by the American Society of Hematology, 2021 L St, NW, Suite 900, Washington DC 20036.

Copyright 2011 by The American Society of Hematology; all rights reserved.



## A human promyelocytic-like population is responsible for the immune suppression mediated by myeloid-derived suppressor cells

Samantha Solito,<sup>1</sup> Erika Falisi,<sup>1</sup> Claudia Marcela Diaz-Montero,<sup>2</sup> Andrea Doni,<sup>3</sup> Laura Pinton,<sup>1</sup> Antonio Rosato,<sup>1-4</sup> Samuela Francescato,<sup>5</sup> Giuseppe Basso,<sup>5</sup> Paola Zanollo,<sup>1-4</sup> Georgiana Onicescu,<sup>6</sup> Elizabeth Garrett-Mayer,<sup>6</sup> Alberto J. Montero,<sup>2</sup> Vincenzo Bronte,<sup>4</sup> and Susanna Mandruzzato<sup>1-4</sup>

<sup>1</sup>Department of Oncology and Surgical Sciences, Oncology Section, University of Padova, Padova, Italy; <sup>2</sup>Department of Medicine, Sylvester Comprehensive Cancer Center, University of Miami, Miami, FL; <sup>3</sup>Laboratory of Immunology and Inflammation, Istituto Clinico Humanitas, Istituto Di Ricovero e Cura a Carattere Scientifico (IRCCS), Rozzano, Milan, Italy; <sup>4</sup>Istituto Oncologico Veneto IOV-IRCCS, Padova, Italy; <sup>5</sup>Laboratory of Oncohematology, Department of Pediatrics, University of Padova, Padova, Italy; and <sup>6</sup>Department of Medicine and Division of Biostatistics and Epidemiology, Medical University of South Carolina Hollings Cancer Center, Charleston, SC

**We recently demonstrated that human BM cells can be treated in vitro with defined growth factors to induce the rapid generation of myeloid-derived suppressor cells (MDSCs), hereafter defined as BM-MDSCs. Indeed, combination of G-CSF + GM-CSF led to the development of a heterogeneous mixture of immature myeloid cells ranging from myeloblasts to band cells that were able to suppress alloantigen- and mitogen-stimulated T lymphocytes. Here, we further investi-**

**gate the mechanism of suppression and define the cell subset that is fully responsible for BM-MDSC-mediated immune suppression. This population, which displays the structure and markers of promyelocytes, is however distinct from physiologic promyelocytes that, instead, are devoid of immunosuppressive function. In addition, we demonstrate that promyelocyte-like cells proliferate in the presence of activated lymphocytes and that, when these cells exert suppressive activity, they**

**do not differentiate but rather maintain their immature phenotype. Finally, we show that promyelocyte-like BM-MDSCs are equivalent to MDSCs present in the blood of patients with breast cancer and patients with colorectal cancer and that increased circulating levels of these immunosuppressive myeloid cells correlate with worse prognosis and radiographic progression. (*Blood*. 2011;118(8):2254-2265)**

### Introduction

One of the mechanisms of immune tolerance induced by cancer is based on the expansion of myeloid-derived suppressor cells (MDSCs), a heterogeneous population of immature myeloid cells, which accumulate in the blood, lymph nodes, BM, and tumor sites in patients and experimental animals with neoplasia, capable of inhibiting both adaptive and innate immunities.<sup>1,2</sup> The heterogeneity of MDSCs has always been a hallmark of this cell population since its original description, and many studies advanced that MDSCs might be composed of cells at several stages of differentiation of the myeloid lineage (Lin) sharing the same functional properties.<sup>2</sup> To explain this heterogeneity, it was advanced that the patterns of cytokines/chemokines that arm myeloid cells with inhibitory function may be tumor dependent. For all these reasons, MDSCs have been shown to express different surface markers, depending both on the stage of myeloid development examined and the differentiation context provided by factors secreted by cancer cells.

In this respect, we recently demonstrated that the cytokines GM-CSF, G-CSF, and IL-6 allowed a rapid generation of MDSCs from precursors present in human BM and that the immunoregulatory activity of BM-derived MDSCs (BM-MDSCs) depended on the C/EBP $\beta$  transcription factor.<sup>3</sup>

In the present study, we further characterized BM-MDSC mediated-immune suppression. Analogously to tumor-induced MD-

SCs, BM-MDSCs consist of a heterogeneous population of immature myeloid cells. We thus investigated whether the immune regulatory function of BM-MDSCs could be attributed to different myeloid subsets induced by cytokine treatment or rather to a specific subpopulation. Our results indicate that only one immature cell population, with structure and phenotype resembling promyelocytes, is responsible for the whole immune suppression mediated by BM-MDSCs and that a cell population with a similar phenotype is expanded in patients with breast cancer and patients with colorectal cancer.

### Methods

#### BM samples, human cohorts, and treatments

Fresh BM aspirate samples with normal cytologic characteristics were obtained from patients enrolled in the protocol AIEOP-BFM-ALL 2000, with suspected leukemia or lymphomas, patients with lymphatic leukemia after 78 days without recurrences, and patients with lymphatic leukemia after BM transplantation as a part of the diagnostic follow-up. Informed consent was obtained from all participating persons, in compliance with the Declaration of Helsinki, before the study that was approved by the ethics committee of the Azienda Ospedaliera of Padova. For more details, see supplemental Methods (available on the *Blood* Web site; see the Supplemental Materials link at the top of the online article).

Submitted December 20, 2010; accepted June 21, 2011. Prepublished online as *Blood* First Edition paper, July 6, 2011; DOI 10.1182/blood-2010-12-325753.

The publication costs of this article were defrayed in part by page charge payment. Therefore, and solely to indicate this fact, this article is hereby marked "advertisement" in accordance with 18 USC section 1734.

The online version of this article contains a data supplement.

© 2011 by The American Society of Hematology

BM aspirates were subjected to lysis to remove red blood cells, with a hypotonic solution of ammonium chloride. Cells were plated ( $2 \times 10^6$  cells/well) into a 24-well tissue culture plate (Becton Dickinson) in IMDM (Gibco Invitrogen) supplemented with 10% FBS (Gibco), 0.01M HEPES, penicillin/streptomycin, and  $\beta$ -mercaptoethanol. Cells were cultured with 40 ng/mL G-CSF and GM-CSF for 4 days at 37°C, 8% CO<sub>2</sub>. Human recombinant GM-CSF was a gift from J. F. Parkinson (Bayer Healthcare Pharmaceuticals), human recombinant G-CSF was purchased from Sanofi Aventis.

### Patients with solid tumors

Peripheral blood specimens were collected from patients with stage IV colorectal cancer ( $n = 25$ ) at the University of Miami Sylvester Comprehensive Cancer Center (UMSCC) and stage IV breast cancer ( $n = 25$ ) at UMSCC and at the Medical University of South Carolina Hollings Cancer Center starting a new line of therapy. Venous blood was collected in K2 EDTA lavender-topped tubes (BD) before initiation of therapy, after every other cycle of therapy, and at the time of progression. Protocol Review Committees at Hollings Cancer Center and UMSCC and Institutional Review Boards at both institutions approved this study. Written consent was obtained from all subjects.

### Patients with solid tumors: statistical

Random effects linear regression was used to model the association between MDSCs and time in responders and nonresponders. The outcome was log (MDSCs), and predictors were time, response status, and an interaction between time and response. Random intercepts were included to account for correlation of repeated measures of MDSCs over time from the same patients. The coefficient on the interaction term was tested to determine whether the change in MDSCs over time was the same compared with difference in responders and nonresponders whereby an  $\alpha$  level of 0.05 was used. Results were displayed graphically whereby each patient's MDSC responses are shown over time, with the estimated regression model shown as solid straight lines. Standard model diagnostics were used to ensure that assumptions about residuals were met. Kaplan-Meier analysis was used to estimate survival distributions, and differences in survival were tested with log-rank tests. Linear regression was used to determine association between circulating tumor cells (CTCs), Swenerton score (SS), and MDSCs, including estimation of slope, correlation coefficient, and statistical significance of the association. Overall survival (OS) was defined as time of study enrollment to date of death.

### Flow cytometric analysis, Abs, and reagents

Cells were harvested and incubated with FcReceptor (FcR) Blocking Reagent (Miltenyi Biotec) to saturate FcR and then labeled with monoclonal Abs. For a detailed description of the Abs and of the methods used for labeling, see supplemental Methods. Data acquisition was performed with FACSCalibur or LSRII flow cytometer (Becton Dickinson), and data were analyzed with FlowJo software (TreeStar Inc).

### Cytospin preparation

Cytospins were obtained by centrifuging  $1 \times 10^4$  cells on microscope slides and stained with May-Grünwald-Giemsa dye (Bio-Optica) for 5 and 15 minutes, respectively. Cell morphology was examined by microscopic evaluation of stained cells using a Leica DM 2000 microscope (Leica Microsystems) with Leica lenses at 40 $\times$  magnification and without immersion oil. Pictures were taken using a Leica DFC 295 camera (Vashaw Scientific Inc), acquired with Leica Acquisition Suite Version 3.5 (Meyer Instruments) and processed with Adobe Photoshop CSI (Adobe Systems).

### Confocal microscopic analysis

Cells were fixed with 4% paraformaldehyde on polylysinated 14-mm round Menzel-Glaser glass in the dark for 15 minutes at room temperature and permeabilized for 5 minutes with 0.1% Triton X-100 (Sigma-Aldrich) in PBS, pH 7.4, before incubation for 1 hour at room temperature with PBS

2% BSA (Sigma-Aldrich) and 5% normal goat serum (Sigma-Aldrich). Cells were stained with mAb diluted in PBS 0.5% Tween for 1 hour at room temperature in the dark. Slides were then washed with the same buffer and incubated with the secondary Abs for 1 hour at room temperature in the dark. For a detailed description of the Abs and of the methods used for confocal microscopy, see supplemental Methods.

### Separation of BM-MDSC subsets

Lin<sup>-</sup> and Lin<sup>+</sup> fractions were separated from BM-MDSCs with Lineage Cell Depletion Kit (Miltenyi Biotec), a magnetic labeling system for the depletion of mature hematopoietic cells, following the manufacturer's instructions.

Myeloid fractions were also separated through cell sorting. Briefly, single-cell suspensions of ex vivo BM or BM-MDSCs were stained with anti-CD11b-PE, anti-CD16-FITC, and anti-CD3 $\epsilon$ -PC7 and sorted on a MoFlo (DakoCytomation). CD11b<sup>low</sup>/<sup>-</sup>/CD16<sup>-</sup> cells, CD11b<sup>+</sup>/CD16<sup>-</sup> cells, and CD11b<sup>+</sup>/CD16<sup>+</sup> cells were isolated, excluding lymphocytes, on the basis of CD3 expression and forward/side scatter parameters. All the fractions were obtained with a purity of  $\geq 90\%$ . Alternatively, myeloid populations were isolated through 2 consecutive magnetic sortings; in the first round, BM-MDSCs were depleted of CD3 $\epsilon$ <sup>+</sup>/CD19<sup>+</sup>/CD56<sup>+</sup> lymphocytes, with a cocktail of immunomagnetic beads obtained by combining anti-human CD3 $\epsilon$ , CD19, and CD56 beads (Miltenyi Biotec). Subsequently, the CD3 $\epsilon$ <sup>+</sup>/CD19<sup>-</sup>/CD56<sup>-</sup> fraction was depleted of CD11b<sup>+</sup> cells with immunomagnetic anti-human CD11b beads (Miltenyi Biotec).

### CFSE or CellTrace labeling and proliferation assay

PBMCs were isolated from the peripheral blood of healthy donors by density centrifugation as described.<sup>4</sup> Cell purity was checked by FACS analysis on forward/side scatter parameters, and viability was checked by Trypan blue dye exclusion.

PBMCs were stained with CFSE (Invitrogen Molecular Probe; range, 2-4 $\mu$ M) or with 2 $\mu$ M CellTrace Violet Cell Proliferation Kit (Invitrogen Molecular Probe), according to the manufacturer's instructions. For a detailed description of the methods of the labeling and proliferation assay, see supplemental Methods.

### Isolation of human monocytes and granulocytes

Human granulocytes and PBMCs used for confocal microscopic analysis were obtained from peripheral blood of healthy donors, as described,<sup>4</sup> whereas human monocytes were prepared from PBMCs by short-term adherence to plastic. Briefly, PBMCs were isolated from leukocyte-enriched buffy coats (Transfusion Center) and incubated for 1 hour at 37°C and 5% CO<sub>2</sub> in flasks (Becton Dickinson) with the use of RPMI 1640 medium (Life Technologies) supplemented with 3% human serum. Nonadherent cells were removed by washing gently the flask with RPMI 1640 medium, and adherent monocytes were removed for successive analysis.

### Statistical analysis

The statistical significance to compare parametric groups was determined by the Student *t* test, whereas the Mann-Whitney *U* test was used to compare nonparametric groups. Values were considered statistically significant with  $P < .05$ . Absence of significance was not reported for brevity.

## Results

### BM-MDSCs down-regulate the CD3 $\zeta$ chain expression in CD8<sup>+</sup> T cells and require a cell-to-cell contact to inhibit alloantigen-activated T lymphocytes

BM-MDSCs consist of a heterogeneous combination of immature myeloid cells that, based on the combined staining with anti-CD11b and anti-CD16 Abs, can be qualified as differentiating cells that range from myeloblasts to band cells, albeit with variable

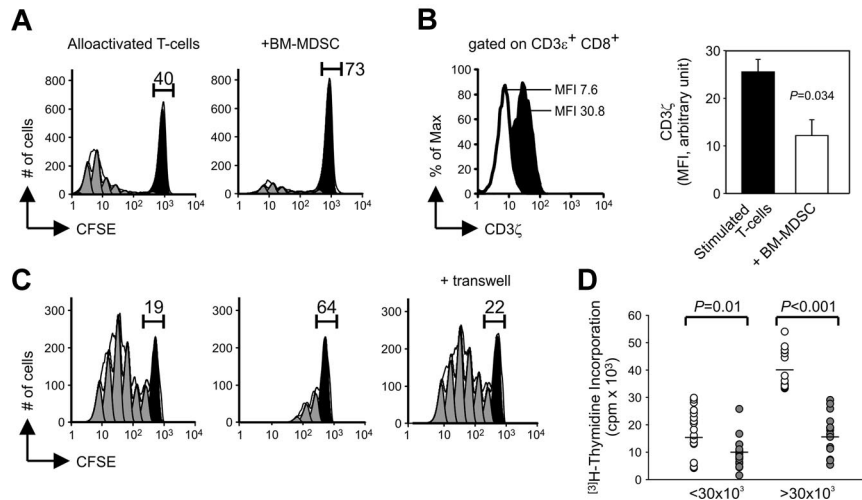


**Figure 1. Characterization of BM-MDSC-mediated immune suppression.** (A) CFSE-labeled PBMCs were stimulated with allogeneic  $\gamma$ -irradiated PBMCs without (left) or with (right)  $\gamma$ -irradiated BM-MDSCs added at a ratio of 1:1. After 7 days, cell cultures were harvested, labeled with anti-CD3 $\epsilon$ , and analyzed in the CD3 $\epsilon^+$ /CFSE $^+$  cell gate. The figure shows a representative experiment of cell division analysis of 3 performed. The percentages of the undivided cells are indicated. (B) After 7 days of culture, cultures set up as in panel A were labeled with anti-CD3 $\epsilon$ , anti-CD8, fixed, and then labeled with anti-CD3 $\zeta$ . Mean fluorescence intensity (MFI) of CD3 $\zeta$  was calculated in the CFSE $^+$ /CD3 $\epsilon^+$ /CD8 $^+$  cell gate. On the left panel, black histogram represents the MFI of stimulated PBMCs without BM-MDSCs, whereas the white histogram refers to MFI of stimulated PBMCs in presence of  $\gamma$ -irradiated BM-MDSCs. On the right panel, MFI values of CD3 $\zeta$  are presented as mean  $\pm$  SE of 3 independent experiments;  $P = .034$ , Student  $t$  test. (C) PBMCs were labeled with CFSE and stimulated with coated anti-CD3 and soluble anti-CD28 (left) and cocultured with BM-MDSCs in the presence (right) or in the absence (center) of a transwell. After 4 days, cells were harvested, labeled with anti-CD3 $\epsilon$ , and analyzed in the CD3 $\epsilon^+$ /CFSE $^+$  gate. The figure shows a representative experiment of 3. The percentages of the undivided cells are indicated. (D) Proliferation of alloactivated PBMCs cocultured either with or without  $\gamma$ -irradiated BM-MDSCs was assessed by  $^3\text{H}$ -thymidine incorporation. White dots represent the proliferation of stimulated PBMCs without BM-MDSCs, and gray dots correspond to the proliferation of alloactivated PBMCs in presence of BM-MDSCs. Twenty independent experiments are shown with proliferation of alloactivated PBMCs  $< 30 \times 10^3$  cpm (columns 1 and 2) and 15 experiments with proliferation  $> 30 \times 10^3$  cpm (columns 3 and 4).  $P = .01$  and  $P < .001$ , Mann-Whitney  $U$  test.

proportions in different cultures.<sup>3</sup> We initially addressed whether some of MDSC functional properties, described both in mice and patients with cancer, were also shared by BM-MDSCs. In this regard, one of the mechanisms proposed to explain T-cell dysfunction induced by MDSCs is the proliferative arrest of Ag-activated T cells caused by loss of CD3 $\zeta$  chain expression,<sup>5</sup> a proximal TCR-associated signaling molecule necessary for correct assembly and function of the TCR itself.

To understand whether BM-MDSC-mediated immune suppression induced a decrease in CD3 $\zeta$  expression, we set up allogeneic MLRs, with CFSE-labeled PBMCs that were stimulated with a pool of  $\gamma$ -irradiated allogeneic PBMCs and cocultured with  $\gamma$ -irradiated BM-MDSCs. After 7 days, cell cultures were harvested, and CD3 $\zeta$  chain expression was determined by intracellular staining after gating on CFSE $^+$ CD8 $^+$ CD3 $\epsilon^+$  cells. As shown in the representative experiment of Figure 1A, BM-MDSCs induced a marked decrease in T-lymphocyte proliferation, and this effect was accompanied by a significant reduction in the intracellular levels of CD3 $\zeta$  chain in CD8 $^+$  T cells cocultured with BM-MDSCs (Figure 1B); this result was also confirmed by gating on CFSE $^+$ CD8 $^+$  T cells (data not shown). Moreover the reduction of CD3 $\zeta$  chain expression was also accompanied by a decrease in the surface expression of CD3 $\epsilon$  chain (supplemental Figure 1A), implying that both chains might be the target of BM-MDSC activity; however, down-regulation of CD3 $\epsilon$  chain expression was less evident in comparison to CD3 $\zeta$  chain.

Several studies have shown that MDSCs inhibit immune responses through cell-to-cell contact;<sup>6,7</sup> to address this point, we set up cultures with CFSE-labeled PBMCs, which were stimulated with anti-CD3/CD28 and cocultured with BM-MDSCs, either in the presence or absence of a transwell. The insert ensures the flow of metabolites between the 2 chambers, so that if the immune suppression of BM-MDSCs depends exclusively on the release of soluble molecules, the separation would not prevent the suppres-

sive program of BM-MDSCs. As assessed by the reduction of the CFSE dilutions in PBMCs stimulated in the presence of BM-MDSCs compared with the control cultures without BM-MDSCs, an inhibitory effect was evident only in the presence of a cell-to-cell contact between lymphocytes and BM-MDSCs, because separation of BM-MDSCs by the insert did not affect T-cell proliferation (Figure 1C).

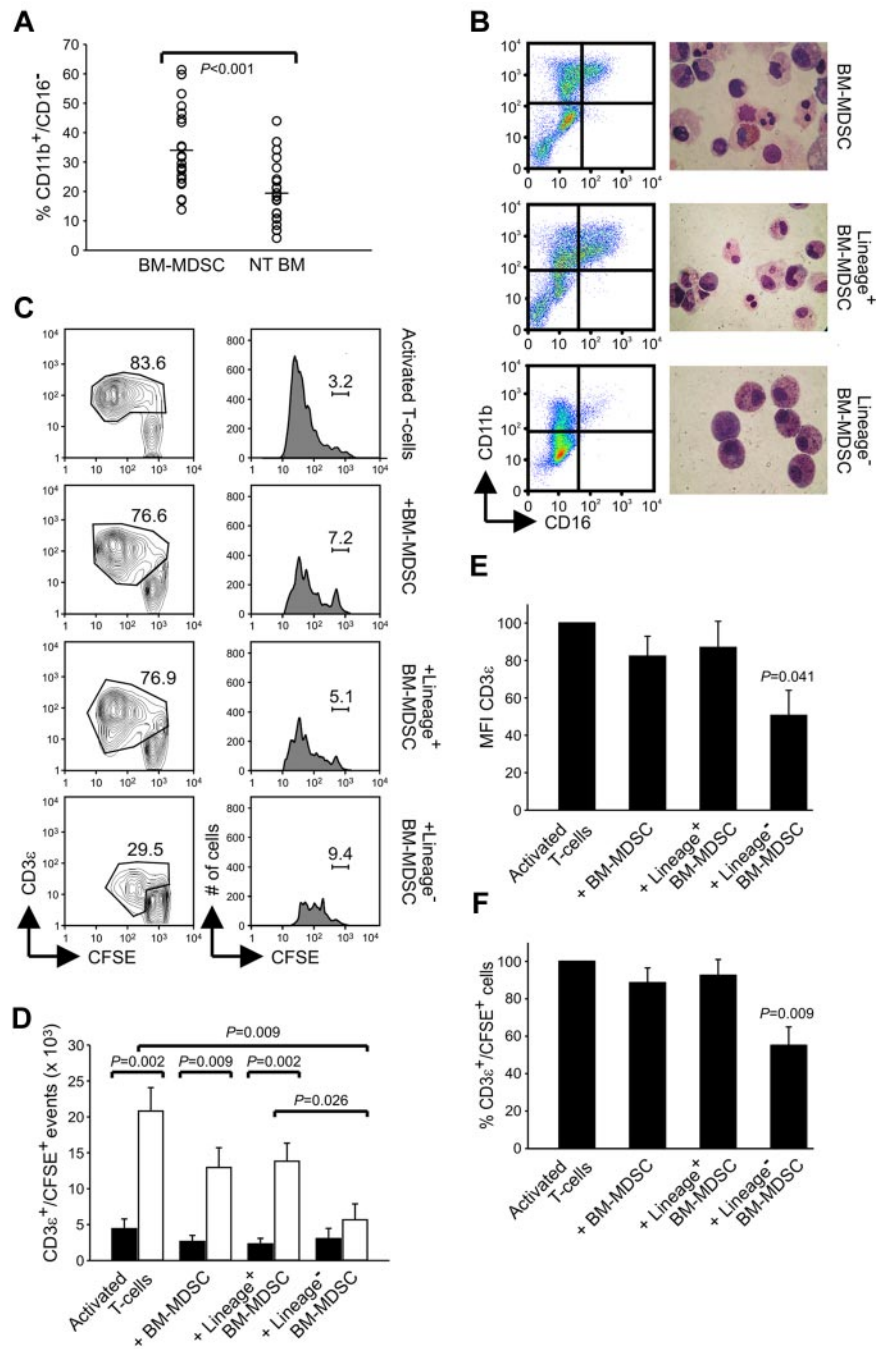
We also performed allogeneic MLRs in which the levels of suppression were evaluated through  $^3\text{H}$ TdR incorporation. MLRs were set up with different combinations of responder and stimulator PBMCs. In these experiments the proliferative rate of responder PBMCs varied, most probably as a result of the different HLA mismatches between effectors and stimulators, which influenced the magnitude of allogeneic response. Interestingly, we observed that in the presence of a high proliferation rate of responder PBMCs ( $> 30 \times 10^3$  cpm), BM-MDSCs could exert a significantly higher suppression of the proliferation, in comparison to a lower proliferation rate of responder lymphocytes (Figure 1D). Indeed, when we evaluated the ability of BM-MDSCs to suppress CD3/CD28-mediated T-lymphocyte activation, that is, a condition in which T lymphocytes are massively activated, suppression was achieved in  $> 90\%$  of the cases, that is, in a higher proportion of cases compared with alloantigen-specific MLRs (data not shown). These results suggest that MDSCs become fully competent in their suppressive function only in the presence of strongly activated T lymphocytes.

#### Lin $^-$ fraction of BM-MDSCs is responsible for the immune suppressive activity

As described earlier, the gradual increase of CD11b and CD16 expression is used to distinguish among all the differentiation stages of myeloid commitment. CD16 is considered a marker for mature myeloid cells; thus, the CD11b $^+$ /CD16 $^-$  cell subset represents a more immature myeloid population than the CD11b $^+$ /

**Figure 2. Lin<sup>-</sup> subset contained within BM-MDSCs shows potent suppressive activity.**

(A) Flow cytometric analysis of BM cells cultured for 4 days with G-CSF + GM-CSF (BM-MDSCs) or without growth factors (NT BM). At the end of the culture, cells were harvested and labeled, and the percentages of CD11b<sup>+</sup>/CD16<sup>-</sup> cells were calculated. The figure represents 22 independent experiments;  $P \leq .001$ , Student *t* test. (B) Flow cytometric profile of CD16 and CD11b expression and May-Grünwald-Giemsa staining on BM-MDSCs before and after immunomagnetic depletion with Lin Ab cocktail. (C) Flow cytometric analysis of the proliferation of allogeneic PBMCs, stained with CFSE and activated with anti-CD3 and anti-CD28 for 4 days, in the presence of either BM-MDSCs or the fractions Lin<sup>+</sup> or Lin<sup>-</sup> sorted from BM-MDSCs. The figure, in which the percentages of undivided CD3ε<sup>+</sup>/CFSE<sup>+</sup> lymphocytes are shown, represents 1 of 3 independent experiments. (D) Number of CD3ε<sup>+</sup>/CFSE<sup>+</sup> events obtained after activation of PBMCs with anti-CD3/CD28 and cocultured in the presence of BM-MDSCs or the subsets Lin<sup>+</sup> and Lin<sup>-</sup> sorted from BM-MDSCs. The figure, in which the black bars refer to undivided cells and the gray bars to divided cells, represent the mean ± SE of 6 independent experiments. The values of *P* are indicated in the figure, Mann-Whitney *U* test. (E-F) Evaluation of MFI of CD3ε chain expression and percentage of the CD3ε<sup>+</sup>/CFSE<sup>+</sup> cells in PBMCs stimulated with anti-CD3/CD28 in the presence of BM-MDSCs or the Lin<sup>+</sup> and Lin<sup>-</sup> fractions. Values are mean ± SE of 6 independent experiments. All comparisons among BM-MDSCs containing cultures versus cultures without BM-MDSCs,  $P = .041$  (E) and  $P = .009$  (F), respectively, Mann-Whitney *U* test.



CD16<sup>+</sup> cell subset.<sup>8</sup> We observed that the in vitro expansion of BM-MDSCs with the combination of G-CSF + GM-CSF gave rise to a significant increase in immature CD11b<sup>+</sup>/CD16<sup>-</sup> elements (Figure 2A;  $P < .001$  compared with untreated BM) and that the presence of these cells was correlated with induction of suppressive activity (data not shown).

Interestingly, other groups previously described in patients with cancer an expansion of Lin<sup>-</sup> population endowed with suppressive activity.<sup>9</sup> We thus decided to explore the function of more immature subsets among BM-MDSCs after cell enrichment by immunomagnetic sorting with a cocktail of Abs targeting Lin Ags, with the aim to deplete mature myeloid populations and B, T, and natural killer lymphocytes from BM-MDSC cultures. This negative-selection procedure yields a population of cells enriched in hematopoietic stem cells and very early myeloid progenitors that are CD11b<sup>low/-/</sup>

CD16<sup>-</sup> (Figure 2B). Although the cell purity is rather high in the Lin<sup>-</sup> fraction, the Lin<sup>+</sup> fraction was heterogeneous and still contained lymphocytes, mature, and immature myeloid cells. The structure of the different populations was examined by May-Grünwald-Giemsa staining of cytospin cell preparations and confirmed that unsorted BM-MDSCs were composed of both mononuclear and polymorphonuclear cells, whereas the Lin<sup>-</sup> fraction was mainly composed of large mononuclear cells (Figure 2B).

To test the suppressive activity of BM-MDSC fractions we measured the proliferation of T cells (allogeneic with respect to BM-MDSCs) by CFSE dilution after CD3/CD28 stimulation in the presence of unsorted, Lin<sup>-</sup>, or Lin<sup>+</sup> BM-MDSC cell subsets. In cultures of T cells stimulated with anti-CD3/CD28, the addition of whole BM-MDSCs caused both a moderate increase in undivided T-cell fraction and a strong reduction in the numbers of CFSE<sup>+</sup>

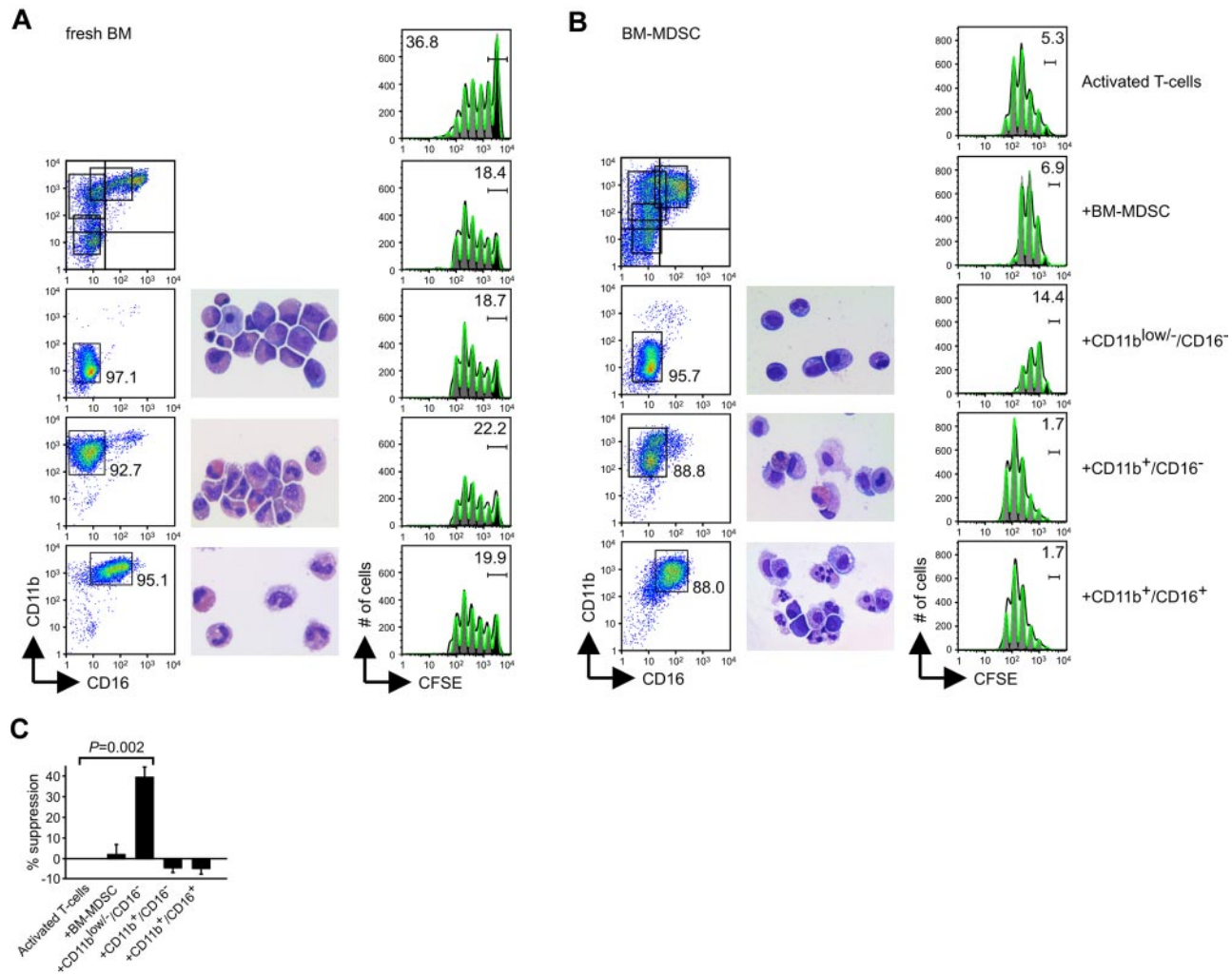


**Figure 3. CD11b<sup>low</sup>⁻/CD16<sup>-</sup> phenotype defines the subset responsible for the immune suppression in BM-MDSCs.** (A) Flow cytometric evaluation of CD11b and CD16 markers in BM-MDSC or sorted CD11b<sup>low</sup>⁻/CD16<sup>-</sup>, CD11b<sup>+</sup>/CD16<sup>-</sup> and CD11b<sup>+</sup>/CD16<sup>+</sup> cell populations from fresh BM samples (left), structural analysis by May-Grünwald-Giemsa staining (center), and CFSE dilution proliferation assay (right) in which values reported on histograms represent the percentages of cells in the parental, undivided generation. (B) Flow cytometric evaluation of CD11b and CD16 markers in BM-MDSCs or sorted CD11b<sup>low</sup>⁻/CD16<sup>-</sup>, CD11b<sup>+</sup>/CD16<sup>-</sup>, and CD11b<sup>+</sup>/CD16<sup>+</sup> cell populations from BM-MDSCs (left), structural analysis by May-Grünwald-Giemsa staining (center), and CFSE dilution proliferation assay (right) in which values reported on histograms represent the percentages of cells in the parental, undivided generation. (C) Suppression of allogenic CFSE<sup>+</sup> PBMCs activated with anti-CD3 and anti-CD28 and cocultured in the presence of 1:1 ratio of the different populations sorted from human BM-MDSCs. The suppression was calculated, analyzing the number of proliferating cells from generation 3 to generation 10, assumed to be 100% without BM-MDSCs. Mean ± SE of 3 independent experiments.  $P \leq .01$ , Student *t* test, all comparisons among BM-MDSCs containing cultures versus cultures without BM-MDSCs.

cells (Figure 2C-D). The Lin<sup>-</sup> fraction was endowed with the highest suppressive activity compared with both the unsorted population and the Lin<sup>+</sup> subset, which basically had the same suppressive ability of the unsorted BM-MDSCs (Figure 2C-D).

We also observed that levels of CD3ε chain expression in activated T cells suppressed by the Lin<sup>-</sup> subset of BM-MDSCs were constantly reduced in terms of MFI (Figure 2E) in all the experiments performed. This decrease in CD3ε expression was also accompanied by a significant reduction in the percentage of CD3ε<sup>+</sup>/CFSE<sup>+</sup> cells (Figure 2F), therefore suggesting that suppression by the Lin<sup>-</sup> subset of myeloid cells was mediated through a profound alteration of signaling machinery associated with a significant reduction in the numbers of CD3<sup>+</sup> T lymphocytes.

#### Suppressive activity of BM-MDSCs is entirely contained within the CD11b<sup>low</sup>⁻/CD16<sup>-</sup> cell subset

Experiments performed with the Lin<sup>-</sup> subset of BM-MDSCs highlighted that cells with the strongest suppressive activity were

present in this fraction, supporting data from other laboratories showing that MDSCs obtained from patients with cancer can be traced among Lin<sup>-</sup> cells.<sup>9</sup> However, this separation protocol does not allow to distinguish various differentiation stages during myeloid commitment. Therefore, to find out whether suppressive activity of BM-MDSCs was either shared by a number of immature subsets or limited to a specific differentiation stage, we separated defined myeloid subsets through cell sorting.

We sorted 3 different myeloid fractions from fresh BM and cultured BM-MDSCs, based on the expression levels of CD11b and CD16 Ags: the low/negative fraction CD11b<sup>low</sup>⁻/CD16<sup>-</sup>, the intermediate subset CD11b<sup>+</sup>/CD16<sup>-</sup>, and the double-positive fraction CD11b<sup>+</sup>/CD16<sup>+</sup>, as shown in Figure 3. Because BM-MDSCs do not contain mature granulocytes (CD11b<sup>+</sup>/CD16<sup>high</sup>), which are instead present in BM cells, we excluded from the analysis the mature granulocyte population (Figure 3A-B).

May-Grünwald-Giemsa staining showed that both unsorted fresh BM cells and cultured BM-MDSCs had an heterogeneous

structure, as confirmed by other phenotypical features; moreover, in our cell cultures we never found contaminating CD14<sup>+</sup>/CD15<sup>-</sup> macrophages that could contribute to suppressive activity of BM-MDSCs (data not shown). The CD11b<sup>low/-</sup>/CD16<sup>-</sup> subset isolated from fresh BM cells comprised cell elements with the appearance of myeloid progenitors and promyelocytes, whereas the corresponding subset isolated from BM-MDSCs contained basophilic cells, resembling promyelocytes (Figure 3A-B). The CD11b<sup>+</sup>/CD16<sup>-</sup> subset separated from fresh BM contained myelocytes, metamyelocytes, eosinophils, and monocytes, whereas BM-MDSCs included mainly cells resembling monocytes and eosinophils. At last, metamyelocytes and band cells were present among CD11b<sup>+</sup>/CD16<sup>+</sup> cells isolated from both populations.

When we tested the potential suppressive activity of the sorted subsets, only the CD11b<sup>low/-</sup>/CD16<sup>-</sup> cell population isolated from BM-MDSCs was able to suppress the proliferation of activated T cells, whereas the CD11b<sup>+</sup>/CD16<sup>-</sup> and CD11b<sup>+</sup>/CD16<sup>+</sup> cell subsets purified from BM-MDSCs were completely devoid of suppressive activity (Figure 3C). Cumulative data reported in Figure 3C show that the entire suppressive activity of BM-MDSCs is contained within a single subset of cytokine-conditioned promyelocytes, which were able not only to block lymphocyte proliferation but also to affect IFN- $\gamma$  production and to induce T-cell apoptosis (data not shown). None of the 3 corresponding subsets isolated from fresh BM cells was able to interfere with T-lymphocyte proliferation (Figure 3A), further highlighting that priming of BM cells with cytokines is mandatory to induce immunoregulatory MDSCs.

#### **Cytokine-stimulated CD11b<sup>low/-</sup>/CD16<sup>-</sup> cell subset consists of immature and large mononuclear myeloid cells**

The phenotype of the suppressive CD11b<sup>low/-</sup>/CD16<sup>-</sup> cell subset was further analyzed by flow cytometry. In the course of our attempt to increase the purity and to minimize the manipulation of sorted cells, we observed that the suppressive CD11b<sup>low/-</sup>/CD16<sup>-</sup> subset could be also separated through a progressive sorting with magnetic beads in which BM-MDSCs were first depleted of CD3<sup>+</sup>, CD19<sup>+</sup>, and CD56<sup>+</sup> cells, and the resulting population was then depleted of CD11b<sup>+</sup> cells. The remaining, negatively selected cell population (CD11b<sup>low/-</sup> BM-MDSCs) had the same phenotypic and suppressive characteristics of the sorted CD11b<sup>low/-</sup>/CD16<sup>-</sup> BM-MDSCs (supplemental Figure 1B).

CD11b<sup>low/-</sup>/CD16<sup>-</sup> cells sorted from fresh BM had a peculiar structure, characterized by a high side scatter, occupying the region of normal granulocytes, but, after 4 days of culture with G-CSF + GM-CSF, these cells gradually reduced their side scatter and increased the forward scatter, thus moving to the monocyte region (supplemental Figure 1C; Figure 4). However, the surface phenotype of the suppressive CD11b<sup>low/-</sup>/CD16<sup>-</sup> cells, separated from BM-MDSCs, indicated that this population lacked the expression of the monocytic marker CD14 and was positive for the CD15 granulocytic Ag (Figure 4A), thus implying that it had characteristics distinct from both mature monocytes and granulocytes.

The suppressive subset was negative for the lineage markers and expressed the myeloid markers CD13 and CD33; IL4R $\alpha$  chain was expressed at low intensity, as previously shown.<sup>4,10</sup> The expression of CD66b was down-regulated in the cytokine-treated subset, compared with the same population sorted from fresh BM cells, whereas CD117 increased its expression after induction with G-CSF + GM-CSF (Figure 4A; supplemental Figure 1C). Two discrete populations with different expression of HLA-DR molecule (low or negative) were noted. The suppressive cells expressed CD39 but lacked CD73, which are both expressed on the surface of

human T-regulatory lymphocytes.<sup>11</sup> Finally, this subset did not express B7-H1 and slightly expressed B7-H2 and B7-H3 (Figure 4A), members of B7 family that are able to regulate immune responses and to induce immunologic tolerance.<sup>12</sup>

We also estimated the proliferative rate of the CD11b<sup>low/-</sup>/CD16<sup>-</sup> cells by intracellular staining of Ki-67<sup>+</sup> cells and observed that 97% of the cells expressed this Ag, indicating that these cells were actively proliferating in response to cytokine treatment (Figure 4A).

It is known that during the differentiation of polymorphonuclear leukocytes, myeloblasts and promyelocytes proliferate and generate primary granules,<sup>13</sup> and one of the proteins contained in these granules is the enzyme myeloperoxidase (MPO). CD11b<sup>low/-</sup>/CD16<sup>-</sup> cells isolated from BM-MDSCs induced from different human samples could assume either 1 of 2 main structural patterns: cells with large nuclei and reduced cytoplasm without granules and cells with more abundant cytoplasm and a discrete number of cytoplasmic granules (Figure 4B). By confocal microscopy, the MPO protein appeared prevalently located, as expected, within granules; however, the cytoplasm of the agranular cells showed a diffuse pattern of expression (Figure 4B). Classic, mature granulocytes presented the typical polylobated nucleus surrounded by azurophilic granules containing MPO, whereas the MPO expression in monocytes seemed to be confined within the lysosomal compartment (Figure 4B), as described.<sup>14</sup>

We also used a novel monoclonal Ab against human arginase 1 (ARG1) to evaluate whether the enzyme was present in CD11b<sup>low/-</sup>/CD16<sup>-</sup> cells and whether it was coexpressed with MPO, as suggested by some studies.<sup>15</sup> The analysis of ARG1 in this suppressive subset showed cells with different expression pattern: in most cells this enzyme was partially colocalized with MPO, but some cells stained negative for ARG1 (Figure 4B). In contrast, mature granulocytes showed a complete colocalization of the 2 enzymes, whereas monocytes did not express ARG1, as already described.<sup>15</sup> The CD11b<sup>low/-</sup>/CD16<sup>-</sup> cells isolated from fresh BM cells stained positive for ARG1 but showed a decrease of MPO expression, compared with the same population separated from BM-MDSCs (Figure 4C). In comparison, freshly isolated CD11b<sup>+</sup>/CD16<sup>-</sup> and CD11b<sup>+</sup>/CD16<sup>+</sup> cells, which represent more advanced maturation stages, presented a progressive increase in the signals for both enzymes (Figure 4C).

#### **Activated T lymphocytes sustain the proliferative rate of the BM-MDSC CD11b<sup>low/-</sup> cells and block their differentiation process**

The activation level of T lymphocytes appears to be critical to drive the suppressive activity of BM-MDSCs (Figure 1D). To investigate the relationship between T-cell activation and MDSC suppression, we set up experiments in which either resting or activated T cells, labeled with CellTrace fluorescent stain, were cocultured with BM-MDSC cell subsets, so that we could trace unambiguously the myeloid and lymphoid cell populations in the coculture and evaluate proliferation after 4 days. As expected, we observed a high proliferation rate of activated T cells in the presence of CD11b<sup>+</sup> BM-MDSCs, evaluated in terms of CellTrace dilution and, instead, a reduction in the proliferation of T cells cocultured with the suppressive CD11b<sup>low/-</sup> BM-MDSC fraction (Figure 5A second lane). We also assessed the cell proliferation of the myeloid cell subsets in the cultures by analyzing Ki-67 expression on gated CD3<sup>-</sup>/CellTrace<sup>-</sup> cells. Interestingly, although the CD11b<sup>+</sup> cell subset of BM-MDSCs did not proliferate in culture with either activated or resting T cells (Figure 5A third lane), the suppressive

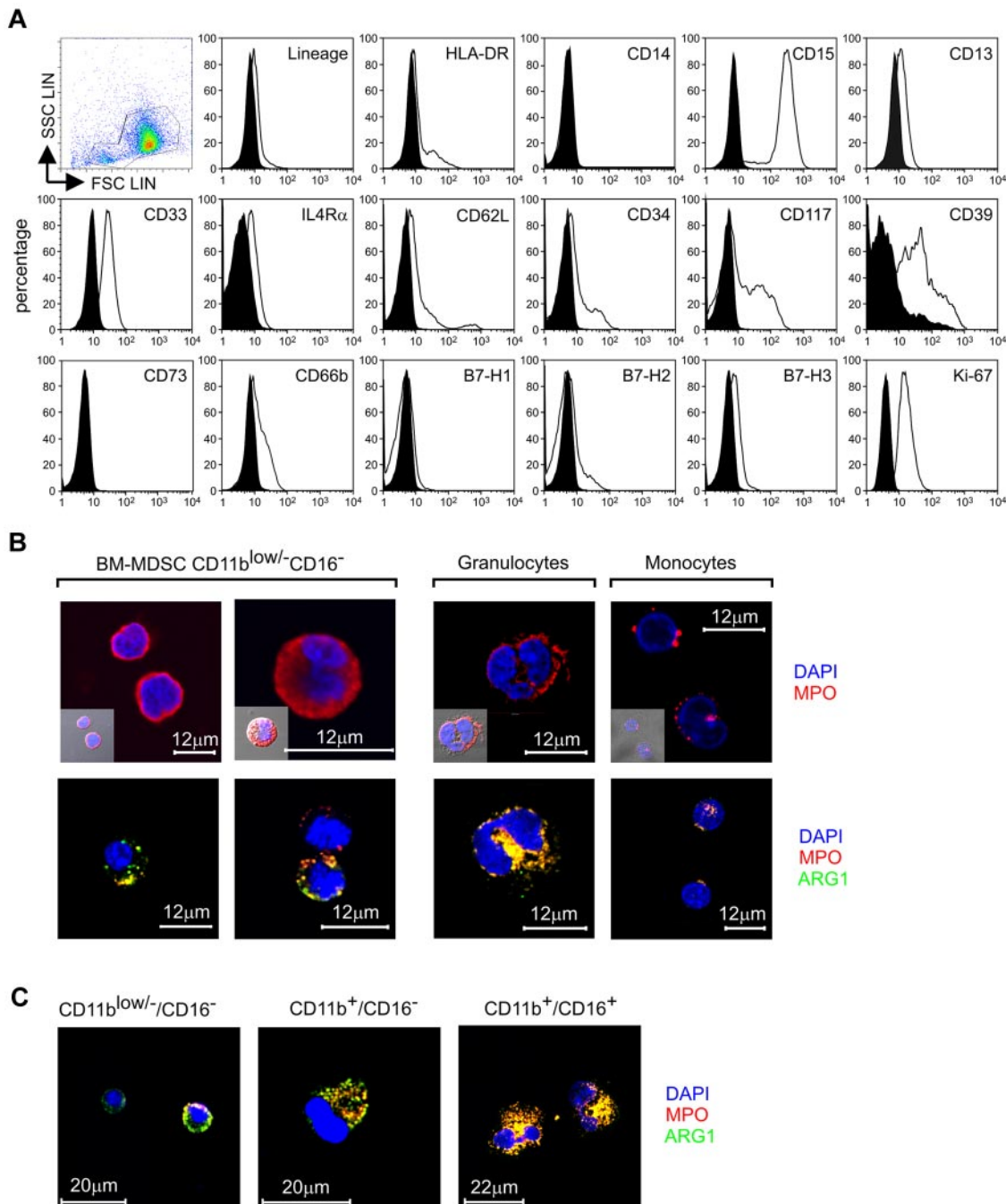


**Figure 4. Phenotypic evaluation of the immune-suppressive subset CD11b<sup>low/-</sup>/CD16<sup>-</sup> contained within BM-MDSCs.** (A) Flow cytometric analysis of CD11b<sup>low/-</sup>/CD16<sup>-</sup> cells sorted from BM-MDSCs. The expression of putative MDSCs markers, markers of mature and immature myeloid cells, and markers associated with tolerance was evaluated relative to isotype control (black histograms). In the figure is presented 1 representative of 2 independent experiments. (B) Confocal microscopic localization of MPO and ARG1 in CD11b<sup>low/-</sup>/CD16<sup>-</sup> cells, freshly isolated neutrophils, and monocytes. Scale bars = 12  $\mu$ m. (C) Localization of MPO and ARG1 in CD11b<sup>low/-</sup>/CD16<sup>-</sup>, CD11b<sup>+</sup>/CD16<sup>-</sup>, and CD11b<sup>+</sup>/CD16<sup>+</sup> cells isolated from fresh BM samples determined by confocal microscopy. Scale bars = 20  $\mu$ m.

CD11b<sup>low/-</sup> cell subset maintained a discrete proliferative capacity in the presence of resting T cells, which was even increased with the presence of activated T cells (geometric mean fluorescent intensity 14.5 vs 29.2, respectively), suggesting that T-cell activation supports the proliferation of suppressive cells.

To understand whether suppressive BM-MDSC CD11b<sup>low/-</sup> cells maintain their phenotype or rather differentiate to more mature myeloid subsets when cocultured with activated T lymphocytes, we analyzed the expression of differentiation myeloid markers after cell coculture. After 4 days of culture we observed that, only in the presence of activated T cells, promyelocyte-like

cells maintained their level of immaturity, as shown by the levels of expression in the markers CD11b and CD16; moreover, whereas HLA-DR and CD34 were maintained or even increased, CD66b, a marker of secondary granules, was down-regulated in the presence of activated T cells (Figure 5B). Control cultures of immature promyelocyte-like cells in the absence of lymphocytes showed a differentiation pattern similar to myeloid cells cocultured with resting T cells (Figure 5B), thus suggesting that only the presence of activated T cells is able to block the default differentiation process of immature promyelocyte-like cells.

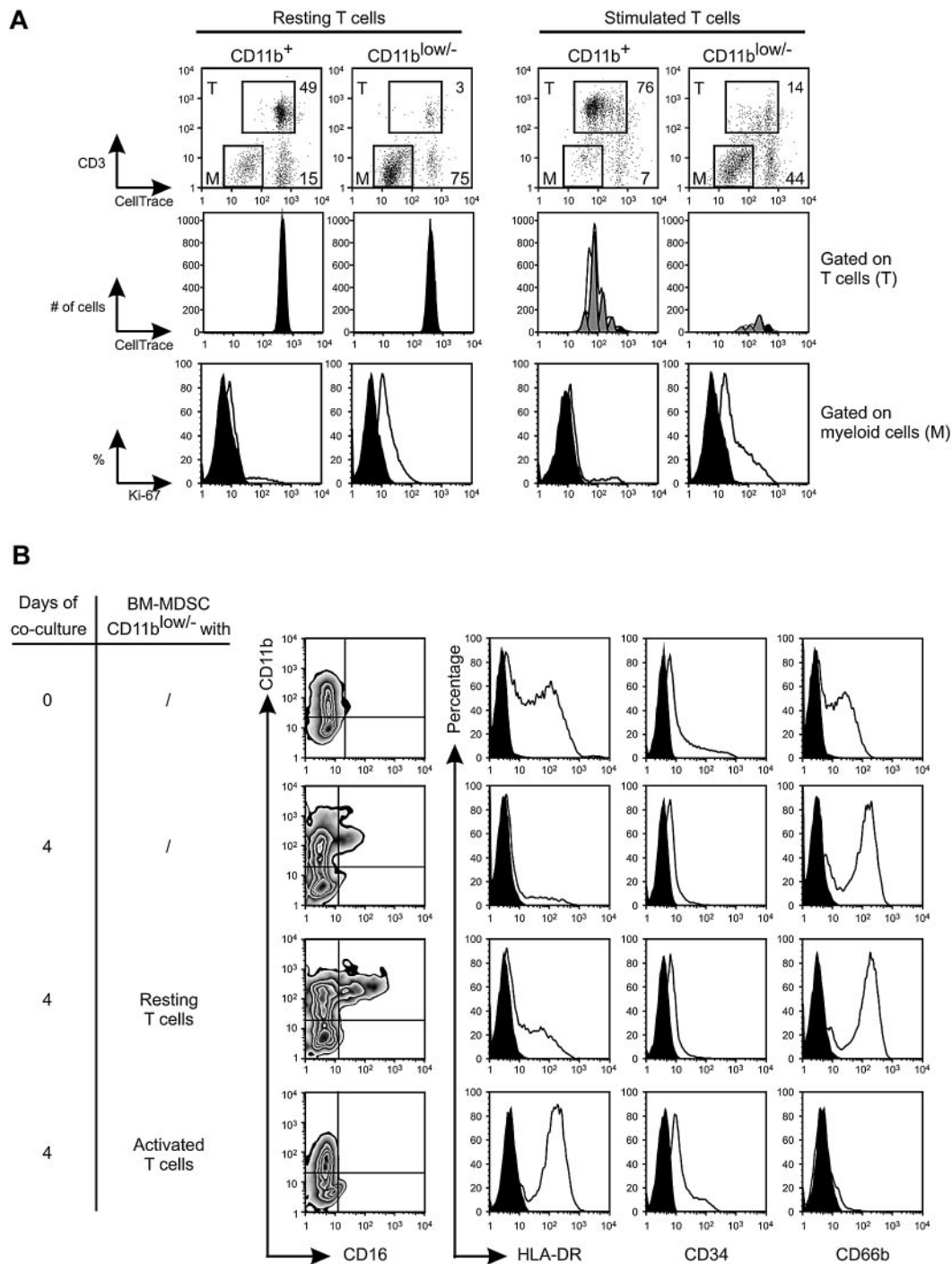


**Figure 5. T-lymphocyte activation is driving BM-MDSC proliferation and immune suppression.** (A) CellTrace-labeled PBMCs were stimulated with anti-CD3/CD28 in the presence of BM-MDSC CD11b<sup>+</sup> and CD11b<sup>low/-</sup> cell subsets, added at a ratio of 1:1. After 3 days, cell cultures were harvested, labeled with anti-CD3ε, and analyzed in the CD3ε<sup>-</sup>/CellTrace<sup>-</sup> gate (M) and in the CD3ε<sup>+</sup>/CellTrace<sup>+</sup> (T) cell gate. The numbers indicated in the top graphs refer to the percentage of cells gated on either T cells (T) or on myeloid cells (M). The central histograms show the profile of CellTrace dilution of either resting or stimulated T cells (gate T) cocultured with BM-MDSCs CD11b<sup>+</sup> and CD11b<sup>low/-</sup> subsets. Black and gray curves refer to undivided and proliferating cells, respectively. The bottom histograms show Ki-67 expression in BM-MDSCs CD11b<sup>+</sup> and CD11b<sup>low/-</sup> subsets (gate M) cocultured with either resting or stimulated T cells. Black histograms indicate isotype control. The figure shows a representative experiment of 3 performed. (B) Flow cytometric evaluation of CD11b, CD16, HLA-DR, CD34, and CD66b markers in CD11b<sup>low/-</sup> cell subset sorted from BM-MDSCs either before or after the coculture with resting or anti-CD3/anti-CD28-activated T cells. The expression of these markers was compared with the autofluorescence signal (black histograms). In the figure, 1 representative of 3 independent experiments is presented.

Taken together these data indicate that promyelocyte-like cells proliferate, their functional activity is associated with a delay in the differentiation pathway, and both proliferation and block in the differentiation pathway account for their expansion and maintenance of an immature phenotype.

**Increased circulating MDSC levels correlate with progression and worse clinical prognosis**

The suppressive myeloid population of BM-MDSCs was mainly Lin<sup>-</sup>, CD11b<sup>low/-</sup>, HLA-DR<sup>low/-</sup>, but positive for myeloid markers

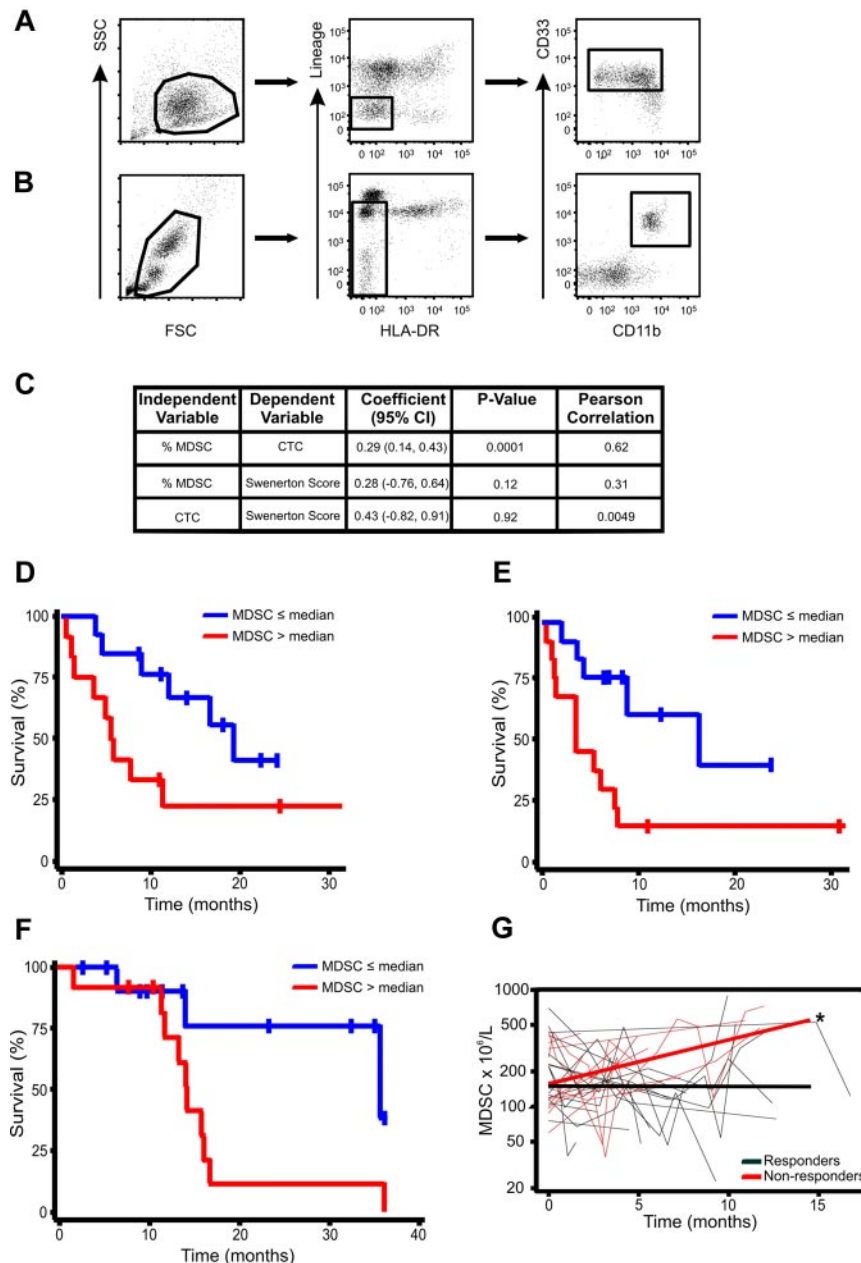


**Figure 6. Increase in circulating MDSC levels over time in patients with advanced solid tumors is associated with decreased survival times and radiographic disease progression.** Gating strategy for BM-MDSCs (A) and whole-blood MDSCs (B) is shown on a representative flow cytometric plot. (C) Random effects regression model and correlation between MDSCs and CTCs. Flow cytometric analysis was performed on peripheral whole blood in a separate cohort of patients with stage IV breast cancer ( $n = 25$ ) before initiation of therapy and at defined intervals during therapy. Blood for CTC determination by the CellSearch was simultaneously drawn. A significant correlation was found between circulating MDSC levels (%) and CTCs ( $P = .0001$ ). (D) Survival analysis by circulating MDSC levels (%) at first blood draw in patients with stage IV breast cancer starting a new line of systemic chemotherapy ( $n = 26$ ). Survival estimates by median percentage of MDSCs ( $\leq 3.17\%$  and  $> 3.17\%$ ) with the use of the first MDSCs observation ( $P = .048$ ). (E) Survival estimates by median percentage of MDSCs ( $\leq 3.04\%$  and  $> 3.04\%$ ) with the use of MDSCs levels drawn at the last visit ( $P = .018$ ). (F) Survival analysis by circulating MDSC levels at time of study enrollment in patients with stage IV colorectal cancer. Survival estimates by median percentage of MDSCs ( $\leq 2.54\%$  and  $> 2.54\%$ ). (G) Analysis of relationship between changes in circulating MDSC levels over time and best radiographic response in patients receiving systemic chemotherapy ( $n = 25$ ). Plot of MDSCs over time by "best response" defined as patients who achieved complete (CR) or partial radiographic response (PR) while on systemic therapy versus patients who did not. MDSCs were drawn prospectively after every other cycle of therapy. Over time circulating MDSCs were significantly higher in nonresponders than in patients with CR or PR as best response ( $*P = .015$  comparing slopes).

CD33 (Figure 4), a subset with phenotype similar to MDSCs previously described in tumor-bearing patients.<sup>9,16</sup> Indeed, in the blood of patients with stage IV breast cancer we could clearly identify a Lin<sup>-</sup>, HLA-DR<sup>-</sup>, CD33<sup>+</sup>, CD11b<sup>+</sup> MDSC population resembling in vitro-generated BM-MDSCs (Figure 6A-B). We previously showed that this cell subset correlated with clinical tumor stage,<sup>16</sup> but it is still unknown whether circulating Lin<sup>-</sup>, HLA-DR<sup>-</sup>, CD33<sup>+</sup>, CD11b<sup>+</sup> cells also correlate with either

metastatic tumor burden or OS in patients with cancer. We thus evaluated the relationship between MDSCs and CTCs measured by the CellSearch assay, a strong, independent predictor of survival in patients with advanced breast cancer.<sup>17,18</sup> In a cohort of patients with stage IV breast cancer ( $n = 25$ ) CTCs (CellSearch) and MDSCs were analyzed simultaneously. A generalized estimating equation regression model was created and fitted individually for each predictor. A significant correlation was observed between

circulating MDSCs and CTCs ( $P = .0001$ ; Figure 6C). As expected, no significant correlation was observed between CTCs and SS ( $P = .92$ ); indeed, CTCs are not a measure of metastatic tumor burden, and levels do not correlate with SS in patients with advanced breast cancer.<sup>17-19</sup> To ascertain whether high circulating MDSC levels were associated with poorer prognosis, survival estimates in the breast cancer dataset were calculated with MDSC levels (%), drawn either before starting a new line of therapy or levels at the last blood draw. Patients with circulating MDSCs  $> 3.17\%$  (median) at baseline had a poorer OS than patients with circulating MDSCs  $\leq 3.17\%$ , with median OS times of 5.5 months (95% confidence interval [CI], 0.5-11.3 months) and 19.32 months (95% CI, 8.7 months to infinity), respectively ( $P = .048$ ; Figure 6D). Likewise, elevated MDSC levels at the last visit were also associated with a significantly poorer OS ( $P = .018$ ), with median survival times of 3.8 months (95% CI, 0.5-7.7 months) and 16.7 months (95% CI, 3.8 months to infinity), respectively (Figure 6E).

We then moved to examine another group of patients with cancer. In a cohort of patients with stage IV colorectal cancer ( $n = 25$ ) we also found that baseline levels of MDSCs before starting chemotherapy also correlated with poorer OS (Figure 6F). Patients with circulating MDSC levels greater than the median value (2.54%) had significantly shorter median OS times than patients with levels below the median value (35.6 vs 14.3 months;  $P = .025$ ; Figure 6F). We next investigated whether levels of circulating MDSCs over time in patients with advanced solid tumors receiving systemic chemotherapy correlated with clinical outcomes. MDSC levels in the same cohort of patients with stage IV colorectal cancer were drawn every other chemotherapy cycle. Patients underwent routine radiographic assessments as clinically indicated, typically every 2-3 months. Over time MDSC levels were significantly higher in patients who had radiographic evidence of progressive disease than in levels in patients who achieved either a CR or PR as their best radiographic response ( $P = .015$ ; Figure 6G). Taken together, these clinical data suggest, for the first time, that circulating MDSC levels, phenotypically similar to those described in human BM experiments, are clinically relevant and appear to (1) increase over time in patients with progressive disease, (2) correlate with an established prognostic marker (CTCs) in advanced breast cancer, and (3) show that persistently high or increasing levels after chemotherapy are associated with poorer survival.

## Discussion

The aim of our study was to dissect the differentiation stage of the suppressive myeloid cells by taking advantage of the *in vitro* generation of MDSCs from the BM precursor.<sup>3</sup> The suppressive activity is fully induced in BM-MDSCs only after direct contact with activated T lymphocytes, indicating that suppressive cells are primed by the activation status of target cells and by a cell membrane signal, a result analogous to data obtained with mouse MDSCs.<sup>10</sup> Moreover, this result is in line with the consideration that myeloid suppressors play a role in turning off potential harmful immune responses carried out by activated T lymphocytes.<sup>1,20</sup> Our results extend this idea, leading us to hypothesize that the activity of MDSCs is dictated by the activation level of the T lymphocytes. In fact, suppressive cells are unable to harm resting lymphocytes, and the direct contact between these 2 cells might ensure that the

signals delivered by MDSCs are confined only to target cells and not to bystander cells.

It is known that anti-CD3- and anti-CD28-activated T cells secrete GM-CSF and IL-6,<sup>21</sup> cytokines that drive the BM-MDSC development from BM; however, we observed that BM-MDSCs also are able to produce *in vitro* IL-6 during the culture with growth factors (data not shown). Moreover, it was recently shown that T lymphocytes, on TCR activation, produce soluble factors that enhance fibroblasts production of IL-6.<sup>22</sup> An attractive hypothesis is that activated T cells release cytokines that might sustain the induction of the suppressive cells or maintain their tolerogenic activity, an autoregulative loop that has already been shown in a different system.<sup>10</sup>

Among different cytokine combinations, GM-CSF and IL-6 were the most effective in generating, from healthy donor PBMCs, suppressive CD33<sup>+</sup> cells that inhibited the proliferation and IFN- $\gamma$  production by autologous human T cells after CD3/CD28 stimulation.<sup>23</sup> These cells were large mononuclear CD11b<sup>+</sup> HLA-DR<sup>low</sup> CD66b<sup>+</sup> cells with basophilic and granular cytoplasm. When molecules and enzymes participating in inhibitory pathways were evaluated by either quantitative RT-PCR or cytofluorometry, NOS2, TGF $\beta$ , VEGF, and NOX2 were found to be up-regulated, whereas no significant changes in comparison with the nonsuppressive, normal CD33<sup>+</sup> cells were detected for B7-H1, B7-H2, and B7-H4.<sup>23</sup> It thus appears that cytokines might induce different cells with immunoregulatory properties when acting on either BM or blood-circulating precursors. Whether these cells represent stages of the same differentiation process is an issue that requires further investigation. It is clear, however, that MDSCs described in the present study are different from either fully differentiated or activated granulocytes and monocytes.

We observed that the reduction of lymphocyte proliferation induced by BM-MDSCs is accompanied by a decreased expression not only of the CD3 $\zeta$  but also of the CD3 $\epsilon$  chain and by a reduction in absolute numbers of T lymphocytes. It is known that the absence or reduction of CD3 $\zeta$  chain impairs T-cell signaling and contributes to immune cell dysfunction and evidence is accumulating that expression of the CD3 $\zeta$  chain is markedly decreased in both peripheral blood and tumor-infiltrating lymphocytes in patients with different types of tumors.<sup>24,25</sup> Significantly less is known about the importance of the  $\epsilon$  chain of the CD3/TCR complex in tumor immunity, even if some reports have shown down-regulation of CD3 $\epsilon$  chain in patients with lung cancer and SCID.<sup>26-28</sup>

In this study we addressed the extent and relevance of cell heterogeneity of MDSCs, generally accepted as a common feature of this cell population, with the aim to define whether immunoregulatory properties of human BM-MDSCs can be attributed to  $\geq 1$  cell subsets. We observed that the treatment of BM cells with G-CSF + GM-CSF resulted in a significant accumulation of immature myeloid cells (Figure 2A).<sup>3</sup> In this regard, we observed that one of the differences existing between untreated BM and BM-MDSCs was represented by the expansion of immature myeloid cells expressing low levels of CD11b and negative for CD16, a phenotype that is typically associated with myeloblasts and promyelocytes, but not with more differentiated cells (Figure 2A and <sup>3</sup>). The accumulation of immature CD11b<sup>+</sup>/CD16<sup>-</sup> cells in BM-MDSCs led us to test the hypothesis that this myeloid population was entirely responsible for the suppression exerted by BM-MDSCs. Our results clearly indicate that the only subset responsible for the immune suppression exerted by BM-MDSCs is contained within the CD11b<sup>low</sup>-/CD16<sup>-</sup> cell population of BM-MDSCs, and other immature but more differentiated subsets, such

as CD11b<sup>+</sup>/CD16<sup>-</sup> and CD11b<sup>+</sup>/CD16<sup>+</sup> cells, are completely devoid of suppressive activity; accordingly, this subset was able to proliferate in the presence of activated T cells, a feature that is lost by more mature subsets. Interestingly, we also observed that BM-MDSC CD11b<sup>low/-</sup> were able to exert suppressive activity both on CD4<sup>+</sup> and CD8<sup>+</sup> subsets and to induce apoptosis of T cells, an event that was marginal in T cells activated without BM-MDSC CD11b<sup>low/-</sup> (data not shown).

Remarkably, the suppressive cell subset had a phenotype corresponding to promyelocytes, and, indeed, these cells structurally resembled promyelocytes, with a large regular, symmetric nucleus, high nucleus/cytoplasm ratio, and basophilic cytoplasm. We sorted the corresponding subset from fresh BM (CD11b<sup>low/-</sup>/CD16<sup>-</sup>), containing mainly promyelocytes. The 2 subsets were indistinguishable from a structural point of view, but they differed completely in terms of ability to suppress activated T lymphocytes, because normal promyelocytes were unable to exert any inhibitory activity (Figure 3A). Here, for the first time, we show that MDSCs proliferate, that this activity is linked to a block in the differentiation pathway, and, interestingly, that both suppression and maturation depend on the activation status of the T lymphocytes (Figure 5).

Because suppressive activity of myeloid cells is limited to a specific subset of promyelocytic-like cells, and the more differentiated populations are completely devoid of regulatory activity, this implies that suppressive activity is not a stable trait of MDSCs but rather a transitory state, possibly ending or being sustained according to local signals coming from the microenvironment where the immature cells migrate. These results, therefore, suggest that MDSCs maintain a plasticity that enables them to differentiate and suspend their tolerogenic program.

We found that ARG1 was expressed in the suppressive CD11b<sup>low/-</sup>/CD16<sup>-</sup> cell subset and partially colocalized with MPO, suggesting its main distribution within primary granules, as suggested by Munder et al.<sup>15</sup> However, in comparison with the same population isolated from fresh BM, this subset had an increased expression of MPO, which presented both an expected granular and an uncommon agranular localization. We are currently evaluating whether the altered expression of these enzymes is only a marker of these cells or whether it is related also to their suppressive function.

Finally, one of the challenges in studying MDSCs in humans has been that the phenotype is not as well defined as in mice. We

show that MDSCs, defined as Lin<sup>-</sup>, HLA DR<sup>-</sup>, CD33<sup>+</sup>, CD11b<sup>+</sup>, can be easily traced among blood circulating cells in patients with advanced breast and patients with colorectal cancer, with levels correlating with clinical outcomes.

## Acknowledgments

The authors thank Drs A. Anselmo for help and advice with FACS, C. Frasson for FACS, and P. Gallo for artwork preparation.

This work was supported by grants from the Italian Ministry of Health, Fondazione Cassa di Risparmio di Padova e Rovigo, Italian Association for Cancer Research (AIRC), Association for International Cancer Research (AICR; grant 08-0518), and Fondazione Cassa di Risparmio di Verona, Vicenza, Belluno e Ancona and Associazione Italiana Ricerca sul Cancro (AIRC; grant 6599).

## Authorship

Contribution: S.S. performed research, analyzed and interpreted data, and wrote the manuscript; E.F. performed flow cytometry and confocal microscopy studies; C.M.D.-M. performed flow cytometric analysis of all data from patients with solid tumors, analyzed and discussed results; A.D. performed confocal microscopy study; L.P. performed research; A.R. generated monoclonal Ab against ARG1; S.F. performed BM samples enrollment; G.B. discussed results and provided vital material for the study; P.Z. discussed the results; G.O. and E.G.-M. performed statistical analyses of data from patients with breast cancer and with colorectal cancer; A.J.M. obtained informed consent on all patients with solid tumors, helped write results on relevant section, and edited manuscript; V.B. discussed and analyzed the results and wrote the manuscript; and S.M. designed the study, analyzed and interpreted data, and wrote the manuscript.

Conflict-of-interest disclosure: The authors declare no competing financial interests.

The current affiliation for V.B. is Immunology Section, Verona University Hospital and Department of Pathology, Verona, Italy.

Correspondence: Susanna Mandruzzato, Oncology Section, Department of Oncology and Surgical Sciences, Via Gattamelata, 64 35128 Padova, Italy; e-mail: susanna.mandruzzato@unipd.it.

## References

- Gabrilovich DI, Nagaraj S. Myeloid-derived suppressor cells as regulators of the immune system. *Nat Rev Immunol*. 2009;9(3):162-174.
- Peranzoni E, Zilio S, Marigo I, et al. Myeloid-derived suppressor cell heterogeneity and subset definition. *Curr Opin Immunol*. 2010;22(2):238-244.
- Marigo I, Bosio E, Solito S, et al. Tumor-induced tolerance and immune suppression depend on the C/EBPβ transcription factor. *Immunity*. 2010;32(6):790-802.
- Mandruzzato S, Solito S, Falisi E, et al. IL4Rα<sup>+</sup> myeloid-derived suppressor cell expansion in cancer patients. *J Immunol*. 2009;182(10):6562-6568.
- Rodriguez PC, Ochoa AC. Arginine regulation by myeloid derived suppressor cells and tolerance in cancer: mechanisms and therapeutic perspectives. *Immunol Rev*. 2008;222:180-191.
- Dugast AS, Haudebourg T, Coulon F, et al. Myeloid-derived suppressor cells accumulate in kidney allograft tolerance and specifically suppress effector T cell expansion. *J Immunol*. 2008;180(12):7898-7906.
- Apolloni E, Bronte V, Mazzoni A, et al. Immortalized myeloid suppressor cells trigger apoptosis in antigen-activated T lymphocytes. *J Immunol*. 2000;165(12):6723-6730.
- Elghetany MT, Ge Y, Patel J, Martinez J, Uhrova H. Flow cytometric study of neutrophilic granulopoiesis in normal bone marrow using an expanded panel of antibodies: correlation with morphologic assessments. *J Clin Lab Anal*. 2004;18(1):36-41.
- Almand B, Clark JI, Nikitina E, et al. Increased production of immature myeloid cells in cancer patients: a mechanism of immunosuppression in cancer. *J Immunol*. 2001;166(1):678-689.
- Gallina G, Dolcetti L, Serafini P, et al. Tumors induce a subset of inflammatory monocytes with immunosuppressive activity on CD8<sup>+</sup> T cells. *J Clin Invest*. 2006;116(10):2777-2790.
- Deaglio S, Dwyer KM, Gao W, et al. Adenosine generation catalyzed by CD39 and CD73 expressed on regulatory T cells mediates immune suppression. *J Exp Med*. 2007;204(6):1257-1265.
- Latchman Y, Wood CR, Chernova T, et al. PD-L2 is a second ligand for PD-1 and inhibits T cell activation. *Nat Immunol*. 2001;2(3):261-268.
- Borregaard N, Cowland JB. Granules of the human neutrophilic polymorphonuclear leukocyte. *Blood*. 1997;89(10):3503-3521.
- Bunbury A, Poticchio I, Maitra R, Santambrogio L. Functional analysis of monocyte MHC class II compartments. *FASEB J*. 2009;23(1):164-171.
- Munder M, Mollinedo F, Calafat J, et al. Arginase I is constitutively expressed in human granulocytes and participates in fungicidal activity. *Blood*. 2005;105(6):2549-2556.
- Diaz-Montero CM, Salem ML, Nishimura MI, Garrett-Mayer E, Cole DJ, Montero AJ. Increased circulating myeloid-derived suppressor cells correlate with clinical cancer stage, metastatic tumor burden, and doxorubicin-cyclophosphamide chemotherapy. *Cancer Immunol Immunother*. 2009;58(1):49-59.

17. Cristofanilli M, Budd GT, Ellis MJ, et al. Circulating tumor cells, disease progression, and survival in metastatic breast cancer. *N Engl J Med*. 2004;351(8):781-791.
18. Cristofanilli M, Broglio KR, Guarnieri V, et al. Circulating tumor cells in metastatic breast cancer: biologic staging beyond tumor burden. *Clin Breast Cancer*. 2007;7(6):471-479.
19. Cristofanilli M, Hayes DF, Budd GT, et al. Circulating tumor cells: a novel prognostic factor for newly diagnosed metastatic breast cancer. *J Clin Oncol*. 2005;23(7):1420-1430.
20. Marigo I, Dolcetti L, Serafini P, Zanovello P, Bronte V. Tumor-induced tolerance and immune suppression by myeloid derived suppressor cells. *Immunol Rev*. 2008;222:162-179.
21. Harris KM, Lenz P, Hankey KG, et al. Products of anti-CD3/anti-CD28 activated lymphocytes induce differentiation and maturation of dendritic cells and have adjuvant-like activity in vitro and in vivo. *Clin Immunol*. 2008;129(1):58-68.
22. Barnas JL, Simpson-Abelson MR, Brooks SP, Kelleher RJ Jr, Bankert RB. Reciprocal functional modulation of the activation of T lymphocytes and fibroblasts derived from human solid tumors. *J Immunol*. 2010;185(5):2681-2692.
23. Lechner MG, Liebertz DJ, Epstein AL. Characterization of cytokine-induced myeloid-derived suppressor cells from normal human peripheral blood mononuclear cells. *J Immunol*. 2010;185(4):2273-2284.
24. Schule J, Bergkvist L, Hakansson L, Gustafsson B, Hakansson A. Down-regulation of the CD3-zeta chain in sentinel node biopsies from breast cancer patients. *Breast Cancer Res Treat*. 2002;74(1):33-40.
25. Otsuji M, Kimura Y, Aoe T, Okamoto Y, Saito T. Oxidative stress by tumor-derived macrophages suppresses the expression of CD3 zeta chain of T-cell receptor complex and antigen-specific T-cell responses. *Proc Natl Acad Sci U S A*. 1996;93(23):13119-13124.
26. de Saint Basile G, Geissmann F, Flori E, et al. Severe combined immunodeficiency caused by deficiency in either the delta or the epsilon subunit of CD3. *J Clin Invest*. 2004;114(10):1512-1517.
27. Prado-Garcia H, Aguilar-Cazares D, Meneses-Flores M, Morales-Fuentes J, Lopez-Gonzalez JS. Lung carcinomas do not induce T-cell apoptosis via the Fas/Fas ligand pathway but down-regulate CD3 epsilon expression. *Cancer Immunol Immunother*. 2008;57(3):325-336.
28. Kuang DM, Zhao Q, Xu J, Yun JP, Wu C, Zheng L. Tumor-educated tolerogenic dendritic cells induce CD3epsilon down-regulation and apoptosis of T cells through oxygen-dependent pathways. *J Immunol*. 2008;181(5):3089-3098.